From discrete anions to extended solids: new uranium thiophosphates

Dissertation
zur Erlangung des Grades
„Doktor der Naturwissenschaften“
am Fachbereich Chemie und Pharmazie
der Johannes-Gutenberg-Universität Mainz

Christine Gieck
geboren in Groß-Umstadt

Mainz, 2003

Die experimentellen Untersuchungen zu der vorliegenden Arbeit wurden am Institut für Anorganische Chemie und Analytische Chemie der Johannes-Gutenberg-Universität in Mainz in der Zeit von November 1997 bis Mai 2002 unter der Leitung von Prof. Dr. W. Tremel durchgeführt.

Für meine Mutter

The most important phrase in science,
the one which heralds new results
is not "Eureka" but "That's funny..."

Isaac Asimov

Table of Contents

1 Introduction

The preparation and characterization of micro- and mesoporous oxide-based materials has been an important issue during the last decades. The most important class of microporous inorganic compounds are the zeolites, crystalline materials with porous network structures. Zeolite frameworks consist of corner-sharing SiO_4 and AlO_4^- tetrahedra. The negative charge of the porous 3D alumosilicate framework is counterbalanced by templating alkali metal cations residing in the cavities.

Zeolites are generally prepared by hydrothermal synthesis techniques, where the size of the cavities can be "fine tuned" by choosing suitable countercations. The introduction of surfactant liquid crystals serving as templates in the reaction mixture resulted in the formation of mesoporous silicate and alumosilicate frameworks with pore sizes ranging from 15 to 100 Å.[1]

The substitution of either SiO_4 or AlO_4^- with different tetrahedral oxidic units yielded a class of so-called "zeotype" materials, whose properties resemble the parent compounds. For example, the substitution of AlO_4^- yielded zeotype silicates of boron,[2] gallium, iron[3] and titanium,[4] while the introduction of orthophosphate units into the framework resulted in the formation of porous aluminium- and galliumphosphates.[5-7]

The properties of the corresponding porous non-oxidic chalcogenides were investigated only recently. The most important difference between oxygen and the heavier chalcogen atoms is the preference of the latter elements to form stable infinite Q_n chains instead of Q-Q double bonds.[8] This ability of the chalcogens leads to the formation of a multitude of possible connectivity patterns.

Most of these non-oxidic zeotype compounds are air- and moisture-sensitive and cannot be precipitated from aqueous solutions. The vast majority was obtained from high-temperature reactions in a polychalcogenide or alkali metal halide flux. New synthetic routes include the self-assembly of suitable anionic precursors like $Ge_4Q_{10}^{4-}$ (Q = S, Se) in

solutions containing organic templates.[9-15] The properties of the reaction products are determined by the polarity of the solvent and the structure of the templating surfactant molecule aggregates.

The most successful candidates for the formation of porous or low-dimensional network structures are the thio- and selenophosphates of transition metals. Their easy accessibility by solid-state reactions, the large variety of possible connectivity patterns and the comparative stability of the precursors resulted in the synthesis and characterization of an intriguing variety of transition metal chalcogenophosphates.

The arrangement of the different building blocks in the crystal structures of these compounds depends on the preferred coordination environment for the metal centers and the structure of the $P_xQ_y^{z-}$ (Q = S, Se) ligands. For example, the combination of the tetrahedral PQ_4 ligand, which acts as a twofold bidentate connector between two metal centers, with a MQ_6 octahedron results in a triangular connectivity for the metal atom.[16] The combination of a MQ_8 polyhedron with four bidentate PQ_4 ligands leads to the formation of a pseudotetrahedral environment for the central metal atom.[17] The high and variable coordination numbers of transition metal atoms combined with the condensation equilibria of chalcophosphates may lead to structural arrangements of astounding complexity.

The most important class of ternary metal chalcogenophosphates are the hexathiodiphosphates of divalent transition metals. This so-called MPS_3 structure type[18] is adopted for M = Cr, Mn, Fe, Ni, Cd and Zn. These compounds contain the MS_6 octahedron coordinated by six S atoms belonging to three ethane-like $P_2S_6^{4-}$ groups. The resulting crystal structure can be derived form the $CdCl_2$ structure type by replacing the Cl atoms with sulfur and 1/3 of the metal cations with P_2 dumbbells. The corresponding selenophosphates, $MPSe_3$, crystallize in most cases in a similar structure type based on the atom arrangement found in CdI_2.[19] Both MPS_3 and $MPSe_3$ consist of 2D layers separated by *van der Waals* gaps. The presence of these gaps, as well as the ability of the metal centers to

act as electron acceptors,[20] leads to a multitude of intercalation products.

Lithium metal hexadithiophosphates[20,21] can be prepared either by electrochemical intercalation of lithium between the layers or by ion exchange reactions. For example, the compound $Li_xNi_{1-x}PS_3$ is used as a cathode material in room-temperature lithium batteries.[22]

Recent research interests include the preparation of nanocomposites with the 2D MPS_3 system acting as the host layer system and planar organic molecules or polymers[23] as the intercalated guest species. Transparent thin films of $MnPS_3$ and $CdPS_3$, which were prepared by exfoliation,[24] are useful host matrices for nonlinear optical chromophores in optical devices.[25]

The replacement of the divalent metal atoms in the crystal structure of MPQ_3 with 1/2 M^+ and 1/2 M^{3+} cations leads to the formation of a number of heterocharge substitution products, $M'_{0.5}M'''_{0.5}PQ_3$.[26,27] The structure of the resulting cation sublattice can be correlated to the ratio of the metal-chalcogen distances.[26d] For r'/r''' ≈ 1, M' and M''' form distinct triangular sublattices, whereas for r'/r''' > 1, an ordered arrangement of the cations in separate zigzag chains can be observed. The existence of these low-dimensional sublattices leads to interesting physical properties, for example $Ag_{0.5}V_{0.5}PS_3$ shows 1D magnetic behaviour[26b] as the result of the existence of one-dimensional vanadium chains in the structure. In the compounds $Cu_{0.5}In_{0.5}PS_3$ and $Cu_{0.5}Cr_{0.5}PS_3$, where the triangular Cu' sublattice is distorted due to the presence of an off-centering Jahn-Teller effect, ferroelectricity can be observed.[27c]

While the crystal structures of $Hg_2P_2S_6$[28] and the rhombohedral modification of $Sn_2P_2S_6$[19a] are closely related to the parent MPS_3 structure type and the compounds SnP_2S_6,[29] $V_{0.78}PS_3$[30] and $In_4(P_2S_6)_3$[31] crystallize in MPS_3 defect variants, a completely new atom arrangement can be observed for the hexathiodiphosphates of the tetravalent metal cations Ti, Zr, Hf, Th and U.

The orthorhombic TiP_2S_6[32] structure contains the metal cations in an octahedral environment, whereas the tetragonal ZrP_2S_6 structure type consists of M^{4+} (M = Zr, [33] Th, U[34]) coordinated by eight S atoms in a square-antiprismatic fashion. Interestingly, the TiP_2S_6 structure is also adopted for HfP_2S_6,[35] the result was interpreted as a clue for the existence of high-temperature and low-temperature modifications in the $M^{IV}P_2S_6$ system.

The investigation of the group 5 metal/thiophosphate system resulted in a multitude of new compounds, many of them crystallizing in low-dimensional structure types with interesting optical properties. For example, V_2PS_{10}[36] forms infinite one-dimensional chains while 2D-NbP_2S_8,[37] Nb_2PS_{10},[38] $Nb_4P_2S_{21}$,[39] $V_{0.78}PS_3$,[30] V_5PS_{10}[40] and $V_2P_4S_{13}$[41] contain parallel slabs. 3D-NbP_2S_8,[42] $Ta_2P_2S_{11}$[43] and $TaPS_6$[44] consist of three-dimensional networks. The tantalum thiophosphates $Ta_4P_4S_{29}$[45] and $TaPS_6Se$[46] are formal intercalation compounds of $TaPS_6$ with one-dimensional chalcogenide chains residing in the pores of the host lattice.

A reduction of these frameworks can be achieved by adding alkali metal chalcogenides to the reactive flux. In many cases, the structure of the resulting anionic unit can be derived from a ternary compound with a higher-dimensional network. For example, in the case of $K_4Pd(PS_4)_2$,[47] the anion can be obtained by formal excision of the $[Pd(PS_4)_2]^{4-}$ unit from the layered structure of $Pd_3(PS_4)_2$.[48] The Zintl anion $[Cr_2(PS_4)_4]^{6-}$, which is found in $K_6Cr_2(PS_4)_4$,[49] can be interpreted as a reduced fragment of the infinite 1D anionic chain found in $K_3Cr_2(PS_4)_3$.[50]

The aim of this thesis was the preparation and characterization of new uranium thiophosphates, which were, until recently, not investigated.[17b,34] In these compounds, uranium is coordinated by eight ligands, as most anionic units donate two S atoms, a pseudotetrahedral coordination was expected resulting in open 3D networks with large pore sizes. In these cavities, the alkali metal countercations should be able to move freely, resulting in ionic conductivity and ion exchange properties of the compounds.

2 Comprehensive uranium thiophosphate chemistry: Framework compounds based on pseudotetrahedrally coordinated metal centers

Introduction

Actinide chalcogenides, especially those of uranium and thorium have been investigated for a long time. The first crystal structures were already described by Zachariasen[1] more than fifty years ago. One of the intriguing topics in the solid state chemistry of the uranium chalcogenides is the valence state of uranium. The "reduced" compounds (the term "reduced" refers to the oxidation state U^{4+}) such as the monochalcogenides UQ[2] (Q = S, Se, Te), U_3S_5,[3] U_7Te_{12},[4] or UTe_2[5] bridge the gap between localized and itinerant systems due to relative positioning of the 5 *f* and 7 *s* states and the associated localization/delocalization of the 5 *f* electrons. The chalcogen-rich compounds such as UTe_2, U_2Te_3,[6] UQ_3[7] (Q = Se, Te) or UTe_5[8] on the other hand have attracted attention because they are close to the metal-insulator boundary and thus may exhibit low-dimensionality, magnetism or charge density wave behavior. In accordance with the general trends observed for transition elements, high oxidation states of uranium are not achieved in sulfides, selenides, or tellurides. Still, in the chalcogen-rich systems the chalcogen's ability to catenate has led to formal oxidation state assignments beyond 4+ in $Rb_5U_4P_4Se_{26}$ = $Rb_4(U^{5+}{}_4)(PSe_4{}^{3-})_4P(Se_2{}^{2-})_4(Se^{2-})_2$[9] which are still open to debate.[10]

Whereas binary uranium chalcogenides and quaternary uranium chalcophosphates $A_aU_xP_yQ_z$,[11] many of which are accessible from reactive polychalcogenide fluxes, are reasonably well characterized, the information concerning the corresponding ternary chalcogenophosphates $U_xP_yQ_z$ is scarce.[12] By using standard solid-state reaction techniques, four new compounds from the U-P-S system were obtained. Their crystal structures and physical properties were investigated.

Experimental section

Reagents: Starting materials were uranium metal powder (Kristallhandel Kelpin, 99.9 % purity), P_2S_5 (Aldrich, 99 % purity), Na_2S and S powder (Merck, 99.999 %). All starting compounds and products were examined by X-ray powder diffraction, using a Siemens D5000 diffractometer with a CuK_α source.

Sodium sulfide, Na_2S, was obtained by reacting stoichiometric amounts of the elements in liquid ammonia as described in ref. 14. Sodium (2.3 g, 100 mmol) was placed under argon atmosphere into a Schlenck flask. The sample was cooled to -78°C with a dry ice/acetone bath and NH_3 (ca. 30 ml) was condensed into the flask. After the metal was dissolved, elemental sulfur (1.6 g) was added and dissolved by condensing a second portion of NH_3 onto the reactants. The resulting dark blue solution was stirred and the ammonia was allowed to evaporate. A third portion of NH_3 was condensed on the product to ensure that the reaction was complete. After evaporating the ammonia, a light yellow product was obtained. The yellow color indicated a slight contamination with polysulfides.

UP_2S_6 (I). UP_2S_6 was initially synthesized from a polysulfide flux with the formal composition UP_6S_{17}. A 500 mg mixture of uranium metal, phosphorus pentasulfide and sulfur with the molar ratio 1:3:2 was sealed in an evacuated quartz tube with an outer diameter of 1 cm and annealed in a programmable tube furnace at 130°C for ten hours. The sample was heated at a rate of 1°C/min up to 700°C and kept at this temperature for seven days; subsequently, it was cooled to room temperature within a period of one week. The product consisted of black needles with a metallic luster embedded in a dark red glassy matrix, which could be removed by treating the regulus with dry methanol. A single-phase sample of UP_2S_6 was obtained from a 500 mg mixture of uranium metal, P_2S_5 and sulfur with the ratio 1:1:1 using the same reaction conditions. The yield of the dark grey crystalline material was quantitative based on the

initial metal content, as indicated by the X-ray powder diffraction diagram shown in Fig. 1a.

UP_2S_7 (II). UP_2S_7 was initially synthesized from a sodium polysulfide flux with the formal composition $NaUP_3S_9$. A 500 mg mixture of sodium sulfide, uranium metal, phosphorus pentasulfide and sulfur with the molar ratio 1:2:3:2 was sealed in an evacuated quartz tube with an outer diameter of 1 cm and annealed in a programmable tube furnace at 130°C for ten hours. The sample was heated at a rate of 1°C/min up to 700°C and kept at this temperature for seven days; subsequently, it was cooled slowly to room temperature during the period of one week. The product consisted of dark prisms embedded in a dark red glassy matrix, which could be removed by treating the regulus with dry methanol. After the composition of the compound was known, a single-phase sample of UP_2S_7 was obtained from a 500 mg mixture of uranium metal, P_2S_5 and sulfur with the ratio 1:1:2 using the same reaction conditions. The yield of the dark grey crystalline material was quantitative based on the initial metal content as shown by the X-ray powder diffraction diagram presented in Fig. 1b.

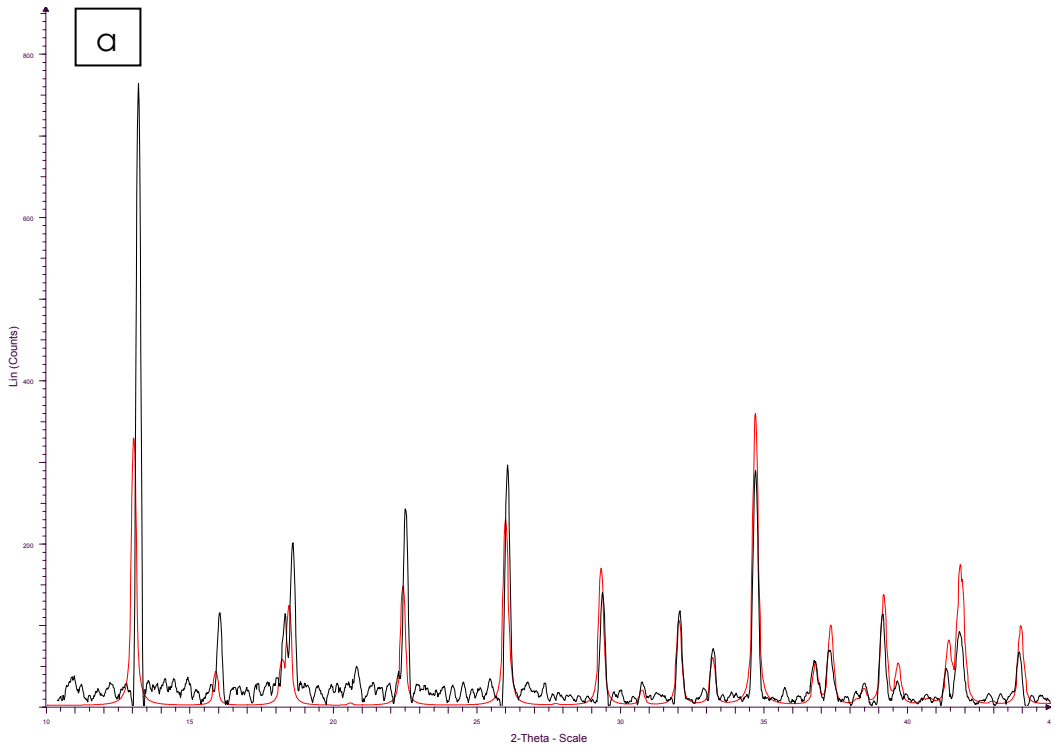

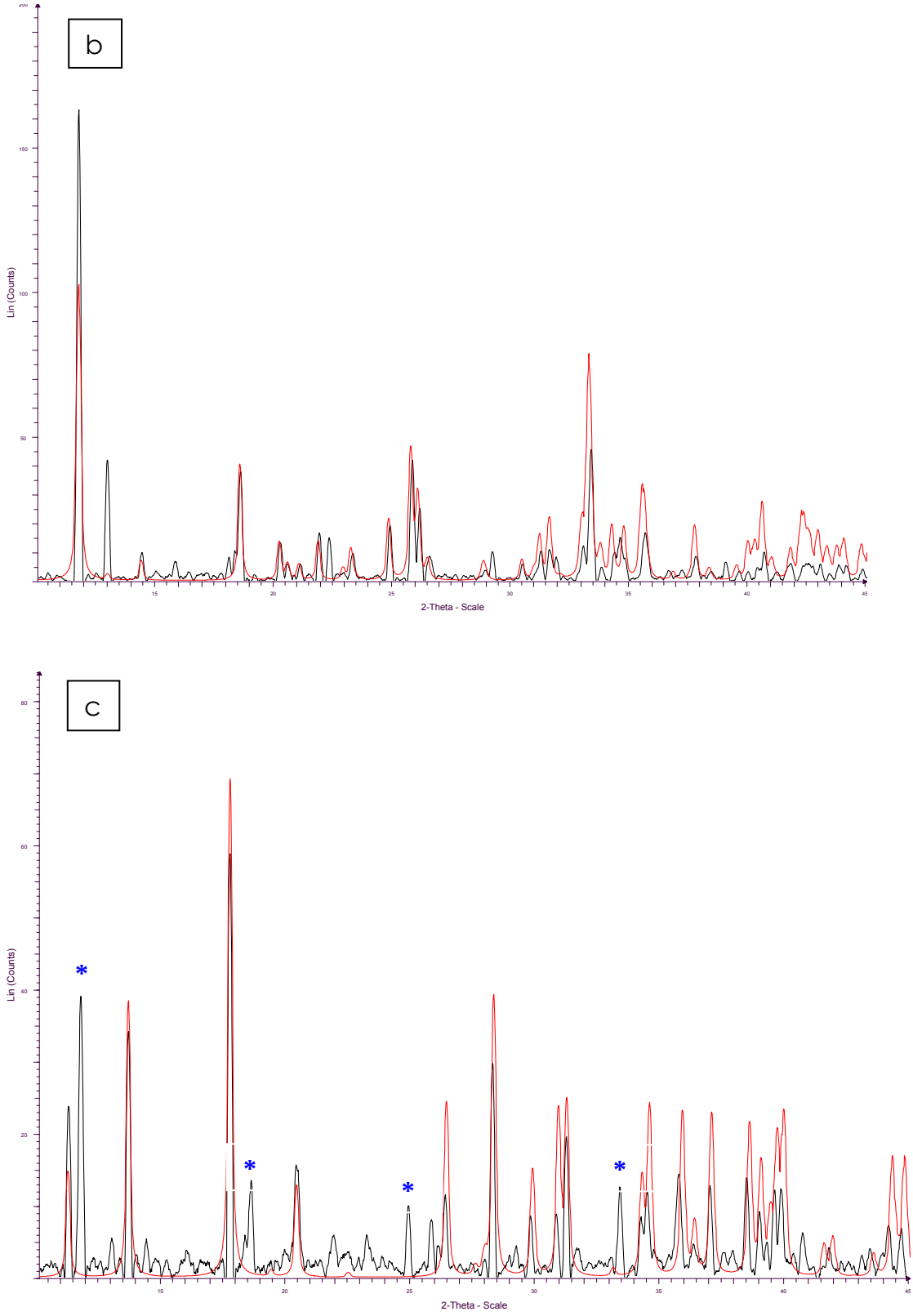

Figure 1. X-ray powder diffraction diagrams (black: measured diffractograms, red: calculated values) of UP_2S_6, UP_2S_7 and $U(P_2S_6)_2$; asterisks indicate impurities.

$U(P_2S_6)_2$ (III). $U(P_2S_6)_2$ (Figure 4) was initially synthesized from a sodium polysulfide flux with the formal composition $NaUP_5S_{15}$. A 500 mg mixture of sodium sulfide, uranium metal, phosphorus pentasulfide and sulfur with the molar ratio 1:2:5:4 was sealed in an evacuated quartz tube with an outer diameter of 1 cm and annealed in a programmable tube furnace at 130°C for ten hours. The sample was heated at a rate of 1°C/min up to 700°C and kept at this temperature for seven days; subsequently, it was cooled to room temperature during one week. The product consisted of dark red blocks embedded in a dark red glassy matrix, which could be removed by treating the regulus with a mixture of dry methanol and carbon disulfide (20:1). A single-phase sample of $U(P_2S_6)_2$ was obtained from a 500 mg mixture of uranium metal, P_2S_5 and sulfur with the ratio 1:2:2 using the same reaction conditions. The yield of the dark red crystalline material was about 90% based on the initial metal content, as evidenced by the X-ray powder diffraction diagram given in Fig. 1c.

$U_3(PS_4)_4$ (IV). $U_3(PS_4)_4$ (Figure 5) was synthesized from a sodium polysulfide flux with the formal composition $NaU_2P_3S_{18}$. A 500 mg mixture of sodium sulfide, uranium metal, phosphorus pentasulfide and sulfur with the molar ratio 1:4:3:20 was sealed in an evacuated quartz tube with an outer diameter of 1 cm and annealed in a programmable tube furnace at 130°C for ten hours. The sample was heated at a rate of 1°C/min up to 700°C and kept at this temperature for 7 days; subsequently, it was cooled to room temperature within the period of one week. The product consisted of dark red blocks embedded in a dark red glassy matrix, which could be removed by treating the regulus with a mixture of dry methanol and carbon disulfide (20:1). Attempts to prepare $U_3(PS_4)_4$ using a stoichiometric mixture of the educts were not successful.

Physical measurements

Powder X-ray diffraction. Samples in the system U-P-S were characterized using a Siemens D5000 powder diffractometer with a CuK_α source. The obtained powder patterns were indexed using theoretical powder patterns of **I-IV** calculated with the POWDERCELL[15] program.

Magnetic susceptibility measurements. The magnetic susceptibilities of the compounds UP_2S_6, UP_2S_7 and $U(P_2S_6)_2$ were measured between 4 and 300 K at a magnetic field (*H*) of 10 kOe using a MPMS Quantum Design SQUID magnetometer. Samples were ground to a fine powder to minimize possible anisotropic effects and loaded into PVC containers. Corrections for the diamagnetism of the PVC sample container were made by measuring the magnetic response of the empty container under identical conditions. Measurements at different field strengths confirmed that ferromagnetic impurities were absent. The diamagnetic correction was estimated from Pascal's constants to be 161.6 * 10^{-6} cm^3 mol^{-1} (UP_2S_6), 176.6 * 10^{-6} cm^3 mol^{-1} (UP_2S_7) and 304.2 * 10^{-6} cm^3 mol^{-1} ($U(P_2S_6)_2$).[16]

Infrared spectroscopy. FT-IR spectra (400-2000 cm^{-1}, ≈ 5 cm^{-1} resolution) were recorded on a FT-IR spectrophotometer (2030 Galaxy FT-IR, Mattson Instruments) equipped with a TGS/PE detector and a silicon beam splitter. The samples were finely ground with dry CsI, and pressed into transparent pellets.

Raman spectroscopy. Raman spectra (80-870 cm^{-1}) of freshly cleaved single crystals were obtained by means of a LabRAM HR 800 (Jobin Yvon, Horiba). This notch filter-based spectrometer system was equipped with an optical microscope (Olympus BX 41) and a Si-based, peltier-cooled charge coupled device (CCD) detector. Spectra were excited with the 632.8 nm emission of a He-Ne laser.

Semiquantitative microprobe analysis. Semiquantitative microprobe analysis was performed in a Zeiss DSM 962/Philipps PSEM 500 scanning electron microscope equipped with a KEVEX energy dispersive spectro-

scopy detector. Data acquisition was performed with an accelerating voltage of 20 kV and a 1 min accumulation time.

Crystal structure determination. The crystal structures were determined from single crystal X-ray diffraction data. Single crystals were selected from the reaction mixture, embedded in a thin film of epoxy glue and fixed at the tip of a glass fiber on a Bruker SMART CCD diffractometer equipped with a monochromated MoK_α source (λ= 0.71073 Å) and a graphite monochromator. The crystal to detector distance was 5 cm. Crystal decay was monitored by recollecting 50 initial frames at the end of the data collection. Data were collected by a scan of 0.3° in ω in groups of 600 frames at φ settings of 0°, 120° and 240°. The exposure time was 30 s/frame. The collection of the intensity data was carried out with the SMART program.[17] Cell parameters were initially calculated from reflections taken from approximately 30 frames of reflections. The final lattice parameters were calculated from all reflections observed in the actual data collection. The data from the data collections were processed using the SAINT[18] program and corrected for absorption using SADABS.[19] A summary of the experimental and crystallographic data is given in Table 1.

The structures were solved using direct methods, which revealed the atomic positions and refined using the SHELXTL 5.1 program package.[20] The final refinements were carried out on F_O^2. Atomic scattering factors for spherical neutral free atoms were taken from standard sources and anomalous dispersion corrections were applied.[21] Calculations performed at an intermediate stage in which the relative positional occupancies were refined, revealed a fractional occupancy of only 50% for the position U2 in $U_3(PS_4)_4$, but did not indicate any nonstoichiometry.

The final coordinates and equivalent isotropic temperature factors of all atoms are given in Tables 2, 4, 6 and 8.

Results and discussion

Crystal structures

UP_2S_6 crystallizes in a 3D network structure[12b] (ZrP_2S_6 structure type,[22] $P4_2/m$, Z = 2). Figure 2a depicts the unit cell in a view along ***c***, a view of the cell along ***a*** is given in Figure 2b. Each end of the $P_2S_6^{2-}$ group acts as a bidentate ligand for two uranium atoms with one S atom (S1) coordinated to one U atom and the second S atom (S2) linked to both uranium positions. As a result, the U atoms are square-antiprismatically coordinated by eight sulfur atoms belonging to four $P_2S_6^{4-}$ anions.

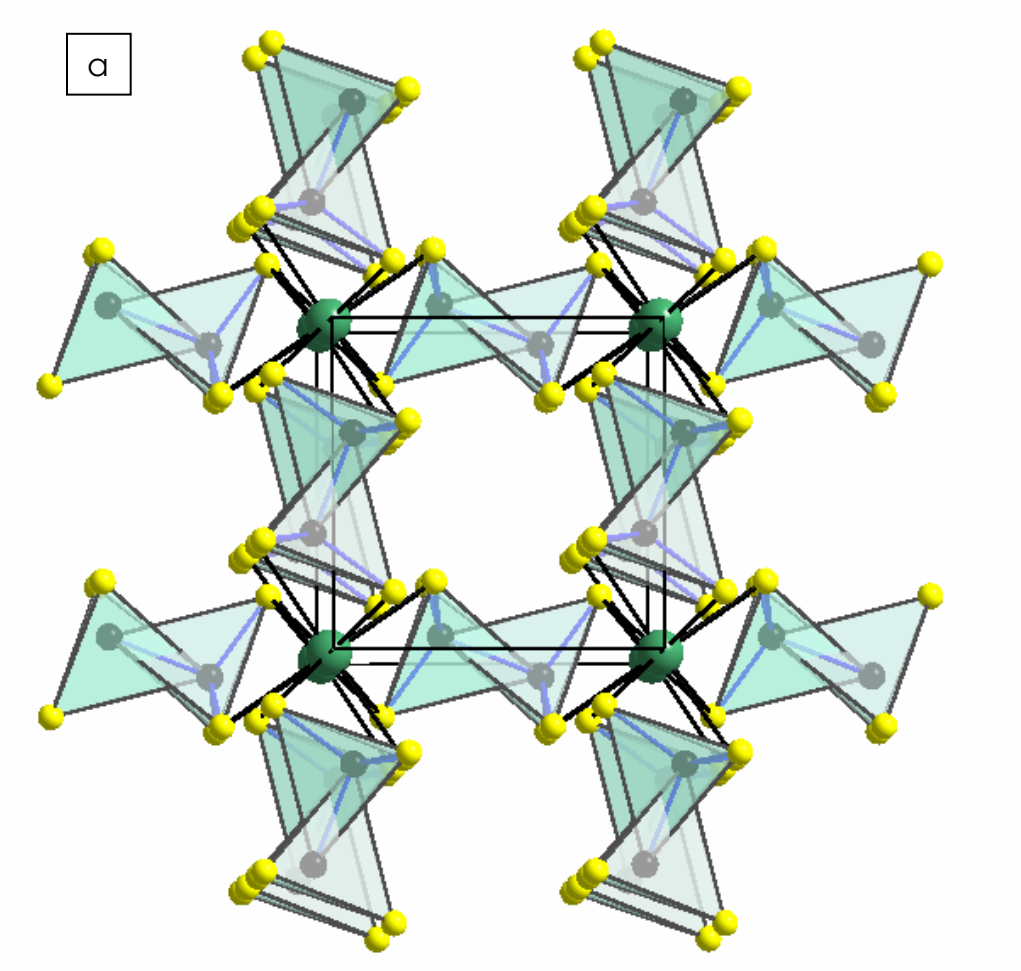

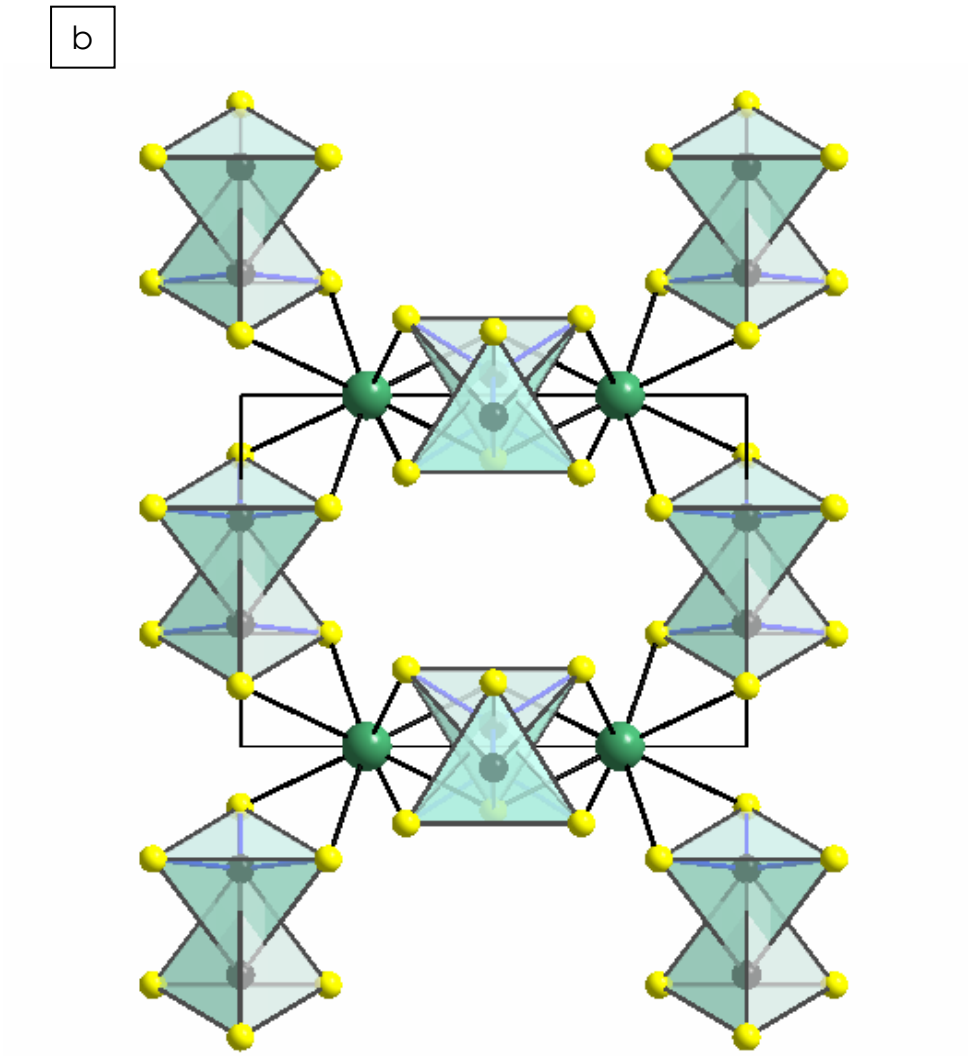

Figure 2. (a) Crystal structure of UP_2S_6, view along the *c* axis. (b) Crystal structure of UP_2S_6 in a view along the *a* axis. Green spheres represent the uranium atoms, black spheres the phosphorus atoms and yellow spheres the sulfur atoms.

As illustrated in Figure 2b, this leads to the formation of $[(U_2(P_2S_6)_6]$ units, similar to those encountered in the $[(U_2(PS_4)_6]^{10-}$ anions in $K_5U(PS_4)_3$,[11a] where the $U_2(PS_4)_2$ core is terminated on each side by two PS_4^{3-} ligands in a bidentate fashion. The U-S distances between 2.748(2) and 2.973(2) Å are comparable with those in other uranium sulfides, the P-P separation

of 2.221(5) Å and the P-S bond lengths of the $P_2S_6^{4-}$ ligands (ranging between 2.014(2) Å and 2.038(4) Å) are unexceptional. The SPS angles of 112.1(1) and 114.1(2)° and the SPP angles between 104.4(2) and 106.6(1)° indicate a slightly distorted staggered conformation (*D_{3d}*) of the anion.

UP_2S_7. The structure of UP_2S_7 is closely related to the ZrP_2S_7 structure,[23] which was described originally in the monoclinic space group *C2/c*. The present crystal data for UP_2S_7, however, indicated a higher symmetry[24] and the structure was solved in the orthorhombic space group *Fddd*. The Hamilton test[25] showed no significant decrease of the *R* value for a structure solution in *C2/c*, so the higher orthorhombic symmetry should provide a better description of the structure.

In the structure of uranium pyrothiophosphate, UP_2S_7, the U atoms are coordinated by four P_2S_7 units with a crystallographically imposed C_2 symmetry in a distorted square antiprismatic fashion. Each PS_3 end of the $P_2S_7^{4-}$ ligand coordinates two metal atoms in such a way that one S atom (S1) is linked to two U atoms, while the remaining two S atoms (S2 and S3) are each coordinated to one uranium atom ($d_{U\text{-}S}$ = 2.801(3)-2.939(3) Å). Figure 3 shows a perspective view of a $U_2(P_2S_7)_6$ portion of the structure. The P-S distances (2.009(4)-2.123(3) Å) and the bridging PSP angle (106.5(2)°) of the pyrothiophosphate group are unexceptional, whereas the SPS angles (101.5(2)-117.7(2)°) indicate some deviation from the ideal tetrahedral angle.

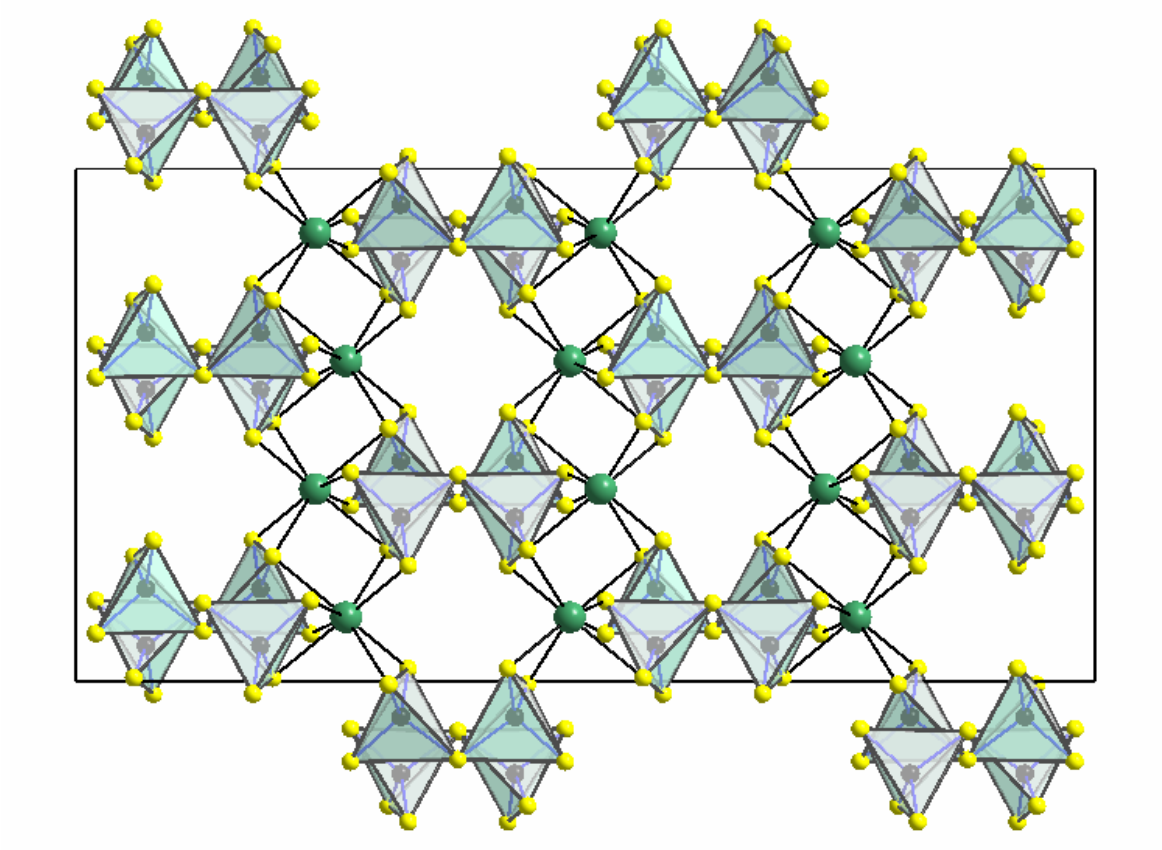

Figure 3. Crystal structure of UP_2S_7, viewed along the *a* axis.

$U(P_2S_6)_2$. The structure of $U(P_2S_6)_2$ contains three interpenetrating diamondoid frameworks, based on elongated adamandoid cages, as illustrated in Figure 4. The shortest vector relating the three independent networks is 9.75 Å. The U atoms are coordinated by eight S atoms of four bidentate P_2S_6 ligands in a pseudotetrahedral fashion. The metal atoms are located on fourfold inversion sites and display crystallographically imposed D_{2d} coordination symmetry. Each uranium atom has a slightly distorted square antiprismatic coordination environment (the distortion being caused by S...S repulsion between the P_2S_6 units) with S(2)-U-S(3) angles of 69.96(3)° for the S atoms of each P_2S_6 ligand. The U-S and P-S distances are unexceptional, selected values are compiled in Table 6. The S(2)-P-S(3) bite angle of 109.90(8)° and the bridging U-S-P angles of 88.47(5)° and 90.23(5)° are compatible with the presence of essentially

planar US_2P rings. The P-U-P angles of 86.54(1)° (2x) and 122.02(1)° (4x) indicate a compression of the $U(S_2PS_2)_4$ "pseudotetrahedron" in harmony with a *c/a* ratio of 0.76.

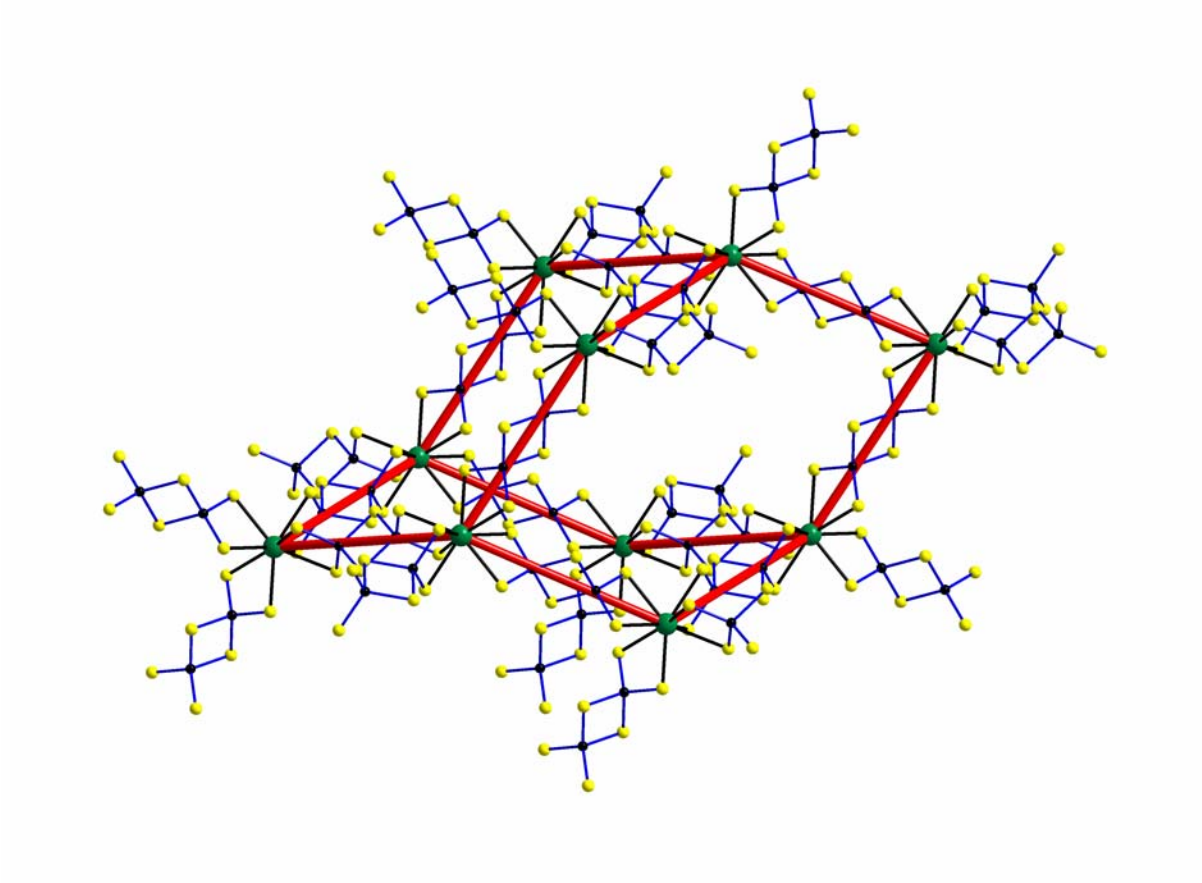

Figure 4. Single adamantane-type network in $U(P_2S_6)_2$.

$U_3(PS_4)_4$. In the crystal structure of $U_3(PS_4)_4$ ($I4_1/acd$, Z = 2) each U atom is coordinated by the sulfur atoms of four bidentate PS_4 ligands in a slightly distorted square antiprismatic fashion. The uranium-sulfur bond lengths range from 2.863(2) to 3.122(2) Å, the P-S distances in the ligand are 2.037(2) and 2.039(2) Å with SPS angles between 104.53(7) and 111.77(7)° corresponding to a slightly distorted T_d symmetry of the PS_4 unit. The structure was initially solved as UPS_4 ($PrPS_4$ structure type[26]) however, unusually high thermal displacement factors for U2 indicated a site disorder for this atomic position. Further refinements showed that only 50% of the U2 sites in the cell are occupied, resulting in the stoichiometry $U_3(PS_4)_4$ with tetravalent metal atoms.

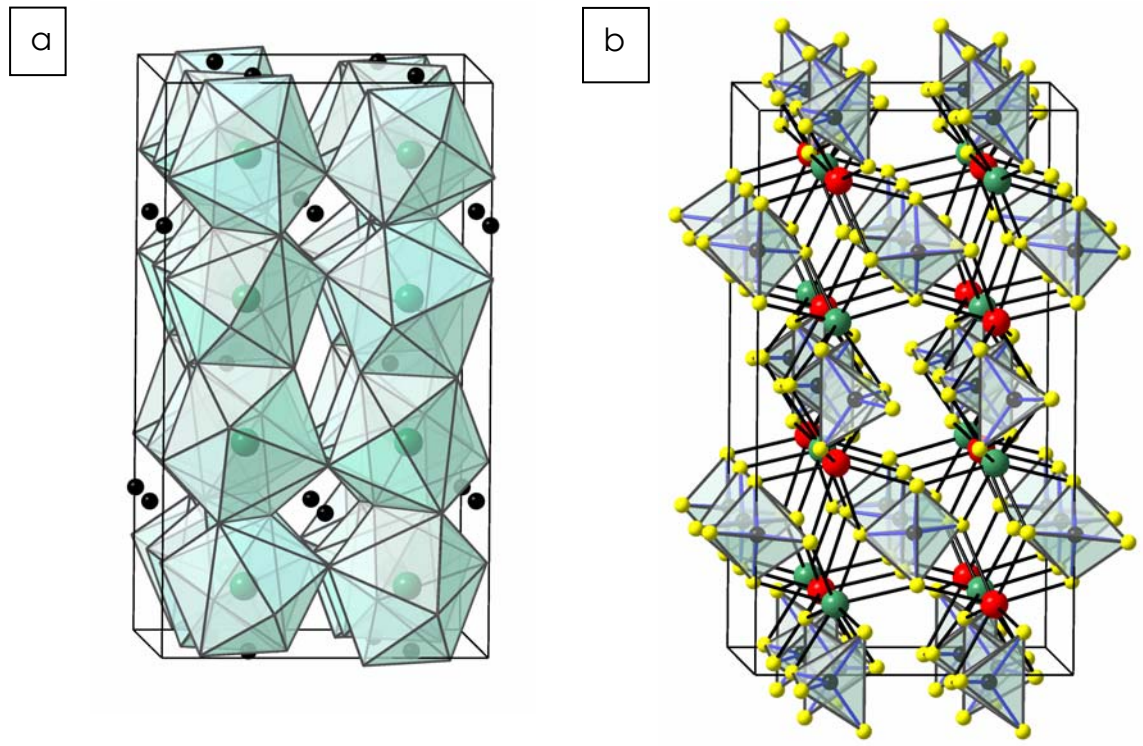

Figure 5. (a) Arrangement of the US_8 polyhedra in the crystal structure of $U_3(PS_4)_4$, viewed along the *a* axis. P-S bonds omitted for clarity.
(b) Crystal structure of $U_3(PS_4)_4$, viewed along the *a* axis. Red spheres represent uranium sites with 50% occupancy.

All reported orthothiophosphates crystallizing in the $PrPS_4$ structure type[27-29] show this systematic discrepancy between the temperature factors of the atoms on the two metal sites, which might indicate a site disorder for these compounds. However, the structure does not show a lattice distortion due to the disorder, but a high symmetry tetragonal space group with statistically occupied M2 positions is formed.

Discussion

Framework formation. It is instructive to study the linkage of the U atoms and the thiophosphate ligands in this group of compounds. The simplest example is UP_2S_6. In the unit cell, the U atoms are arranged in a regular rectangular pattern (*p2mm*) in the *ab* and *ac* planes. Each U atom is coordinated in a pseudotetrahedral fashion by four thiophosphate ligands. The $P_2S_6^{4-}$ anions in turn act as square-planar connectors crosslinking four coplanar metal sites. Therefore, the UP_2S_6 structure may be considered a stuffed analogue of the *anti*-PtS structure type,[30] where the center of the $P_2S_6^{4-}$ group with the coordinates (0, 0, 1/4) is located at the position of the Pt atom in PtS. The *c*/*a* ratio of 1.433 is significantly different from that in PtS because of the lateral extension of the square planar connector. In Figure 2a, $[(P_2S_6)U_4]$ squares are normal to the projection plane, forming mutually perpendicular $[(P_2S_6)U_2]$ strips connected through common U atoms. The U atoms are situated in distorted $P_2S_6^{4-}$ anion tetrahedra, and it is clear that this geometry is a compromise between the pseudotetrahedral coordination of the U atoms and the space and coordination requirements of the $P_2S_6^{4-}$ groups. A remarkable feature is of this compound is the square planar connectivity of the $P_2S_6^{4-}$ ligand.

The UP_2S_7 framework is built up from four connected metal centers and four connecting ligands. As in UP_2S_6, the U atoms exhibit a pseudotetrahedral connectivity. Replacing the $P_2S_7^{4-}$ anion by a pseudo ion at the center of gravity of the pyrophosphate group reveals that the $P_2S_7^{4-}$ unit also acts as a tetrahedral connector, i. e. the UP_2S_7 structure may be described as an analogue of the ZnS structure type. Since the $P_2S_7^{4-}$ ligand is highly elongated, the *c*/*a* ratio increases to 1.93. Furthermore, the presence of a rod-like connector reduces the space filling of the UP_2S_7 structure significantly. However, the open voids of the structure are not large enough to allow the formation of an interpenetrating network.

$U(P_2S_6)_2$ is a novel member of the family of super-diamond networks in „coordination“ polymer chemistry. There is little precedence in metal/chalcogenide systems; the structure of $U(P_2S_6)_2$ is, however, closely related to that related to that of methane tetraacetic acid.[31] Inter-penetration arises by the necessity to fill empty space inside the large cages. In an undistorted (cubic) diamond network each adamantane-type unit possesses three mutually perpendicular inversion axes running parallel to the axes of the unit cell. The interwoven diamondoid networks are arranged in such a way that the nodes of the independent frames are oriented along these inversion axes with identical interframe separations.

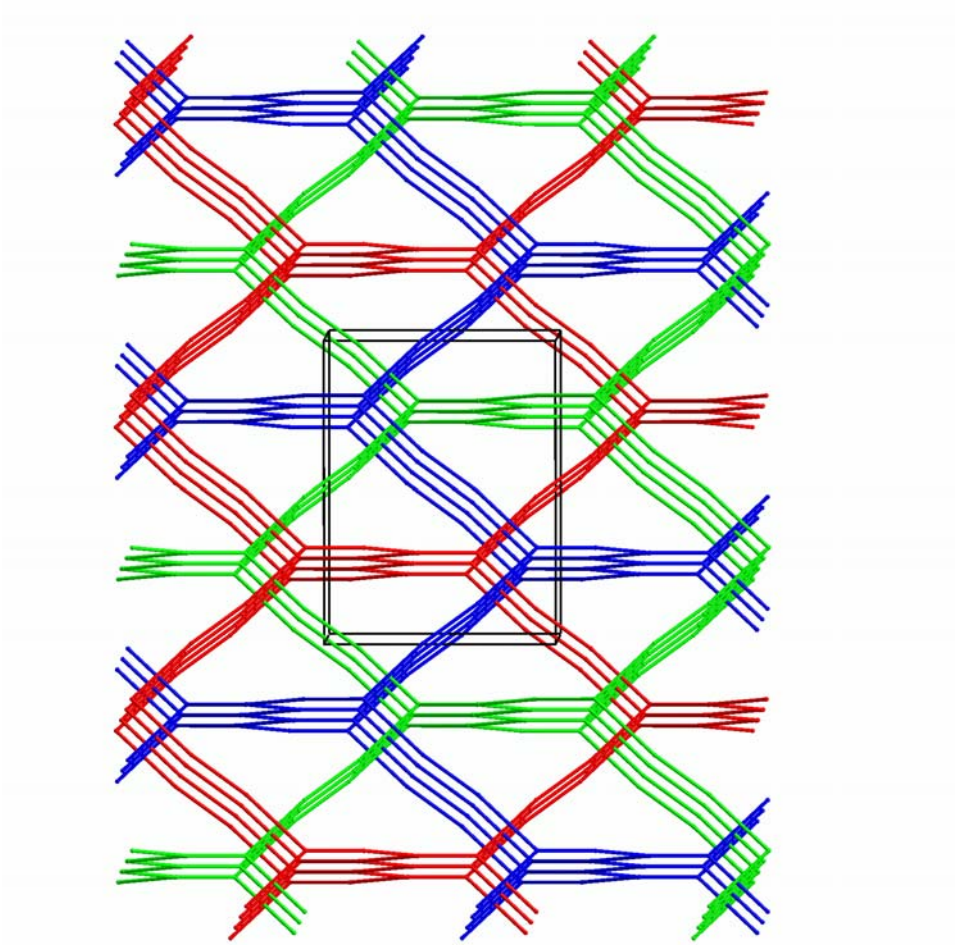

Figure 6. A schematic view of the three equivalent interpenetrating diamondoid frameworks in $U(P_2S_6)_2$. The P_2S_6 groups are represented by rods connecting the P atoms of the P_2S_6 ligands for clarity.

This is illustrated in Figure 6 in a schematic fashion for $U(P_2S_6)_2$. Here the frames of two further independent nets are located between the upper and lower frame. Furthermore, it is apparent that the frameworks are distorted in such a way that the adamantane-type units are elongated along one of the S_4 axes; this reduces the symmetry of the structure from cubic to tetragonal.

The distance between the uranium atoms in the 3D framework structure determines the size of the adamantane-type cage. In order to optimize space filling by stuffing empty space in the structure, independent frameworks undergo „self-assembly" in such a way as to fill each other's empty cages and tunnels. As an example, Si...Si distances of 6.8 Å between the tetrahedral centers in $Si(NCN)_2$[32] are compatible with two interpenetrating diamondoid networks, whereas U...U separations of 9.75 Å in $U(P_2S_6)_2$ require three interpenetrating frameworks for optimum space filling. Rod-ligands with exceptional length such as 4,4´-biphenyldicarbonitril (BPCN) in $[Ag(BPCN)_2]PF_6$[33] can lead to the formation of a nine-fold interwoven diamondoid network with distances of 16.42 Å between the metal centers.

Similarly as for the other three uranium thiophosphates, UP_2S_6, UP_2S_7, and $U(P_2S_6)_2$, the structure of $U_3(PS_4)_4$ can be derived from an elementary A_mB_n structure type. The pseudotetrahedral coordination of the U atoms in $U_3(PS_4)_4$ can be visualized by replacing the PS_4^{3-} anions with single pseudoanions. Each of these pseudoanions resides in a square planar coordination, as shown in Figure 7. The resulting framework structure can be described as a superstructure of the *anti*-PtS structure type, which can be derived from the parent structure by doubling the axes and leaving 50% of the atom sites marked red unoccupied (Figure 5b). A comparison of the *c/a* ratios found for $U_3(PS_4)_4$ (1.777) and PtS (1.761) indicates that the PS_4 unit can be described approximately as a spherical entity, whose introduction into the lattice leads only to a minimal distortion of the *anti*-PtS structure.

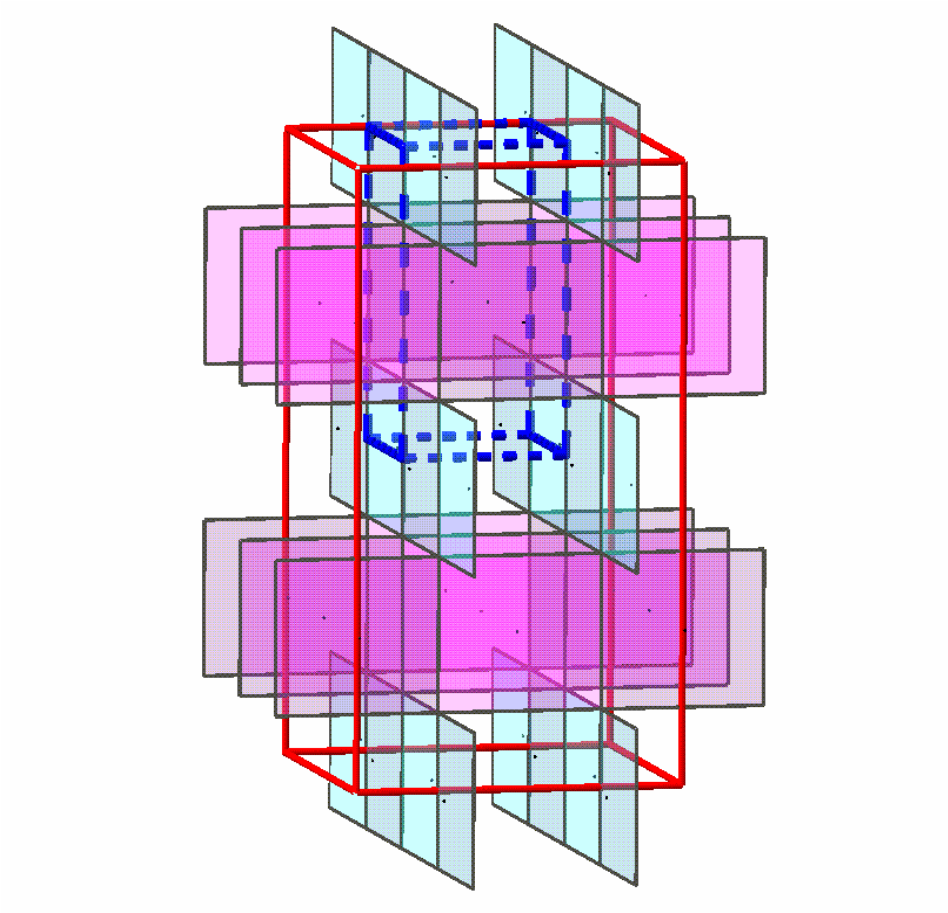

Figure 7. Relation between the PtS structure type (blue unit cell edges) and the $U_3(PS_4)_4$ superstructure (red unit cell edges).

The requirements of both large cavities and linear connectors in the same structure explains the absence of interpenetrating networks in UP_2S_6, UP_2S_7 and $U_3(PS_4)_4$. In the crystal structures of UP_2S_6 and $U_3(PS_4)_4$, the rigid arrangement of the anionic units, which are, formally, two-dimensional connectors between four cations arranged in one plane, prevents the formation of a second framework. In the compound UP_2S_7, non-linear anionic units are present; therefore the pseudotetrahedral coordination sphere of the uranium atoms in the crystal structure is highly deformed. The resulting network contains large pores but due to their shape (3.48 * 16.68 Å) the cavities cannot accommodate additional atoms.

Interpenetration, which can be observed in the crystal structure of $U(P_2S_6)_2$, arises by the necessity to fill empty space inside of large cavities.

The distance between the central atoms, i. e. the length of the rigid ligand group in a 3D framework structure determines the size of the cage. In the compound $U(P_2S_6)_2$, which contains cations with a pseudo-tetrahedral environment created by the quasilinear $P_2S_6^{2-}$ connectors, adamantane-type cages with large cavities are present. In order to obtain optimum space filling, three interpenetrating frameworks are formed. The number of interwoven identical units is dependent on the length of the connecting ligand, for example, in $Si(NCN)_2$,[32] Si...Si distances of 6.8 Å are compatible with two interpenetrating frameworks, while a metal-metal distance of 16.42 Å in $[Ag(BPCN)_2]PF_6$,[33] which contains the 4,4´-biphenyldicarbonitril (BPCN) ligand, leads to the formation of a nine-fold interwoven diamondoid network.

Bonding of the thiophosphate connecting groups. A characteristic structural feature of the title compounds is the bonding mode of the thiophosphate anions. The structural diversity of metal chalcogenides is related to the broad variety of polyanions. Some of them are depicted in scheme I, although this list is not exhaustive at all. In conjunction with the various possible bonding modes (see scheme II) of the polydentate ligands, this leads to a complex and fascinating structural chemistry of the metal chalcogenide family. In order to make it easier to classify and describe the relevant structures, the bonding modes of the three simplest thiophosphate ligands, PS_4^{3-}, $P_2S_6^{4-}$, and $P_2S_7^{4-}$ are examined and compared.

Scheme I

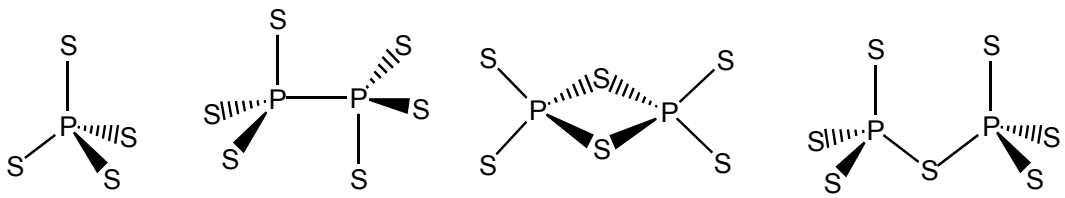

PS_4^{3-} $P_2S_6^{4-}$ $P_2S_6^{2-}$ $P_2S_7^{4-}$

The bonding mode of a thiophosphate (and any other chalcogenometalate) group can be organized according to the number of sulfur atoms connected to metal atoms, i. e. in is possible to distinguish between 4, 3, 2 and 1 connected fragments (scheme II). Any thiophosphate species in scheme I can be 3, 2, and 1 connected at its PS_3 ends. Furthermore, the number of bonding possibilities is increased by symmetrical and unsymmetrical coordination of the PS_3 termini. In general, high connectivity and multiply bridging chalcogen atoms favor higher condensed structures as found in compounds of the coinage or heavy main group metals. Bonding mode **I** has not been observed for chalcogenophosphates so far, but thiophosphates such as $AgZnPS_4$[34] contain entities with fragment **II**. Bonding mode **III** is typically encountered in early transition metal compounds such as $AgTi_2(PS_4)_3$,[35] $ATi_2(PS_4)_3$,[36,37] and $K_3Ti_2P_5S_{18}$[38] whose structures contain interpenetrating $Ti_2(PS_4)_3^-$ networks or infinite one-dimensional $[Ti_2(P_2S_7)_2(PS_4)]^{3-}$ anion chains, whereas mode **IV** is found in $K_3Bi(PS_4)_2$.[39] The 4 connected fragment **V** can be found in the crystal structures of $Cs_3Bi_2(PS_4)_3$[39] and $K_2La(P_2S_6)_{0.5}(PS_4)$.[40] Solids containing the 4 connected fragments **VI** and **VII** have not been reported, but **XII** and **XIII**, the 3 connected counterparts of **V** and **VII**, are common motifs in the structures of $K_5U(PS_4)_3$,[11a] $K_2MP_2S_7$[41,42] and $K_3M_2(PS_4)_3$ (M = V, Cr).[43,44] Connectivities of type **XII** are also encountered for the PS_3 termini in $KBiP_2S_7$.[39] **VIII** and **IX**, the 3 connected counterparts of **I** and **II**, are still waiting to be found. The 2 connected mode **XIV** is characteristic for terminating groups in discrete chalcogeno anions. Soluble prototypes with this type of MQ_4^{2-} (M = Mo, W) coordination are $[M'(MS_4)_2]^{2-}$ (M' = Fe, Co, Ni, Pd, etc.),[44,45] whereas $K_4V(S)(PS_4)_2$[37] with discrete $[V(S)(PS_4)_2]^{4-}$ anions is one recent example from the solid state.

Scheme II

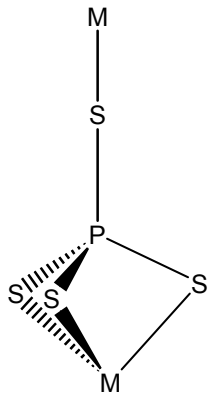

I

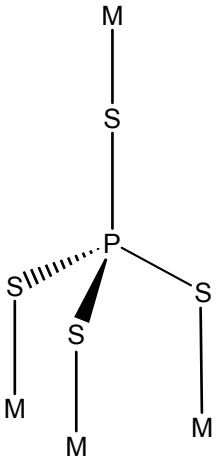

II

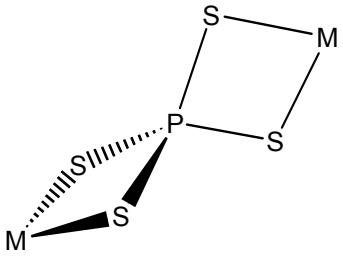

III

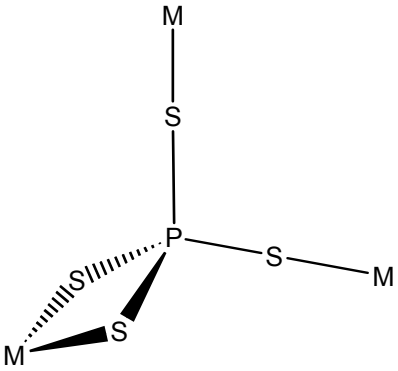

IV

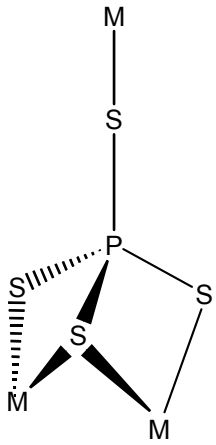

V

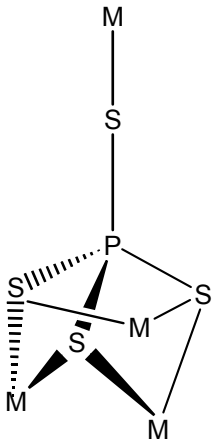

VI

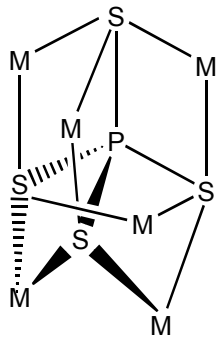

VII

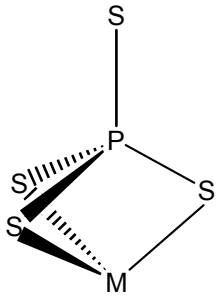

VIII

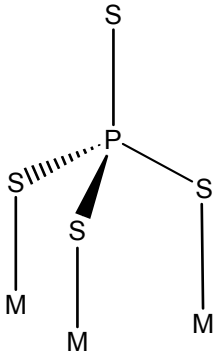

IX

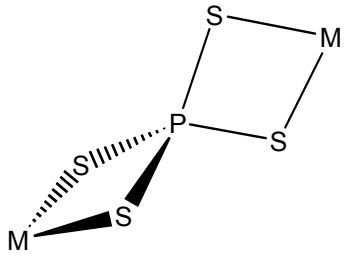

X

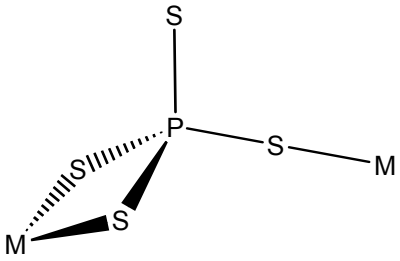

XI

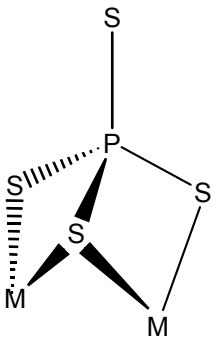

XII

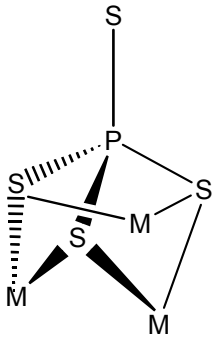

XIII

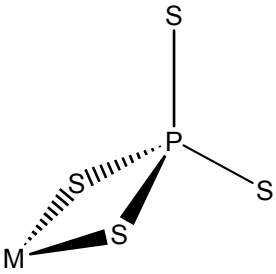

XIV

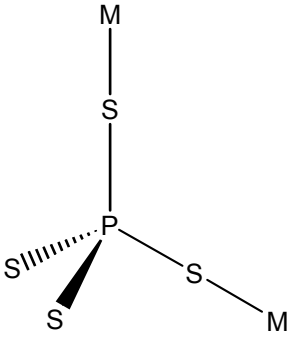

XV

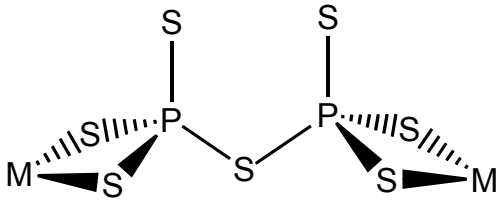

XVI

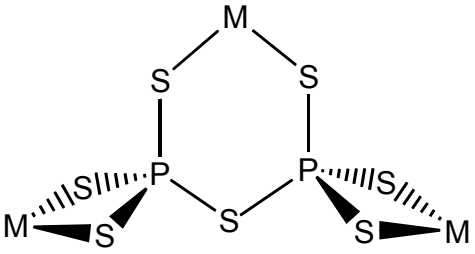

XVII

Several compounds containing $P_2S_6^{2-}$ and $P_2S_7^{4-}$ groups illustrate the seemingly unpredictable coordination modes of the anions. In the structure of $KCrP_2S_7$[46] the PS_3 termini are symmetrically bonded in mode **XVII**, the chain compound $K_3Ti_2P_5S_{18}$[38] contains a pyrothiophosphate in the type **XVI** geometry. Except for uranium, metals with high coordina-

tion numbers (e. g. lanthanides) or the heavy main group metals favor unsymmetrical coordination geometries.

Network formation requires the presence of high symmetry branching units such as $Ti(PS_4)_3$ (3-fold)[36] or $Nb_2(S_2)_2(PS_4)_4$ (4-fold)[47] combined with connecting elements having linear, tetrahedral or square planar coordinating abilities (e. g. PS_4^{3-}, $P_2S_6^{2-}$/$P_2S_6^{4-}$ or $P_2S_8^{4-}$ groups). Typical examples are the compounds **I**-**IV**, $NaTi_2(PS_4)_3$,[36] $Ag_2NbTi_3P_6S_{25}$,[35] $ANb_2P_2S_{12}$,[47] $CsMP_2S_8 \equiv Cs_2M_2(PS_4)_2(P_2S_8)$ (M = Sn, Ti)[48] and $CsTa_4P_3S_{19}$.[49]

Vibrational spectroscopy

UP_2S_6. The Raman spectrum of the compound UP_2S_6 displays six signals in the 150-600 cm^{-1} range, corresponding to the expected Raman active modes for the ethane-like $P_2S_6^{4-}$ anion with D_{3d} symmetry.[50] The sharp absorption at 385 cm^{-1} represents the dominant symmetrical P-P vibration, while the two signals at 559 and 596 cm^{-1} are the result of P-S stretching vibrations. The remaining three signals at 162, 241 and 263 cm^{-1} are tentatively assigned to different bending vibrations of the PS_3 units (see Table 10 for details).

The far-infrared spectrum (400-850 cm^{-1}) of UP_2S_6 contains three absorption bands, which were assigned to different antisymmetric stretching modes of the PS_3 units. Both the Raman and the IR data for the $P_2S_6^{4-}$ anion in UP_2S_6 are in accordance with the values reported for the compound $MnPS_3$.[51]

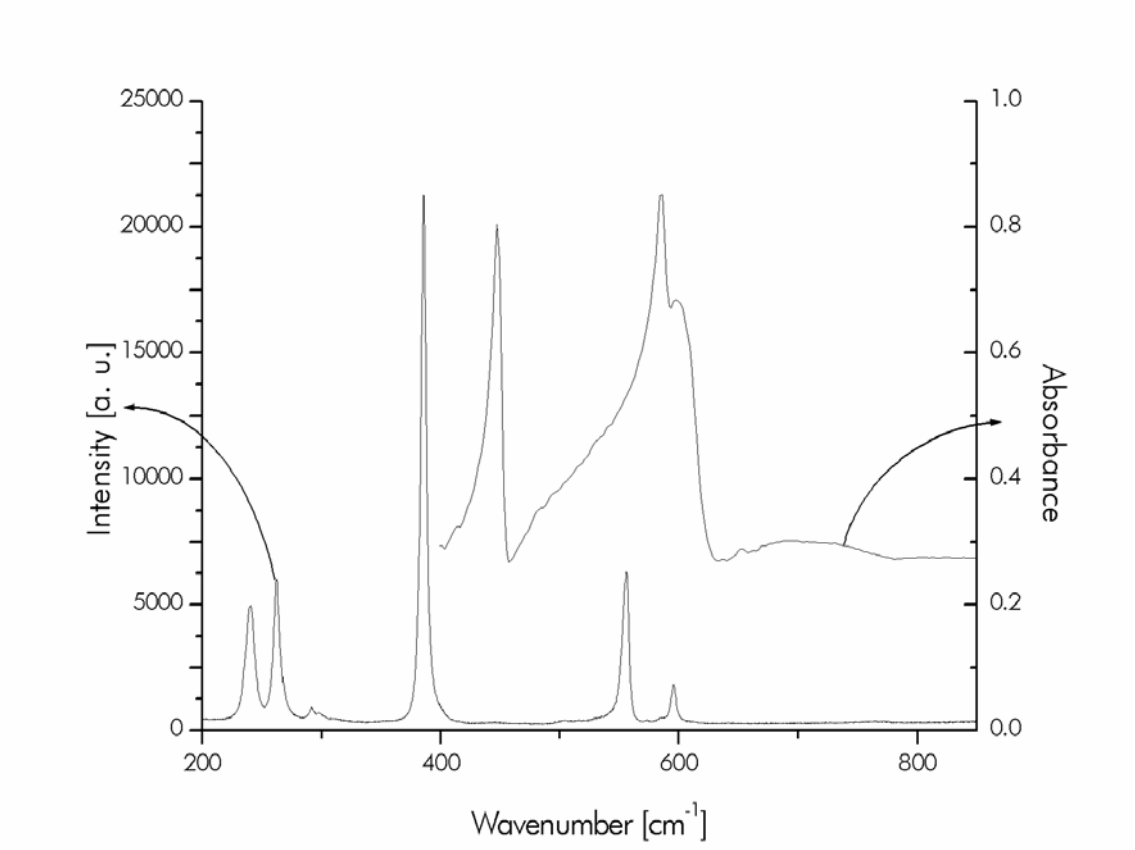

Figure 8. Room-temperature infrared and Raman spectra of UP_2S_6.

UP_2S_7. The Raman spectrum of UP_2S_7 is dominated by an intense band at 410 cm^{-1}. A closer investigation of the peak profile showed, however, that this measured signal might consist of an overlap of two independent Raman peaks at 410 and 409 cm^{-1}, respectively. These signals were tentatively assigned to symmetric vibrations of the PS_3 groups and the bridging PSP unit in analogy to the data reported for the compound $Ag_4P_2S_7$,[52] which also contains the $P_2S_7^{4-}$ anion in the C_2 conformation. The remaining weak bands are assigned to different PS_3 deformation modes, a detailed overview is given in Table 11.

The FIR spectrum of UP_2S_7 contains an intense absorption at 457 cm^{-1} from the antisymmetric PSP vibration and four weaker signals at 592, 575, 512 and 413 cm^{-1} caused by different antisymmetric vibrations of the

terminal PS_3 units. All bands were tentatively assigned by analogy to the values reported for $Ag_4P_2S_7$.[52b]

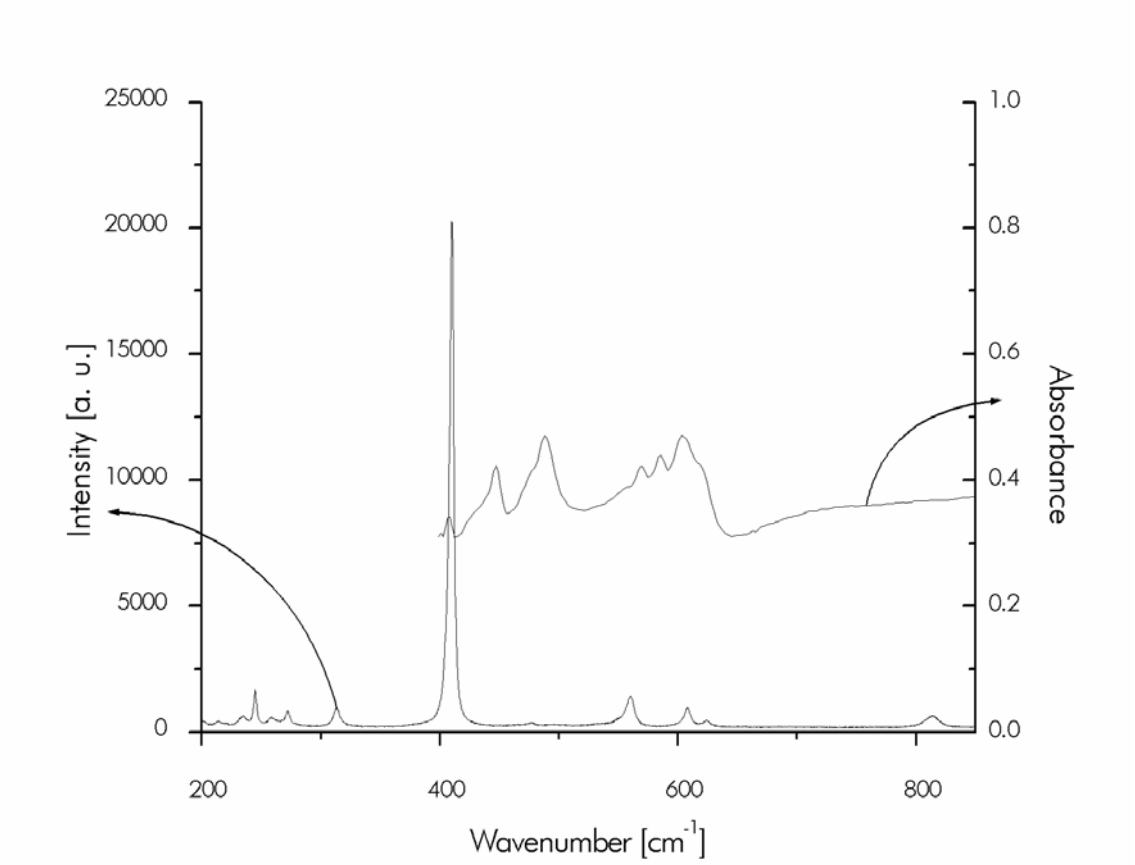

Figure 9. Room-temperature infrared and Raman spectra of UP_2S_7.

$U(P_2S_6)_2$. The Raman spectrum of $U(P_2S_6)_2$ contains two characteristic bands at 430 and 404 cm^{-1} which could be assigned to vibrations of the bridging P_2S_2 group of the $P_2S_6^{2-}$ unit (*D_{2h}* symmetry). The remaining weak signals in the Raman spectrum of $U(P_2S_6)_2$ are, as in the case of the silver thiophosphate $Ag_2P_2S_6$,[53] mostly caused by overtones or combinations. Table 12 shows further details.

The infrared spectrum of this compound displays an absorption at 403 cm^{-1}, which corresponds to a symmetric distortion of the ring, while the recorded signals at higher wavenumbers are the result of different combinations of normal modes. The vibrational spectra of $U(P_2S_6)_2$ were interpreted by analogy to $Ag_2P_2S_6$.

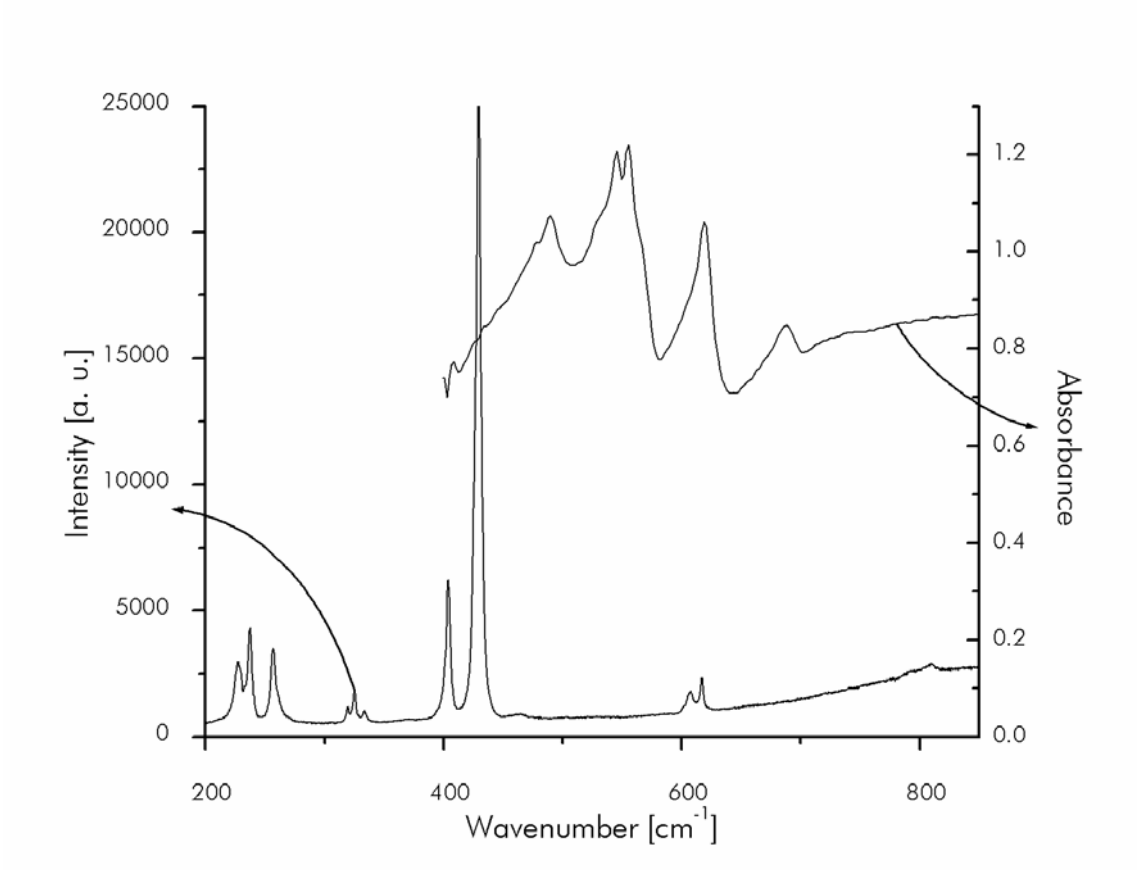

Figure 10. Room-temperature infrared and Raman spectra of $U(P_2S_6)_2$.

Magnetic behavior

Figure 11 shows the reciprocal magnetic susceptibility $1/\chi_{mol}$ for UP_2S_7, the measured magnetic moments μ for UP_2S_7, UP_2S_6, and $U(P_2S_6)_2$ are displayed in Figures 12 to 14.

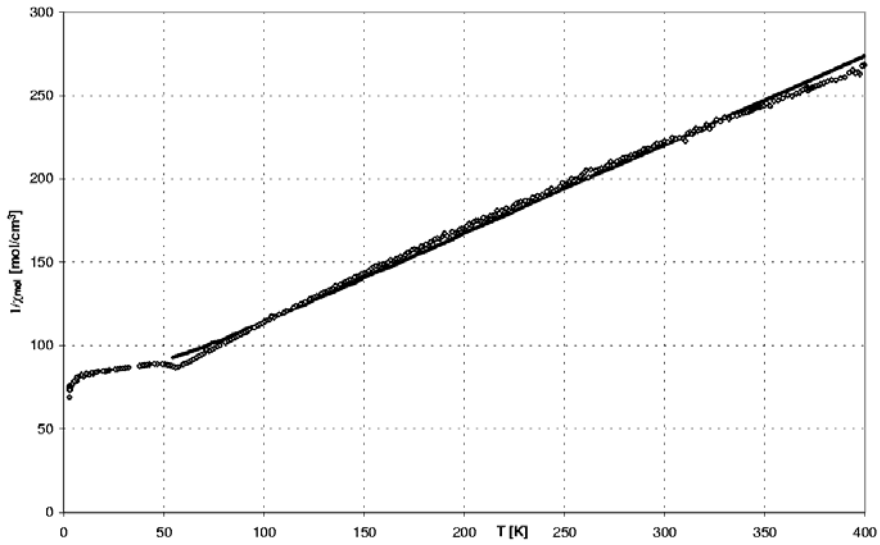

Figure 11. Comparison of measured (dots) and calculated (line) inverse magnetic susceptibilities for UP_2S_7.

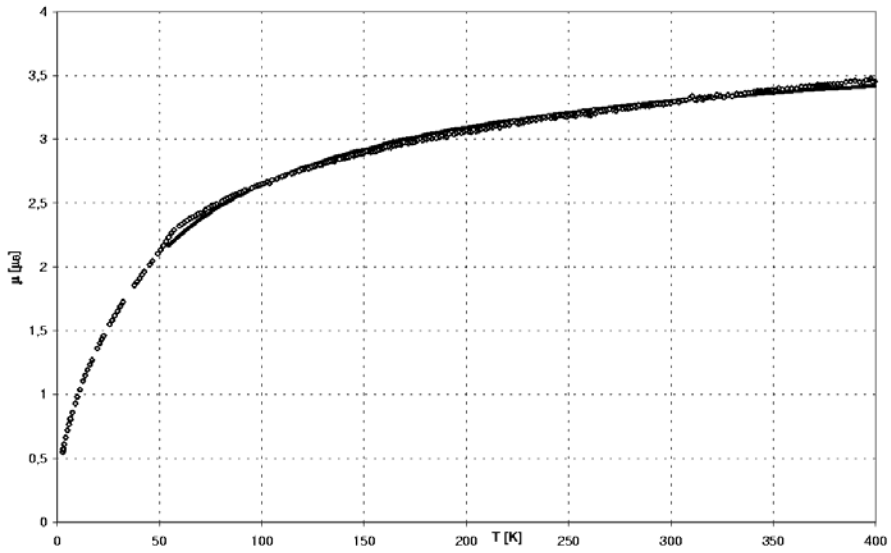

Figure 12. Comparison of measured (dots) and calculated (line) magnetic moments for UP_2S_7.

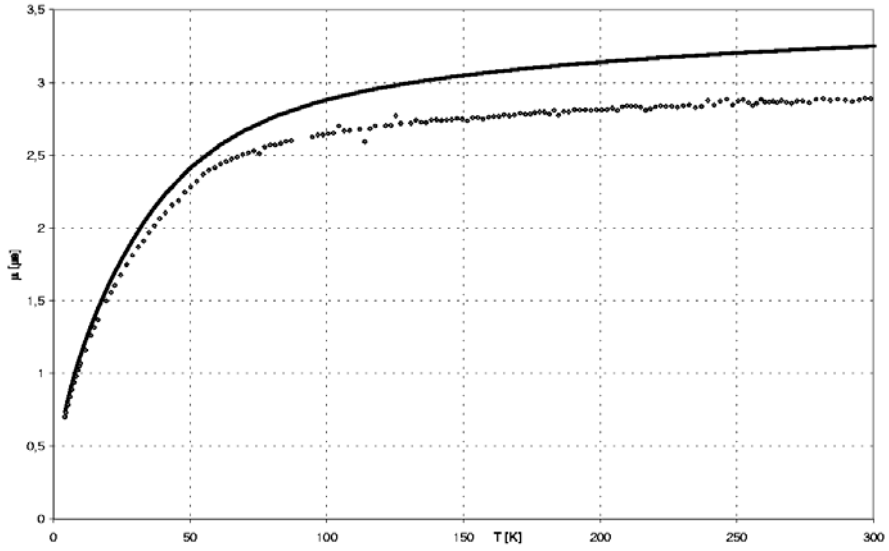

Figure 13. Comparison of measured (dots) and calculated (line) magnetic moments for UP_2S_6.

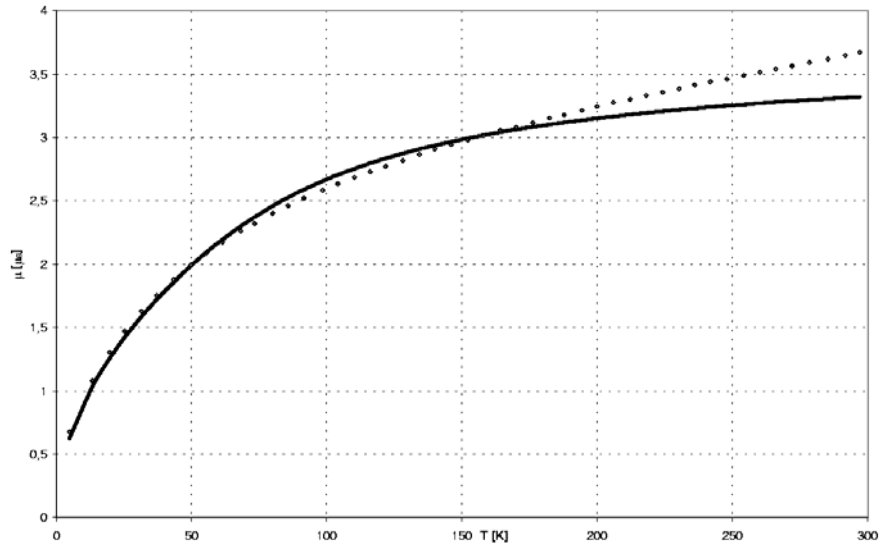

Figure 14. Comparison of measured (dots) and calculated (line) magnetic moments for $U(P_2S_6)_2$.

For the interpretation of the magnetic behavior ligand field calculations were carried out. The magnetic susceptibilities were calculated by taking into account electron-electron interaction, spin orbit coupling, and crystal field effects using the angular overlap (AO) model.[54–56] The influence of the magnetic field was described by the

magnetic field operator $\mu_B H(\hat{L} + 2\hat{S})$ (μ_B = Bohr magneton). For the calculations all 91 possible L, S, J, M_J states for the f^2-configuration of U^{4+} were considered. The electron-electron interaction parameters (F_2, F_4, F_6) and the spin orbit coupling constant (ζ) were taken from the literature[57] and are given in Table 13. The AO parameters $e_\sigma(d)$ and $e_\pi(d)$ representing σ- and π-bonding between U^{4+} and S^{2-} ions for a given distance d were obtained in the case of UP_2S_7 by fitting procedures leading to $e_\sigma(d)$ = 1124 cm^{-1} and $e_\pi(d)$ = 137 cm^{-1} with d = 2.81 Å (cf. Table 13). AO parameters $e_\sigma(d)$ and $e_\pi(d)$ for different U^{4+}-S^{2-} distances in UP_2S_7 as well as in UP_2S_6 and $U(P_2S_6)_2$ were calculated assuming a d^{-7} dependence.[58] The π–interactions for threefold bonded sulfur has been neglected setting $e_\pi(d)$ = 0 cm^{-1}, assuming sp^3 hybridization.[59,60]

For UP_2S_7, cooperative magnetic interactions had to be taken into consideration as the calculated susceptibilities χ^I_{mol} deviated strongly from the experimental ones. This has been accomplished by using the molecular field approximation according to equation (1).[56,61,62]

$$\chi^{-1}_{mol} = \left(\chi^I_{mol}\right)^{-1} - \lambda \qquad (1)$$

In (1) the molecular field constant λ represents the isotropic part of the magnetic interaction. The best agreement of the experimental and calculated data (cf. Figures 10, 11) was achieved with λ = -1.44 mol/cm^3. The negative molecular field constant indicates antiferromagnetic interactions between the U^{4+} ions. This can be explained by considering the shortest U^{4+}-U^{4+} distance of 4.54 Å in UP_2S_7. The local minimum of the inverse susceptibility around 54 K indicates the presence of an ordering temperature. Comparable values of the molecular field constant λ for U^{4+} compounds with similar ordering temperatures (T_N) are given for UOS, λ = -7 mol/cm^3, T_N = 55 K,[63,64] and UOSe, λ = 0 mol/cm^3, T_N = 100 K.[63,65]

The compounds UP_2S_6 and $U(P_2S_6)_2$ both show typical paramagnetic behavior. The magnetic moments μ in Figures 12 and 13 are calculated by the method described above using the parameters given in Table 13.

The deviations of the calculated values from the measured ones are possibly due to impurities of the investigated samples. The magnetic behavior of both compounds does not show cooperative magnetic interactions, which is understandable considering the larger distances between the paramagnetic centers in comparison to UP_2S_7.

The AO parameters (cf. Table 13) are comparable to the ones found for the U^{4+}-halide ion interaction in $Cs_2[UCl_6]$, e_σ = 1489 cm^{-1}, e_π = 338 cm^{-1} and in $Cs_2[UBr_6]$, e_σ = 1356 cm^{-1}, e_π = 331 cm^{-1}.[57,66] The crystal field parameters for UO_2[67] lead to AO parameters of e_σ = 1908 cm^{-1} and e_π = 545 cm^{-1}.

The $e_\sigma(d)$ parameters of the U^{4+}–S^{2-} interaction (e_σ(2.81 Å) = 1124 cm^{-1}) determined here are at least five times larger than those reported for the lanthanide ion–S^{2-} interactions in $Nd_3ClS_2[SiS_4]$ (e_σ(2.84 Å) = 80.3 cm^{-1})[68] and in $Tb_4[SiS_4]_3$ (e_σ(2.809 Å) = 203 cm^{-1}).[69] This observation is in line with the fact that the 5*f* orbitals are more extended than the 4*f* orbitals, leading to a larger overlap with the orbitals of the ligand.

3 Synthesis and characterization of $Rb_5U(PS_4)_3$, $CsU_2(PS_4)_3$ and $Na_2U(PS_4)_2$

Introduction

During the past two decades, numerous new alkali metal/transition metal chalcogenophosphates have been obtained using the reactive flux method[1-3] In several cases, a high alkali metal content leads to the formation of isolated anions.[4-6] A formal oxidation of these Zintl anions can be realized by decreasing the alkali metal/transition metal ratio. The resulting compounds consist of higher-dimensional anionic networks. For example, the $^{1}_{\infty}[Cr_2(PS_4)_3]^{3-}$ chains in the crystal structure of $K_3Cr_2(PS_4)_3$[7] can formally be derived from the Zintl anion $Cr_2(PS_4)_4^{6-}$, which is found in $K_6Cr_2(PS_4)_4$,[4] by linking the $Cr_2(PS_4)_4^{6-}$ units via the terminal PS_4 groups.

The structure of the anionic frameworks in heavy metal chalcogenophosphates is not only determined by the stoichiometry, but also by the radii of the alkali metal cation(s). For example, while $CsLiU(PS_4)_2$ (**X**) forms a 3D framework with the Cs^+ cations located in one-dimensional tunnels running along the *c* axis, the sodium analogue $Na_2U(PS_4)_2$ (**VII**) consists of $[U(PS_4)_2]_x$ double layers with highly disordered Na^+ ions residing in the cavities of the structure and in the *van der Waals* gap between the layers. The results indicate a strong template effect of the alkali metal cations, similar to the observations made in zeolite chemistry, where new compounds with tailor-made pore shapes and sizes can be prepared by adding different quaternary alkyl ammonium salts to the educts.[8]

Experimental section

Materials: Starting materials were uranium metal powder (Kristallhandel Kelpin, 99.9 %), P_2S_5 (Aldrich, 99 %), alkali metal sulfides A_2S (A = Na, Rb, Cs) and S powder (Riedel, 99.999 %). All starting compounds and products were examined by X-ray powder diffraction, using a Siemens D5000 diffractometer with a CuK_α source.

Alkali metal sulfides, A_2S (A = Na, Rb, Cs) were made by reacting stoichiometric amounts of the elements in liquid ammonia as described in chapter 2.

$Rb_5U(PS_4)_3$ (V). $Rb_5U(PS_4)_3$ was obtained by reaction of uranium metal with a rubidium thiophosphate melt. A 500 mg mixture of rubidium sulfide, uranium metal, phosphorus pentasulfide and sulfur with the molar ratio 5:2:3:6 was sealed in an evacuated quartz tube with an outer diameter of 1 cm. The sample was placed in a programmable tube furnace, heated up to 650°C at a rate of 1°C/min and maintained at this temperature for one week. Finally, the furnace was cooled down to room temperature at a rate of 0.1°C/min. The reaction product contained single crystals of $Rb_5U(PS_4)_3$ (dark red prisms). According to the results of X-ray powder diffractometry, the sample is single phase.

$CsU_2(PS_4)_3$ (VI). $CsU_2(PS_4)_3$ was obtained by reaction of uranium metal with a cesium thiophosphate melt. A 500 mg mixture of cesium sulfide, uranium metal, phosphorus pentasulfide and sulfur with the molar ratio 1:4:3:14 was sealed in an evacuated quartz tube with an outer diameter of 1 cm. The sample was placed in a programmable tube furnace and annealed at 130°C for one day. Subsequently, it was heated up to 700°C at a rate of 1°C/min and maintained at this temperature for three days. Finally, the furnace was cooled down to room temperature at a rate of 0.5°C/min. The reaction product contained single crystals of $CsU_2(PS_4)_3$ (red transparent platelets) which were embedded in an amorphous dark orange matrix. The matrix could be removed by washing the crystals with dry methanol.

$Na_2U(PS_4)_2$ (VII). $Na_2U(PS_4)_2$ was obtained by reaction of uranium metal with a sodium thiophosphate melt. A 500 mg mixture of sodium sulfide, uranium metal, phosphorus pentasulfide and sulfur with the molar ratio 4:2:3:1 was sealed in an evacuated quartz tube with an outer diameter of 1 cm. The sample was placed in a programmable tube furnace and annealed at 130°C for one day. Subsequently, it was heated up to 700°C at a rate of 1°C/min and maintained at this temperature for three days. Finally, the furnace was cooled down to room temperature at a rate of 0.1°C/min. The reaction product contained single crystals of $Na_2U(PS_4)_2$ (thin red platelets) embedded in a dark red amorphous polysulfide melt. The crystals were obtained by removing the matrix with a scalpel.

Physical measurements

Crystal structure determination. The crystal structures were determined from single crystal X-ray diffraction data. Single crystals were selected from the reaction mixture, embedded in a thin film of epoxy glue and fixed at the tip of a glass fiber on a Bruker SMART CCD diffractometer equipped with a monochromated MoK_α source (λ= 0.71073 Å) and a graphite monochromator. The crystal to detector distance was 5 cm. Crystal decay was monitored by recollecting 50 initial frames at the end of the data collection. Data were collected by a scan of 0.3° in ω in groups of 600 frames at φ settings of 0°, 120° and 240°. The exposure time was 30 s/frame. The collection of the intensity data was carried out with the program SMART.[9] Cell parameters were initially calculated from reflections taken from approximately 30 frames of reflections. The final lattice parameters were calculated from all reflections observed in the actual data collection. The data from the data collections were processed using the SAINT[10] program and corrected for absorption using SADABS.[11]

The structures were solved using direct methods, which revealed the atomic positions and refined using the SHELXTL 5.1 program package.[12] The final refinements were carried out on F_O^2. Atomic scattering factors for spherical neutral free atoms were taken from standard sources and anomalous dispersion corrections were applied.[13] Calculations performed at an intermediate stage in which the relative positional occupancies were refined, revealed a site disorder for the cation positions in $CsU_2(PS_4)_3$ and $Na_2U(PS_4)_2$, but did not indicate any nonstoichiometry. The final coordinates and temperature factors of all atoms are given in Tables 2, 4 and 6.

Vibrational and spectral properties. Optical measurements were made at room temperature with a Varian CARY5 double-beam, double-monochromator spectro-photometer operating in the 200-2000 nm region. The instrument was equipped with an integrating sphere and controlled by a personal computer. For the diffuse reflectance measurements, $BaSO_4$ was used as reference material (100% reflectivity assumed).[14] The absorption of the $Rb_5U(PS_4)_3$ solution in acetonitrile[15] was measured in transmission mode using a standard quartz glass cell.

The IR spectroscopic data for $Rb_5U(PS_4)_3$ shows absorptions at 600 (ν_3), 400 (ν_1), 220 (ν_4) and 160 cm^{-1} (ν_2). Absorbances in a related spectral range have been observed for thiophosphates such as $Na_3PS_4 * 8\ H_2O$[16] or $KPdPS_4$.[17] According to the results of the X-ray structure determination, the spectroscopically relevant unit is the PS_4^{3-} anion. For this tetrahedral species 4 Raman (ν_1-ν_4) and 2 IR (ν_3 and ν_4) bands are expected.[18] Due to the symmetry reduction in the structure of the title compound, all vibrational bands are visible in the IR spectrum. Neglecting the high- and low-frequency parts of the spectrum (combinations and lattice + deformation modes), the vibrational spectrum of $Rb_5U(PS_4)_3$ is essentially a juxtaposition of bands characteristic of the US_8 unit (outside the detection range; U - S stretching modes are expected in the frequency range below 140 cm^{-1}) and of those of the PS_4^{3-} anion. This result confirms the proposed description of the crystal structure in terms

of ionic fragments but also the predominance of nearest neighbor interactions of covalent character.

UV/Vis spectra of $Rb_5U(PS_4)_3$ were recorded for the solid compound and for a solution of $Rb_5U(PS_4)_3$ in acetonitrile/toluene containing 2,2,2 crypt. The results of the diffuse reflectance measurement obtained for solid $Rb_5U(PS_4)_3$ are in accordance with the values reported for the isotype $K_5U(PS_4)_3$.[5] The UV/Vis spectrum of the solution, which is shown in Figure 2, displays a characteristic absorption maximum at λ_{max} = 617 nm. Surprisingly, this value was also reported for solutions of $K_3Cr(PS_4)_2$,[7] $K_4VP_2S_9$,[6] $K_5Ti(PS_4)_3$[6] and $K_4Pd(PS_4)_2$.[19] The formation of reaction products with apparently the same properties from different starting materials indicates a decomposition of the free Zintl ions upon addition of the solvent. The intense blue color of the solutions can be attributed to the intermediate formation of the S_3^- radical anion.[20]

Results and discussion

$Rb_5U(PS_4)_3$ ($K_5U(PS_4)_3$ structure type[5]) contains binuclear $[(U_2(PS_4)_6]^{10-}$ units which are well separated from each other by the Rb^+ cations. The structure of the anion is shown in Figure 1. The centrosymmetric $[U_2(PS_4)_6]^{10-}$ building block consists of a $U_2(PS_4)_2$ core, which is terminated on each side by two PS_4^{3-} thiophosphate ligands in a bidentate fashion. In the core, two PS_4^{3-} ligands bridge two U atoms by employing three S atoms each. The remaining S atom is nonbonding. Compared to the idealized T_d anion symmetry, metal coordination decreases the S-P-S angle, whereas the angle associated with the S atoms not attached to U is considerably expanded. The U atoms are coordinated by four PS_4^{3-} ligands, where each of the terminal thiophosphate groups furnishes two S atoms to complete the distorted square antiprismatic S coordination of the metal. The U-U distance within the dimer is 4.655(1) Å. The average U-

S distance is comparable to those observed in other uranium chalcogenides[21] with individual U-S distances ranging from 2.813(1) to 3.083(1) Å.

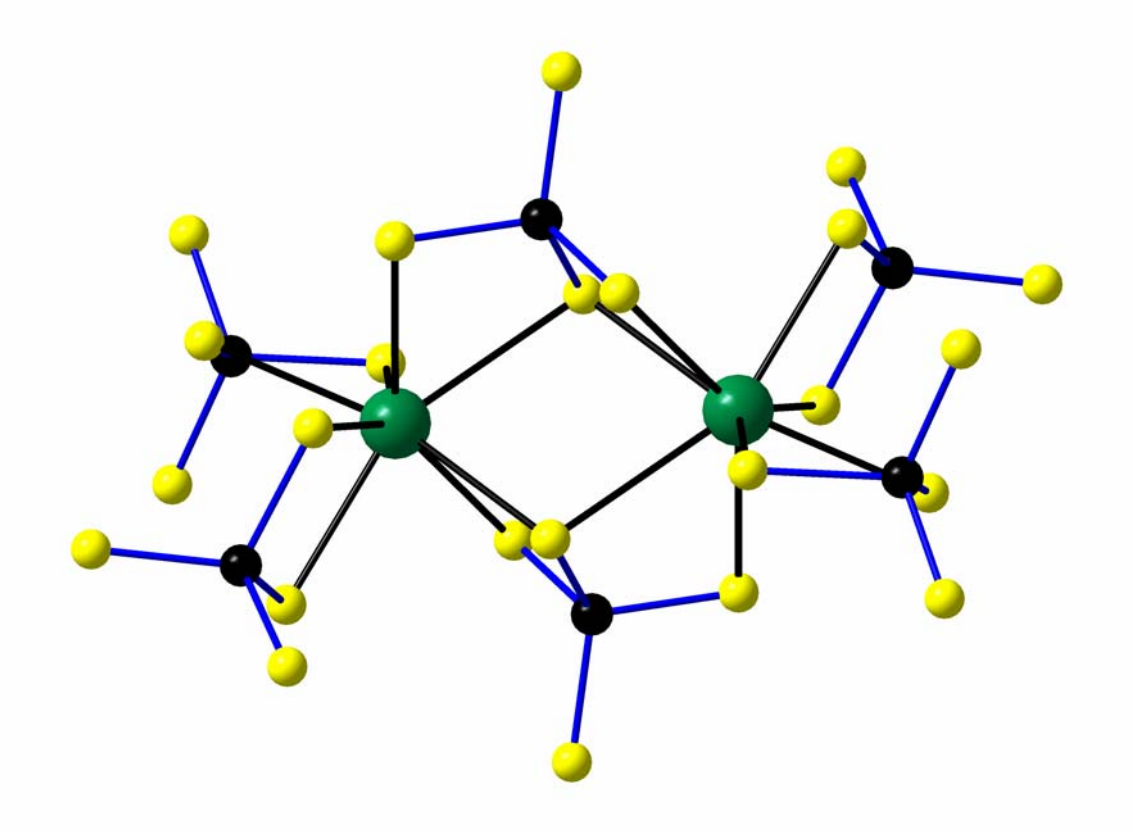

Figure 1. Structure of the $[U_2(PS_4)_6]^{10-}$ anion.

$Rb_5U(PS_4)_3$ is insoluble in polar aprotic solvents such as DMF or acetonitrile, but - following established procedures in Zintl anion chemistry[22] - the preparation of solutions containing the free Zintl-type anion $[U_2(PS_4)_6]^{10-}$ was attempted by adding a crown ether acting as a complexating ligand for the alkali metal.

However, a comparison of the UV-Vis spectrum recorded for the solution of $Rb_5U(PS_4)_3$ with the data obtained for several investigated compounds containing Zintl-type anions ($K_3Cr(PS_4)_2$,[4] $K_4VP_2S_9$,[6] $K_5Ti(PS_4)_3$[6] and $K_4Pd(PS_4)_2$[19]) revealed that all these solutions show exactly the same absorption maximum (617 nm). This result is due to the formation of the blue S_3^- unit, which can also be prepared by dissolving a sodium polysulfide with the formal composition NaS_3 in DMF[20]. The S_3^- radical anion, which is also the chromophore found in lapislazuli,[23]

remains stable in polar aprotic solvents but quickly disintegrates upon contact with air or moisture.

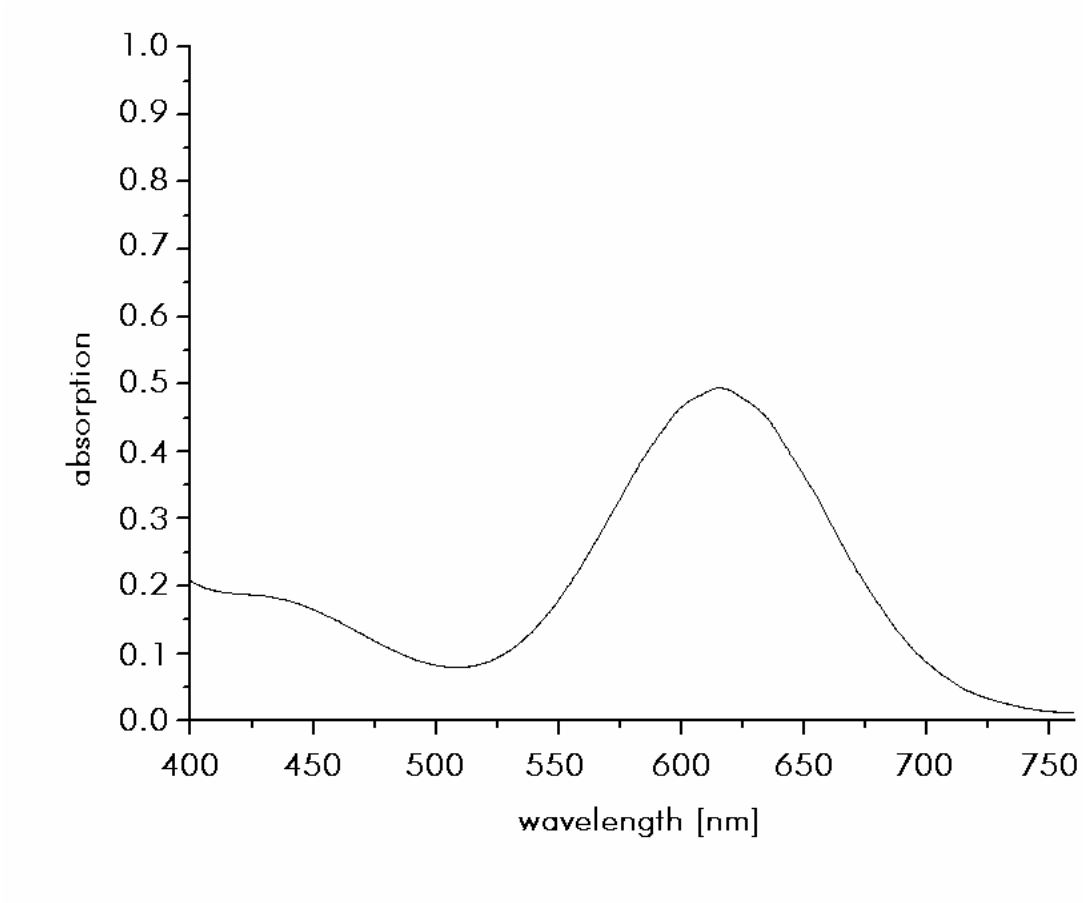

Figure 2. UV-Vis spectrum for $[U_2(PS_4)_6]^{10-}$ with 2,2,2-crypt in toluene/acetonitrile.

For the transition metals, the formation of a complex with the solvent molecules can be expected. However, compared to the strong absorption of the S_3^- unit, the intensity of the absorption bands for the transition metal complexes are too weak to be detected in the UV-Vis spectra of the solutions. Figure 2 shows the UV-Vis spectrum obtained for a solution of $Rb_5U(PS_4)_3$ with 2,2,2-crypt in toluene/acetonitrile.

$CsU_2(PS_4)_3$ crystallizes in the monoclinic space group *$P2_1/c$* with four formula units per cell. The anionic framework of $CsU_2(PS_4)_3$ can be described as a system of $U_2(PS_4)_6$ building blocks (U1) linked by additional

uranium atoms (U2). The resulting three-dimensional structure is composed of uranium atoms connected by tetrahedral PS_4 units with the cesium cations residing in the cavities of the polyanionic framework. Figure 3 shows the arrangement of the $U_2(PS_4)_6$ groups in the unit cells of $Rb_5U(PS_4)_3$ and $CsU_2(PS_4)_3$. The compound $CsU_2(PS_4)_3$ contains two different one-dimensional tunnel systems running parallel to the crystallographic *b* axis. A perspective view of the crystal structure of $CsU_2(PS_4)_3$ along *b* is shown in Figure 4. The larger tunnels (diameter 6 Å) are filled with the Cs^+ cations (fractionally distributed over three distinct crystallographic sites), whereas the smaller ones (size 4.3 * 6.9 Å) remain empty. The arrangement of the cations in the tunnels can be visualized as a system of distorted planar hexagonal layers parallel to the $(\bar{1}02)$ plane.

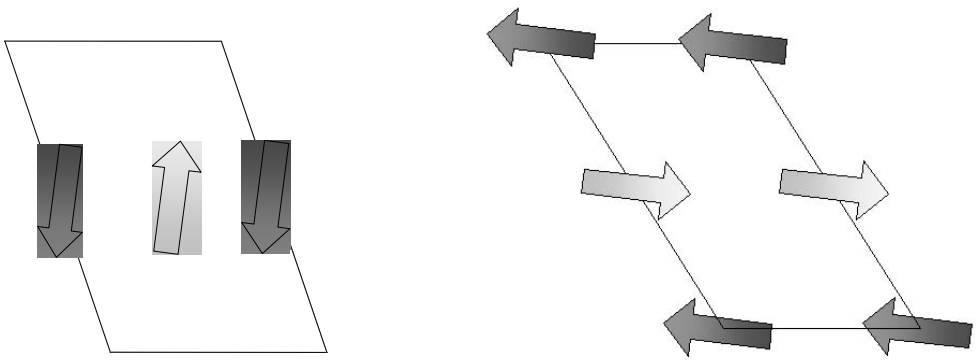

(a) $Rb_5U(PS_4)_3$ (b) $CsU_2(PS_4)_3$

Figure 3. Arrangement of the $U_2(PS_4)_6$ units in the crystal structure of (a) $Rb_5U(PS_4)_3$ and (b) $CsU_2(PS_4)_3$, projection along *b* axis. Dark grey: y = 0; light grey: y = ½; arrowheads pointing towards the reader.

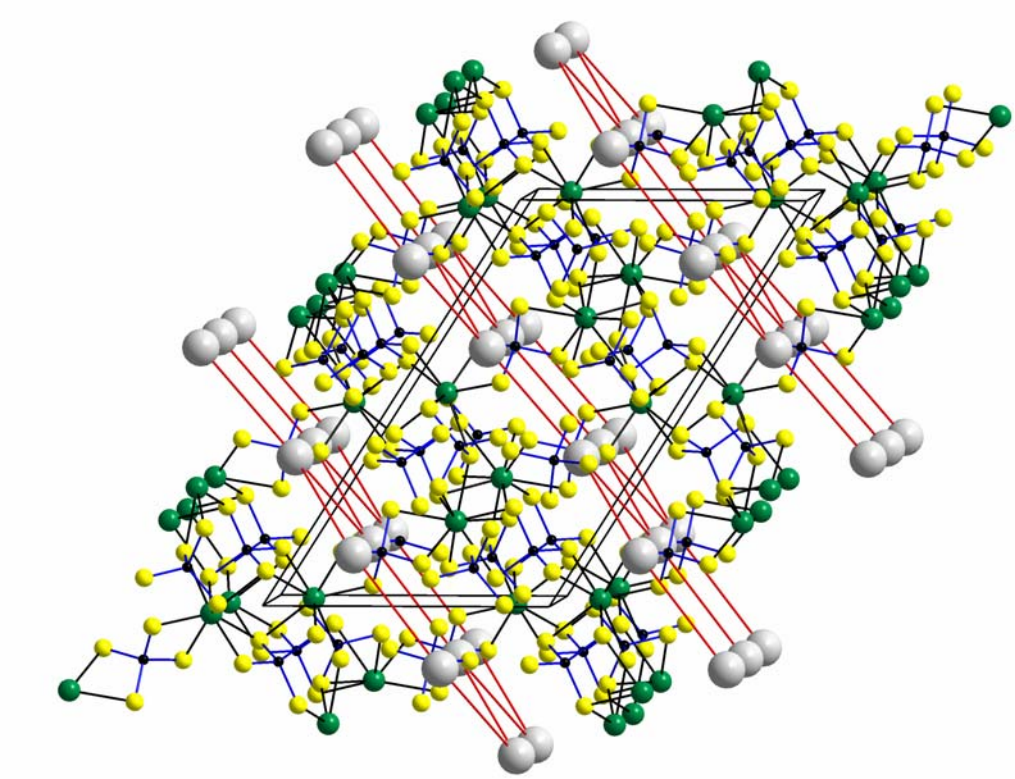

Figure 4. $CsU_2(PS_4)_3$, view along ***b*** axis; Cs: grey spheres; Cs1 and Cs3 positions omitted for clarity.

$Na_2U(PS_4)_2$ crystallizes in the monoclinic space group ***Cc*** with 20 formula units per unit cell. The structure contains linear $[U_2(PS_4)_5]_x$ chains running along $[110]$ and $[\bar{1}10]$ linked by the uranium atoms on U5. The resulting framework consists of two $[U(PS_4)_2]_x$ layers per unit cell with disordered sodium cations residing in the cavities of the framework and in the gap between the layers.

The arrangement of the PS_4 tetrahedra linking the uranium atoms in the structure of $Na_2U(PS_4)_2$ (B) shows an important difference to the $U_2(PS_4)_6$ clusters found in $A_{11}U_7(PS_4)_{13}$ (A = K (**VIII**), Rb (**IX**)), $Rb_5U(PS_4)_3$ and $CsU_2(PS_4)_3$ (A). While the units found in (A) are centrosymmetric (C_i), the connecting tetrahedra in (B) are related by a 2-fold rotation axis, resulting in a distorted D_{2h} symmetry.

$Na_2U(PS_4)_2$ crystals exhibit a systematic non-merohedral twinning which simulates a larger, orthorhombic cell (*Fddd*, with $c' = 2\,c^*\sin\beta$). However,

the monoclinic habit of the crystals and the large *c* value were taken as evidences for the lower symmetry.

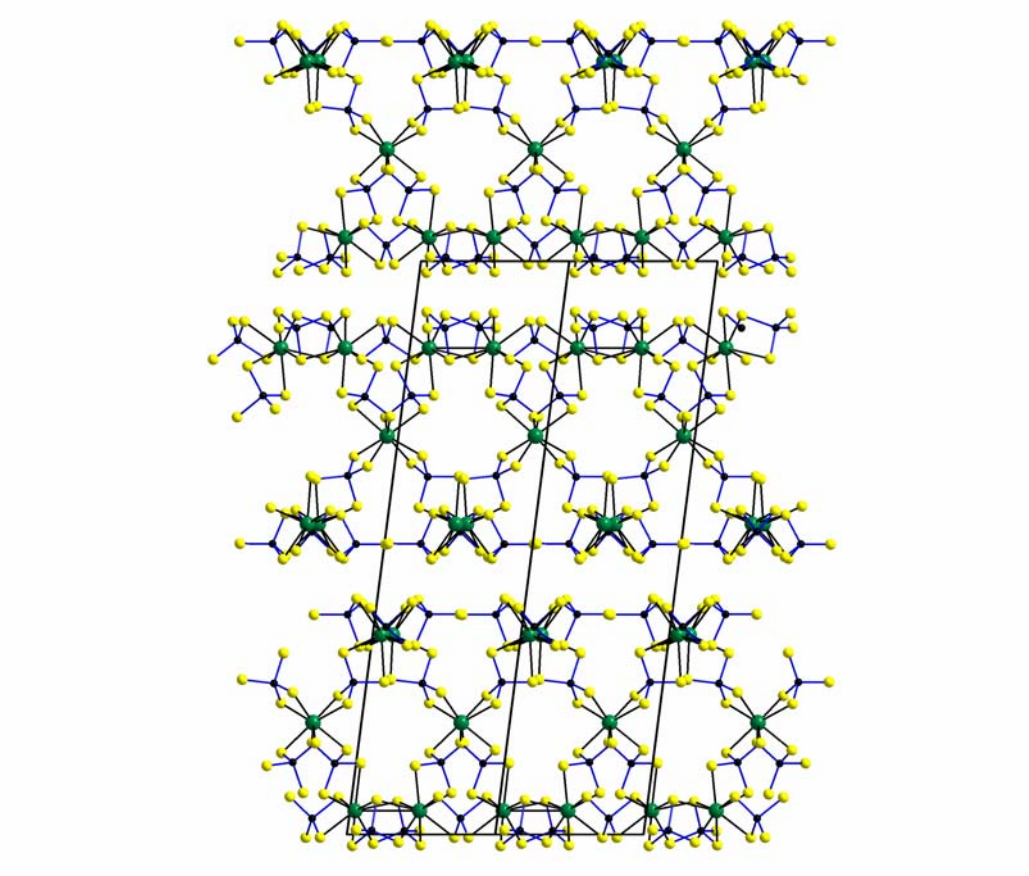

Figure 5. $Na_2U(PS_4)_2$, view along [$\bar{1}$10] axis (cations omitted for clarity).

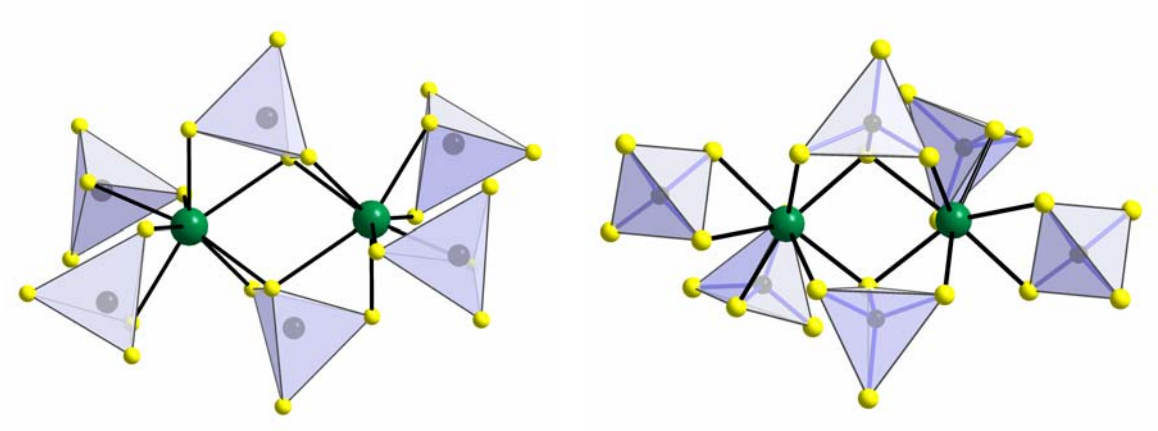

A **B**

Figure 6. Arrangement of the PS_4 tetrahedra in the $U_2(PS_4)_6$ units found in $Rb_5U(PS_4)_3$ (**A**) and $Na_2U(PS_4)_2$ (**B**).

A comparison of the crystal structures of several alkali metal uranium thiophosphates indicates that the structure depends on the cation size, which determines the pore size in the anionic framework. Table 8 shows that only with Cs^+ (cation diameter 3.64 Å), the $CsLiU(PS_4)_2$ (**X**) and $CsU_2(PS_4)_3$ structure types (pore diameter 6 Å) are formed, while with the smaller cations Rb^+ and K^+ only a completely different structure type with a pore size of ~5 Å can be obtained. As soon as the cation diameter is further decreased, the cations become too small to stabilize an anionic network. Instead of a 3D framework with the alkali metal cations located in the pores, an "open structure" consisting of anionic 2D double layers and highly disordered cations is formed for $Na_2U(PS_4)_2$.

This result is in accordance with the observed correlations between the pore diameter and the structure of the (organic) template in zeolite structures, where new compounds with tailor-made pore shapes and sizes can be obtained by adding different quaternary alkyl ammonium salts to the educts.[8]

The multitude of possible connectivity patterns observed in the crystal structures of chalcogenides of group 14 (Si, Ge, Sn) and 15 (P, As) elements leads in many cases to the formation of open framework structures. Bidentate ligands like PS_4^{3-} or $P_2S_6^{2-}$ can act as quasilinear two-fold bridging connectors between 6- or 8-coordinated transition metal atoms, thus leading to a pseudotrigonal or pseudotetrahedral environment for the metal atoms. In many cases, the resulting 3D frameworks contain large cavities, whose size and shape is not only determined by the stoichiometry of the educts, but mainly by the presence and the ionic radii of the templating monovalent countercations like alkali metals,[1-7,25-28] Ph_4P^+[29,30] or NR_4^+.[29-31]

An interesting example for the coexistence of both interpenetrating networks and templating cations in one system is found in the crystal structure of $ATi_2(PS_4)_3$ (A = Li,[5] Na[33]). In this compound, each Ti atom is linked to three bidentate PS_4 ligands, resulting in a pseudotrigonal coordination for the metal centers. The distance between two titanium

atoms in each of the $[Ti_2(PS_4)_3]^-$ networks is 6.08 Å, which is compatible with the formation of two identical interpenetrating frameworks. The highly mobile alkali metal cations provide an additional templating effect, they are arranged in large pores parallel to the *c* axis of the resulting crystal structure.

4 Interlocking inorganic screw helices: Synthesis, structure and magnetism of the novel framework uranium orthothiophosphates $A_{11}U_7(PS_4)_{13}$ (A = K, Rb)

Introduction

Orthothiophosphates are built up from PS_4 groups that are separated and charge balanced by main group elements, transition metals, or *f* block elements. Formally, thiophosphates in general represent higher homologues of oxophosphates. Although there are some similarities originating from the underlying pattern of tetrahedral building blocks, the chemistry of phosphates and thiophosphates is very different and their overlap therefore limited. As for most other chalcogenides, this is caused by the stronger covalency of the P-S bonds relative to the P-O bonds and the redox properties of the S component. Main group and transition metal thiophosphates have been known for more than hundred years.[1] Surveys by Rouxel,[2] Brec[3] and Kanatzidis,[4,5] show a remarkable variety of structures. As in any branch of chemistry where complex structures have to be analyzed, a simple strategy can be used: one decomposes the structures into elementary building blocks, and then tries to identify and explore the matching rules according to which these blocks must be reassembled to yield the considered structure.

In chalcophosphate chemistry (or chalcometalate chemistry in general), a rich structural chemistry emerges from the combination of isolated or condensed P_mS_n motifs and a large variety of metal chalcogenide units. With phosphorus and transition metals, chalcogens generally form low-dimensional compounds, the thiophosphates MPS_3 (e. g. M = Al, Mn, Fe, Co, Ni, Zn) being especially well-characterized representatives of this class of materials.[3]

During the past decade many studies have focused on the chalcophilic late transition metal derivatives, whose structures contain metal

atoms mostly in tetrahedral, square-planar, or octahedral coordination. Much less effort has been devoted to the chalcophosphates of the oxophilic early transition metals.[6-15] Many of these larger metal cations are observed in seven, eight, or higher coordinate environments. These high and variable coordination numbers of the early transition metals,[7-8,13-15] lanthanides[16-25] or actinides[26-30] combined with the condensation equilibria of chalcophosphates[2,5] may lead to structural arrangements of astounding complexity, as the following examples indicate.

Many compounds obtained from the ternary system M-P-S (M = Group 5 metal) contain the bicapped biprismatic M_2S_{12} building unit.[2] Interestingly, the channels of some of the resulting three-dimensional framework structures (e. g. $TaPS_6$[7]) may be filled with chalcogen chains.[31] The structures of several other thiophosphates (e. g. $ATi_2(PS_4)_3$; A = Li, Na[32-34]) are composed of interwoven networks whose channels are filled with alkali metal cations.[32] Finally, the structure of $U(P_2S_6)_2$ (**III**) is based on three interwoven polymeric diamond-type $U(P_2S_6)_2$ frameworks.

The coordination preferences of the metal components seem to be important factors, which determine the structure (and properties) of thiophosphates. Therefore transition metals with high coordination numbers, that is, group 4 metals, lanthanides, or actinides were introduced in order to preclude the formation of octahedrally coordinated metal centers. The example $U(P_2S_6)_2$ (**III**) revealed that the coordination mode of the metal atom combined with the connectivity mode and size of the "linear" (rod-like) $P_2S_6^{2-}$ ligand may lead to the formation of complex network structures. The nonlinear PS_4^{3-} ligand can lead to the formation of metal thiophosphates with helical structure elements.

Experimental section

Materials. The starting materials were uranium metal powder (Kristallhandel Kelpin, 99.9 %), P_2S_5 (Aldrich, 99 %), K_2S, S powder (Riedel, 99.999 %), RbCl (Alfa Aesar, 99.8 %) and LiCl (Alfa Aesar, 99.996 %). All starting compounds and products were examined by X-ray powder diffraction, by means of a Siemens D5000 diffractometer with a CuK_α source.

Potassium Sulfide, K_2S. K_2S was made according to the procedure described in chapter 2.

$K_{11}U_7(PS_4)_{13}$ (VIII). Uranium (0.254 g, 1.06 mmol), P_2S_5 (0.119 g, 0.53 mmol), K_2S (0.059 g, 0.53 mmol), and sulfur (0.068 g, 2.12 mmol) were sealed under vacuum (< 10^{-5} bar) in a silica tube with 8 mm outer diameter and placed in a programmable tube furnace. The tube was heated up to 130°C over a period of 10 h and kept at this temperature for one day. Subsequently, it was heated up to 700°C at a rate of 2°C/min and maintained at that temperature for 50 h. Finally, the sample was cooled down to room temperature at a rate of 0.5°C/min.

The yield of the black crystalline material was quantitative based on the initial metal content as judged by X-ray powder diffraction. Slight impurities of soluble thiophosphates (with presumably discrete anionic structures) were removed by washing with dry ethanol. A semiquantitative microprobe analysis (EDAX) indicated the presence of K, U, P, and S in an approximate atomic ratio of 2:1:2:4. According to the X-ray powder diffractometrical results the sample was a single phase.

$Rb_{11}U_7(PS_4)_{13}$ (IX). A sample with the formal composition UPS_5 (0.250 g, 3.7 µmol) was sealed with a eutectic LiCl/RbCl mixture (1.5 g) under vacuum in a quartz ampoule with an outer diameter of 8 mm. The sample was placed in a programmable tube furnace and heated from room temperature up to 700°C at a rate of 10°C/h, kept at that temperature for 60 h and cooled down to room temperature at a rate of 0.5°C/min. The reaction product contained dark red needle-shaped

crystals embedded in a LiCl/RbCl matrix. The LiCl/RbCl mixture could be removed by treating the product with dry methanol.

The yield of the black crystalline material was approximately 90 % based on the initial metal content as judged by X-ray powder diffraction. A semiquantitative microprobe analysis (EDAX) indicated the presence of Rb, U, P and S in an approximate atomic ratio of 2:1:2:4. Attempts to prepare $Rb_{11}U_7(PS_4)_{13}$ from high temperature reactions or from thiophosphate fluxes did not lead to the desired results. $Rb_{11}U_7(PS_4)_{13}$ could, however, be obtained by treating a sample of the formal composition $CsU_2(PS_4)_5$ at 700°C in a LiCl/RbCl mixture. In this case, small amounts of another phase with the composition $Li_3Rb_6U_3P_5S_{23}$ (**XII**) were formed as black plate-like crystals.

Physical measurements

Crystal structure determination. Single crystals of $K_{11}U_7(PS_4)_{13}$ and $Rb_{11}U_7(PS_4)_{13}$ were selected from the reaction mixtures, embedded in a thin film of epoxy glue and fixed at the tip of a glass fiber on a Bruker SMART CCD diffractometer[35] equipped with a monochromated MoK_α source (λ = 0.71073 Å) and a graphite monochromator. Cell parameters were initially calculated from reflections taken from approximately 30 frames. The final lattice parameters were calculated from all reflections observed in the actual data collection. A summary of details concerning the data collections, structure solutions and refinements is given in Table 1. The collected data were processed by using the SAINT[36] program and corrected for absorption by using SADABS.[37] The systematic absence conditions (*hkl*, *h + k + l = 2n*; *hk0*, *h+k = 2n*) were characteristic for the tetragonal space group $I\bar{4}2d$ (No. 122), and the refinement results proved this choice to be correct. The structures were solved by direct methods and refined in full-matrix least-squares using the SHELXTL

5.1 program suite.[38] The final refinement was carried out on F_O^2. Atomic scattering factors for spherical neutral free atoms were taken from standard sources and anomalous dispersion corrections were applied.[39] From the final refinement cycle the compositions of the crystals used are $K_{11}U_4(PS_4)_{13}$ and $Rb_{11}U_4(PS_4)_{13}$. Calculations performed at an intermediate stage in which the relative positional occupancies were refined, revealed a site disorder for the cation position K7 in $K_{11}U_4(PS_4)_{13}$, but did not indicate any nonstoichiometry. The final atomic parameters are listed in Tables 2 and 4.

Semiquantitative microprobe analysis. Semiquantitative microprobe analysis was performed in a Zeiss DSM 962/Philipps PSEM 500 scanning electron microscope equipped with a KEVEX energy dispersive spectroscopy detector. Data acquisition was performed with an accelerating voltage of 20 kV and a 1 min accumulation time.

FT-IR spectra. FT-IR spectra were recorded on solid samples in a CsI matrix. The samples were ground with dry CsI into a fine powder and pressed into transparent pellets. The spectra were recorded in the far-IR region (700-200 cm^{-1}, ≈ 5 cm^{-1} resolution) with a FT-IR spectrometer (2030 Galaxy-FT-IR, Mattson Instruments) equipped with a TGS/PE detector and a silicon beam splitter.

Optical spectroscopy. Optical diffuse reflectance measurements were made at room temperature with a Varian CARY5 double-beam, double-monochromator spectrophotometer operating in the 200-2000 nm region. The instrument was equipped with an integrating sphere and controlled by a personal computer. The measurement of diffuse reflectivity may be used to determine values for the optical band gap, which are in reasonable agreement with those obtained from single crystal absorption measurements. $BaSO_4$ was used as reference material (100 % reflectivity assumed).[40-42]

Magnetic susceptibility measurements. Variable-temperature magnetic susceptibility data were collected for a sample of $K_{11}U_7(PS_4)_{13}$ (79 mg) with a vibrating sample magnetometer (Foner magnetometer, Princeton

Applied Research), which was operated between 0.2 and 1 T. The instrument was calibrated with $Hg[Co(NCS)_4]$. Measurements at different field strengths confirmed that ferromagnetic impurities were absent. The diamagnetic correction was estimated from Pascal's constants to be -310 * 10^{-6} cm^3/mol.[43]

Results and discussion

The new compound $K_{11}U_7(PS_4)_{13}$ was obtained by reaction of uranium metal with a thiophosphate melt at 700°C. $Rb_{11}U_7(PS_4)_{13}$ was prepared by heating a mixture of the formal composition UPS_5 in an eutectic RbCl-LiCl flux at 700°C. A perspective view of the crystal structure of $A_{11}U_7(PS_4)_{13}$ (A = K, Rb) along the crystallographic *c* axis is shown in Figure 1a. Selected interatomic bond lengths are compiled in Tables 3 and 5.

Principle features of this novel structure type are spiral $U_7(PS_4)_{13}$ chains extending along the view direction. One of these chains is shown in a view along the helix axis in Figure 1b. Four chains are marked by circles in Figure 1a. Each of the individual chains is crosslinked to five neighboring chains by two *exo*-PS_4 groups per linkage. The connectivity of the covalently linked uranium thiophosphate framework generates different types of cavities and a topologically unusual array of tunnels that contain the A^+ counterions.

The coordination geometries of the A^+ counterions are quite irregular with coordination numbers between six and eight with K-S separations varying between 3.160(9) Å and 3.739(8) Å and Rb-S distances between 3.247(7) Å and 3.980(6) Å.

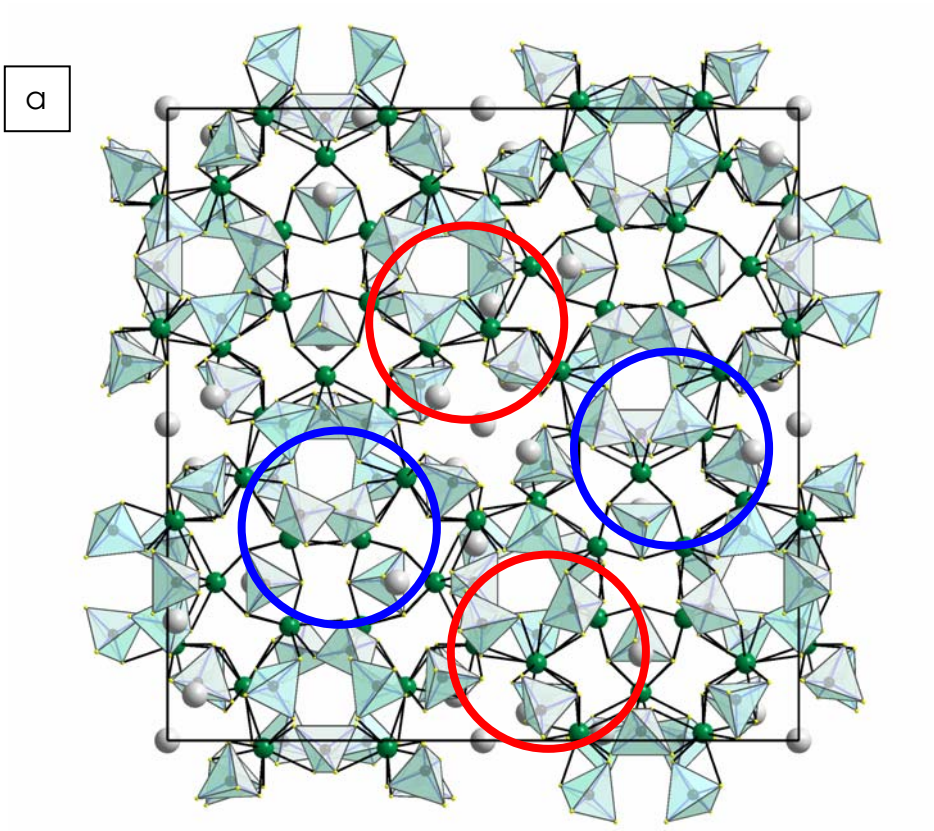
a

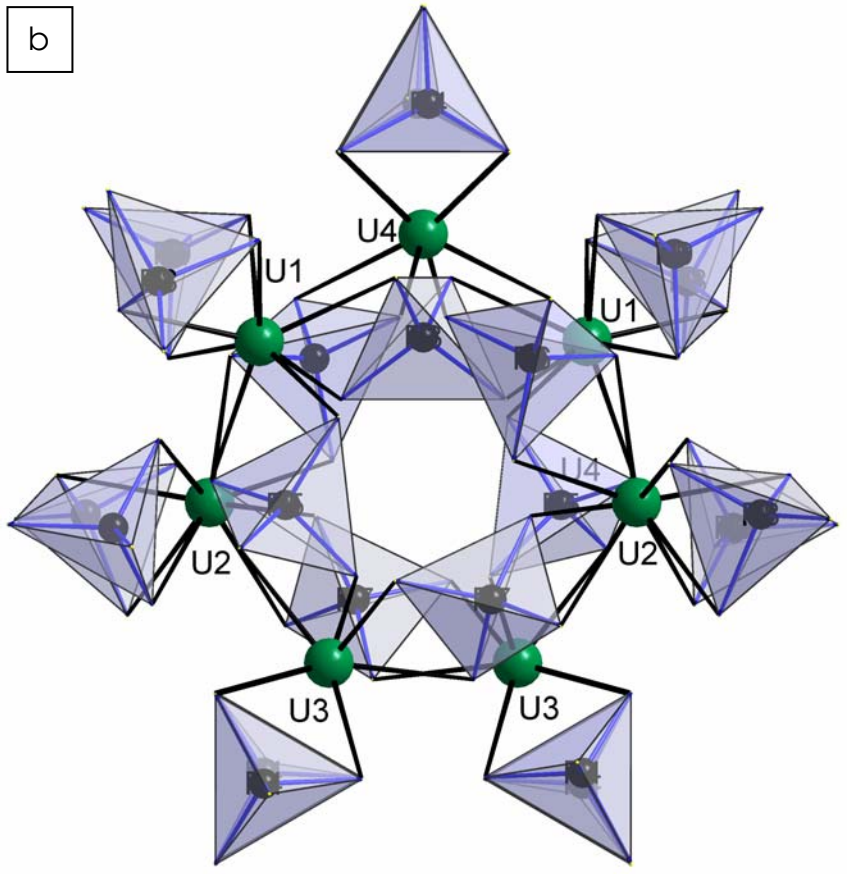
b
U4
U1
U1
U2
U2
U3
U3

Figure 1. (a) View of the unit cell down the *c* axis illustrating the positions of the alkali cations in the structure channels; large red and blue circles indicate the opposite helicity of the chains.
(b) Enlarged view of the circled fragment illustrating the connectivity of the uranium centers by the PS_4 units.

Metal coordination. As in several other uranium chalcogenides the framework structure of $A_{11}U_7(PS_4)_{13}$ (A = K, Rb) is based on bicapped trigonal prismatic US_8 units, US_9 tricapped trigonal prisms and PS_4 tetrahedra. The U coordination is illustrated in Figure 2, which shows a fragment of the structure about U4 that is situated on a crystallographic twofold axis. In the capped prisms, the U atoms have eight S neighbors with distances ranging from 2.753(5) Å to 3.015(5) Å; U2 acquires an additional S neighbor at a slightly larger distance of 3.110(5) Å; this leads to a tricapped trigonal prismatic coordination geometry that is uncommon for uranium chalcogenides.[29] A number of uranium chalcogenides, such as $Cu_2U_3S_7$,[44] US_3,[45] or MUS_3 (M = Ru, Rh)[46] exhibit bicapped trigonal prismatic geometry; square bipyramidal S coordination has been observed in US_2[47], or ternary thiophosphates such as UP_2S_6 (**I**)[26] UP_2S_7 (**II**) or $U(P_2S_6)_2$(**III**).[30]

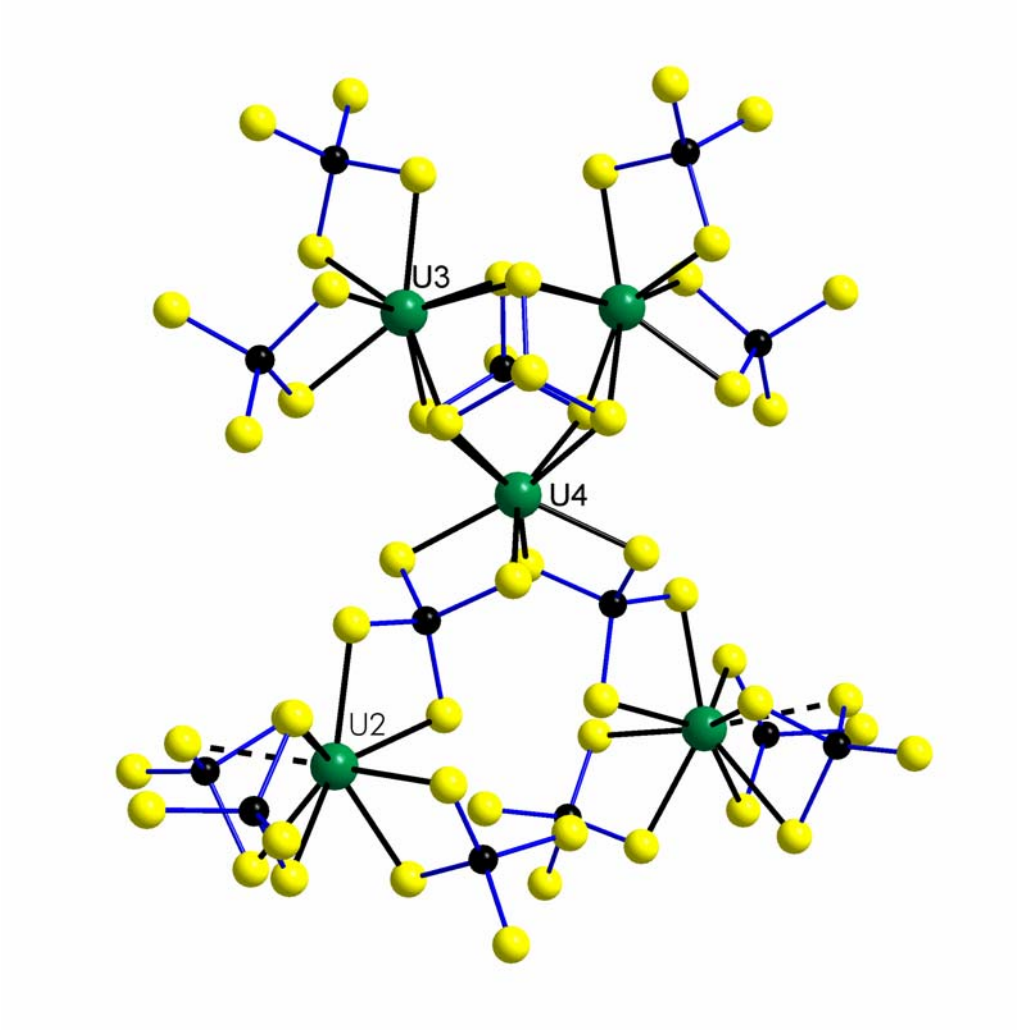

Figure 2. Coordination of the uranium atoms with atomic labeling scheme.

The average U-S distance of 2.873 Å indicates uranium to be in the tetravalent state[48] and compares well with the U-S distances observed in US_2[47] or other U chalcogenides.[26,30,44-46] The PS_4 tetrahedra in $K_{11}U_7(PS_4)_{13}$ are slightly distorted; as expected, the P-S distances to the doubly metal bridging S atoms (d_{P-S} = 2.110(7) Å) are slightly longer than those with a single metal bond (d_{P-S} = 2.032(7) Å) or terminal S atoms (d_{P-S} = 1.930(8) Å). Some of the terminal P-S distances are remarkably short.

Helix formation. In Figure 3 prisms made up of the S atoms of four PS_4^{3-} anions surrounding U3 are depicted; two S atoms of two of the PS_4^{3-} units form one rectangular face of the prism, while two S atoms of the remaining two PS_4^{3-} anions occupy the remaining corners of the prism as well as capping the other two rectangular faces. It should be noted that the two capping PS_4^{3-} anions may have different (right/left) orientation with respect to the prism, that is, because of the chelating nature of the PS_4^{3-} ligand the $[U(PS_4)_4]^{8-}$ unit is a chiral center with one of the capping PS_4^{3-} groups pointing "up" and the other one pointing "down". The upper corner of each unit is condensed with the lower corner of an adjacent unit. As the doubly bidentate PS_4^{3-} groups provide an approximately linear linkage of the U centers and the "pitch angle" of the chains defined by the P-U-P vectors slightly larger than 90°, a helix is formed that ideally should have four (or a multiple of four) prismatic units per repeat distance spiraling around the twofold screw axes parallel to the *c* axis. This can been seen in Figure 3. However, as the helix pitch angle is > 90°, the compound contains only seven $[U(PS_4)_4]^{8-}$ prism units per unit cell. This is illustrated by a simplified view of the U-P backbone of the spiral chains (with the S atoms omitted) in Figure 4. The deviations of the P-U-P (91.2° - 93.7°) and U-P-U (168.0° - 177.4°) angles from their idealized values of 90° and 180°, respectively, lead to an irregular pitch of the helix.

As for any other helix, the "prism helix" in the structure of $A_{11}U_7(PS_4)_{13}$ may be either left or right handed. In this structure, spiral chains around adjacent axes, which are cross-linked by common PS_4^{3-} groups (two PS_4^{3-} groups per linkage), have a different sense of rotation as indicated by the blue and red circles in Figure 1a.

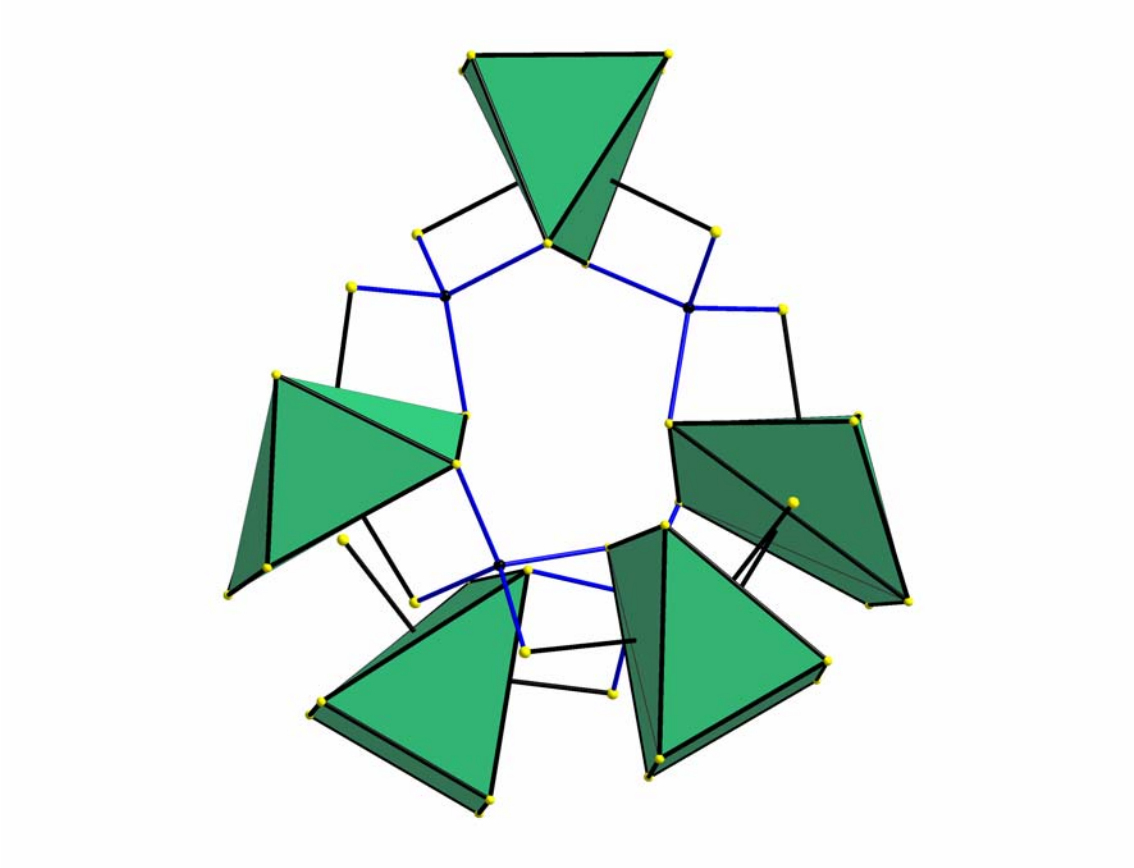

Figure 3. Schematic polyhedral representation of the $[U_7(PS_4)_{13}]^{11-}$ helix in $K_{11}U(PS_4)_{13}$.

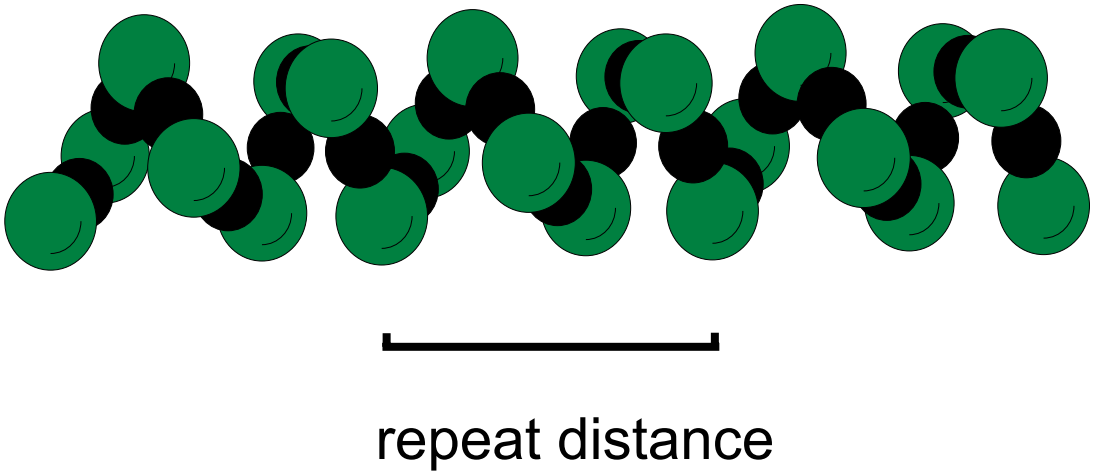

Figure 4. CPK representation of the backbone of the $[U_7(PS_4)_{13}]^{11-}$ helix chain in $K_{11}U_7(PS_4)_{13}$ (S atoms omitted for clarity).

Framework channels. The helix formation and the cross-linking of the helices are illustrated in Figure 1a. Four helices centered about the fourfold inversion axes (along 0, 0, *z* and ½, ½, *z*) form a set of large tunnels with a diameter of approximately 5 Å that contain the majority of the K^+ ions. A second set of smaller tunnels is formed around the twofold screw axes along (¼, ¼, *z*) by four helices linked by PS_4^{3-} groups. These triply-connecting tetrahedra are situated above or below a second set of K^+ ions. The remaining cations are located between the PS_4^{3-} groups spiraling along [001] within the helices. The cation sizes (K^+: 1.39 Å, Rb^+: 1.60 Å)[49] are small compared to the diameter of the large tunnel, and one of the seven crystallographically independent cations (K7) seems to "rattle" within the channels, as indicated by its disorder and the large and strongly anisotropic displacement parameters. This is also the case for the larger Rb^+ ion in the isostructural $Rb_{11}U_7(PS_4)_{13}$. The large tunnel diameter, the high thermal parameters for the A^+ ions inside the tunnel, the existence of the isostructural compounds $A_{11}U_7(PS_4)_{13}$ (A = K, Rb), and the fractional distribution of the A^+ ions over several lattice sites indicate that $A_{11}U_7(PS_4)_{13}$ (A =alkali metal) may act as host for ion exchange.

Vibrational and spectral properties. The IR spectroscopic data for $K_{11}U_7((PS_4)_{13}$ show absorptions at 610 (ν_3), 420 (ν_1), 220 (ν_4) and 170 cm^{-1} (ν_2). Absorbances in a related spectral range have been observed for thiophosphates such as Na_3PS_4 * 8 H_2O[50] or $KPdPS_4$.[51] According to the results of the X-ray structure determination the spectroscopically relevant unit is the PS_4^{3-} anion. For this tetrahedral species 4 Raman (ν_1-ν_4) and 2 IR (ν_3 and ν_4) bands are expected.[52] Due to the symmetry reduction in the structure of the title compound, all vibrational bands are visible in the IR spectrum. Neglecting the high- and low-frequency parts of the spectrum (combinations and lattice + deformation modes), the vibrational spectrum of $K_{11}U_7(PS_4)_{13}$ is essentially a juxtaposition of bands characteristic of the US_8 unit (outside the detection range; U - S stretching modes are expected in the frequency range below 140 cm^{-1}) and of those of the PS_4^{3-} anion. This result confirms the proposed description of

the crystal structure in terms of ionic fragments but also the predominance of nearest neighbor interactions of covalent character.

The optical properties of $K_{11}U_7(PS_4)_{13}$ were determined by studying the UV-visible/near-mid IR diffuse reflectance spectrum which reveals well-defined broad peaks at ≈ 5000 (0.61), ≈ 7100 (0.87), ≈ 8300 (1.02 , ≈ 9650 (1.14), ≈ 11700 (1.44) and ≈ 12500 cm^{-1} (1.54 eV). Based on the oxidation state formalism, a 5 f^2 configuration and semiconducting behavior may be expected. Assuming a $^3H_4$ ground state, other triplet terms arising from this configuration are ^3F and ^3P. Based on their position and spectral width, the absorptions are assigned to *f-f* or *d-d* transitions.[53] $K_2UP_3Se_9$, which contains U^{4+}, displays absorptions at 3725 and 5856 cm^{-1}.[27]

Magnetic properties. The oxidation states of the uranium atoms may be deduced from simple charge balance considerations. The electronic structure of the title compound may easily be understood by electron counting and assigning formal oxidation states according to the formula $[A^+]_{11}[(U^{4+})_7(PS_4^{3-})_{13}]$.

Magnetic measurements between 4 and 300 K were made on poly-crystalline powdered samples of $K_{11}U_7(PS_4)_{13}$ by using a Foner vibrating sample magnetometer. Figure 5 shows the thermal variation of the inverse susceptibility and the effective magnetic moment. The $1/\chi$ versus T curve shows a distinct minimum at approximately 60 K characteristic of an antiferromagnetic transition. In the paramagnetic region, the thermal variation of χ shows some curvature towards the temperature axis. A curve fitting using the modified Curie-Weiss law $\chi = C/(T-\theta) + \chi_0$ in the temperature range 70-300 K led to the values C = 3.78, θ = -14.54 K, χ_0 = 0.01 for the Curie constant, the paramagnetic Neél temperature, and the magnetic susceptibility, respectively, and to an effective magnetic moment of 2.54 μ_B per U atom. The value for the effective paramagnetic moment of uranium is significantly lower than the theoretical value for a U^{4+} free ion value of 3.58 μ_B ($^3H_4$ ground term) and is also lower than that for a totally quenched orbital moment (2.83 μ_B).[54-56] The large reduction of the effective magnetic moment probably results from crystal field

interactions, as observed and theoretically confirmed for $U(P_2S_6)_2$ (**III**) from calculations based on the angular overlap model (chapter 2). The results of calculations for $U(P_2S_6)_2$ (**III**) confirm the presence of a non-magnetic ground state, and a related behavior in the present case can be assumed.

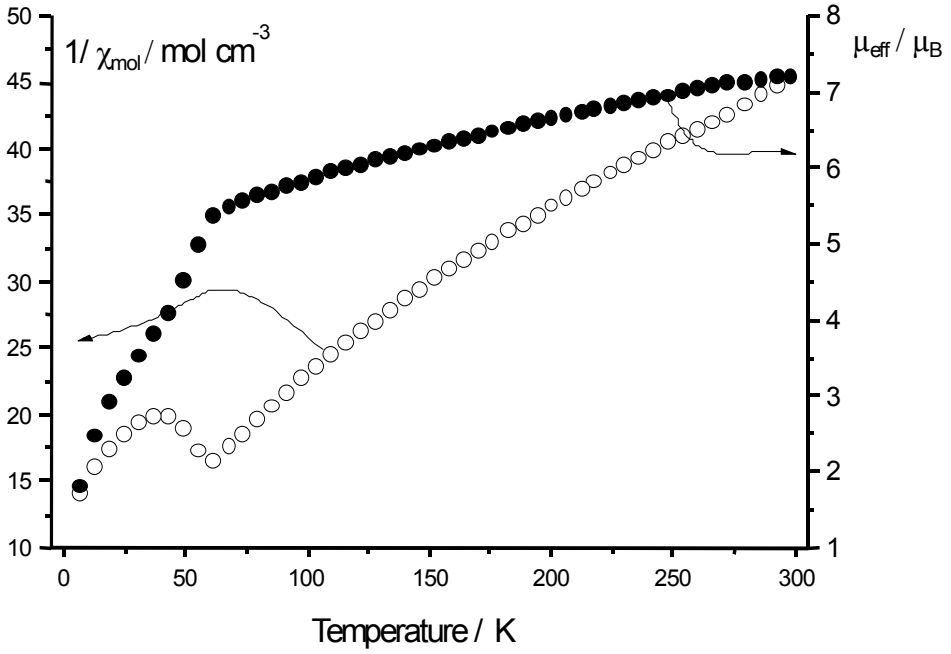

Figure 5. Thermal variation of the inverse molar susceptibility (filled circles) and the effective magnetic moment (open circles) for $K_{11}U_7(PS_4)_{13}$. The data have been corrected for core diamagnetism.

Conclusion

The reaction of K_2S, uranium, P_2S_5, and sulfur leads to the formation of a new framework compound $K_{11}U_7(PS_4)_{13}$, whose tunnel structure is made of interlocked helical chains, which are themselves built from complex polyhedral interconnections. The helix formation in turn is related to the bicapped trigonal prismatic coordination of the uranium centers. A comparison with other uranium ortho- and dithiophosphates indicates

that square-antiprismatic coordination of the metal atoms is compatible with a pseudotetrahedral connectivity within the framework. Based on the results from systematic studies of the ternary system U-P-S and structural considerations, it can be assumed that several other uranium thiophosphates with low density may occur. This would deserve further exploitation of the A-U-P-S system.

The synthesis of interpenetrating framework materials such as $U(P_2S_6)_2$ (**III**) or open framework compounds such as $CsLiU(PS_4)_2$ (**X**) and $K_{11}U_7(PS_4)_{13}$ suggests several areas of additional research. 1) These compounds may be derivatized by "soft chemistry" methods such as ion exchange. 2) The ion transport within the channels is worthwhile to pursue. 3) The compound $Rb_{11}U_7(PS_4)_{13}$ seems to be metastable because it could not be prepared by high-temperature solid state or (poly)thiophosphate flux reactions. 4) Rare earths are widely used to prepare magnetic materials with interesting bulk properties, which are determined by the anisotropy of the ground state of the 4 *f* ions and the nature of the lanthanide-lanthanide and/or lanthanide-transition metal interactions. It might be worthwhile to pursue to interplay of ligand field effects and/or magnetic interactions between the lanthanide/actinide atoms. Although magnetically interacting rare earth centers with organic radicals or Schiff base complexes have been described, magnetic interactions between actinide centers mediated by the σ-bonded PS_4^{3-} ligands would be unusual.

5 $CsLiU(PS_4)_2$, a zeotype uranium thiophosphate obtained from high temperature reactions in salt melts

Introduction

Zeolites can be defined as compounds with fully crosslinked framework structures built from tetrahedral units in which the framework density, i. e. the number of tetrahedral atoms per unit volume is relatively small.[1] These lower framework densities are the result of pores and cavities which often contain extra cations or solvent molecules, but may also be empty. Higher framework densities are encountered among the tectosilicates such as the silicon dioxide polymorphs quartz or cristobalite, where the SiO_4 units are linked to another through oxygen atoms.[2] Although the term zeolite was originally coined for aluminosilicates, it is now applied for many other compounds constructed from TO_4 units with T = Be, B, Ga, Ge, P, As etc.[3] Zeolites have been studied for their applications as catalysts, molecular sieves and ion exchangers.[4] A challenge for materials research is now to expand the scope of zeolitic materials beyond the oxides.

Except for the so-called organic tecton compounds,[5] most compounds with open framework structures are oxidic. Only recently, a number of sulfur or selenium working analogues of zeolites have been reported.[6-14] The majority of these compounds contain the adamantane type $[Ge_4Q_{10}]^{4-}$ (Q = S, Se) cage unit[9-14] whose tetrahedral topology makes it a useful synthon to substitute for the ubiquitous TO_4 units from oxide chemistry. Typically, these micro- or mesoporous network compounds are obtained by an addition copolymerization of divalent transition metals (e. g. Mn,[10a] Fe,[10b,12] Co,[13] Ni,[13a] Cu,[11,13a] Zn,[13] Cd,[10b,13b] Hg[13b]) with the cage compounds $[A]_4[Ge_4Q_{10}]$ [15] (A = alkali metal or ammonium cation) by hydrothermal methods or from aqueous solutions.

Tetrahedral network structures are, however, not restricted to elements with low coordination numbers. For example, in $U(P_2S_6)_2$ (**III**), the uranium atoms are coordinated by dithiophosphate groups in a pseudotetrahedral fashion, and the P_2S_6 units act as linear connectors. The extended network structure may be rationalized based on the length of the P_2S_6 connecting rods. The synthesis of $CsLiU(PS_4)_2$, which contains a microporous framework structure based on a tetrahedral connectivity of the metal centers and the twofold connecting thiophosphate groups, can be regarded as an extension of this synthetic approach.

Experimental section

General. The following reagents were used as obtained: Cs (Chempur, 99.9 %), U (Kristallhandel Kelpin, 99.5 %), P_2S_5 (Aldrich, 99 %), S powder (Merck, 99.999 %), Li_2S (Merck, 98 %), LiCl (Alfa Aesar, 99.996 %), CsCl (Acros, 99 %). All starting compounds and products were examined by X-ray powder diffraction, using a Siemens D5000 diffractometer with a CuK_α source. Cs_2S was made following the procedure described in chapter 2. All substances were handled under argon atmosphere in a stainless steel glove box.

$CsLiU(PS_4)_2$ (X). $CsLiU(PS_4)_2$ was synthesized from a 500 mg mixture of uranium metal, P_2S_5 Li_2S and Cs_2S and sulfur with the molar ratio 2:2:1:1:4 in an evacuated quartz tube. The sample was heated in a furnace at a rate of 1°C/min up to 700°C and kept at this temperature for 3 days; subsequently, it was cooled to room temperature at a rate of 0.2°C/min. The resulting dark brown powder was finely ground and 1.5 g of eutectic LiCl/CsCl mixture were added. After tempering the substance in an evacuated quartz tube for 7 days at 700°C it was cooled to room temperature in 3 days. Black hexagonal crystals were obtained by dissolving the halide melt with distilled water. Microprobe analysis of the

crystals indicated the presence of cesium, uranium, phosphorus and sulfur in a 1:1:2:8 ratio.

Crystal structure determination

The structure of $CsLiU(PS_4)_2$ was determined from single crystal X-ray diffraction data. A single crystal of $CsLiU(PS_4)_2$ was selected from the reaction mixture, embedded in a thin film of epoxy glue and fixed at the tip of a glass fiber on a Bruker SMART CCD diffractometer[16] equipped with a monochromated MoK_α source (λ= 0.71073 Å) and a graphite monochromator. The crystal to detector distance was 5 cm. Crystal decay was monitored by recollecting 50 initial frames at the end of the data collection. Data were collected by a scan of 0.3° in ω in groups of 600 frames at φ settings of 0°, 120° and 240°. The exposure time was 30 s/frame. The collection of the intensity data was carried out with the program SMART.[16] Cell parameters were initially calculated from reflections taken from approximately 30 frames of reflections. The final lattice parameters were calculated from all reflections observed in the actual data collection. The data from the data collections were processed using the SAINT[17] program and corrected for absorption using SADABS.[18]

The structure was solved using direct methods which revealed the atomic positions and refined using the SHELXTL 5.1 program package.[19] The final refinement was carried out on F_O^2. Atomic scattering factors for spherical neutral free atoms were taken from standard sources and anomalous dispersion corrections were applied.[20] From the final refinement cycle the composition of the crystal used is $CsLiU(PS_4)_2$. The reasonableness of the anisotropic thermal parameters for the atoms in the structure suggests a stoichiometric composition. The final atomic parameters are listed in Table 2.

Results and discussion

$CsLiU(PS_4)_2$ crystallizes in the rhombohedral space group $R\bar{3}c$ with eighteen formula units per cell. The structure of $CsLiU(PS_4)_2$ is a unique three-dimensional $U(PS_4)_2^{2-}$ framework with large tunnels running parallel to the crystallographic *c* axis, as shown in Figure 1.

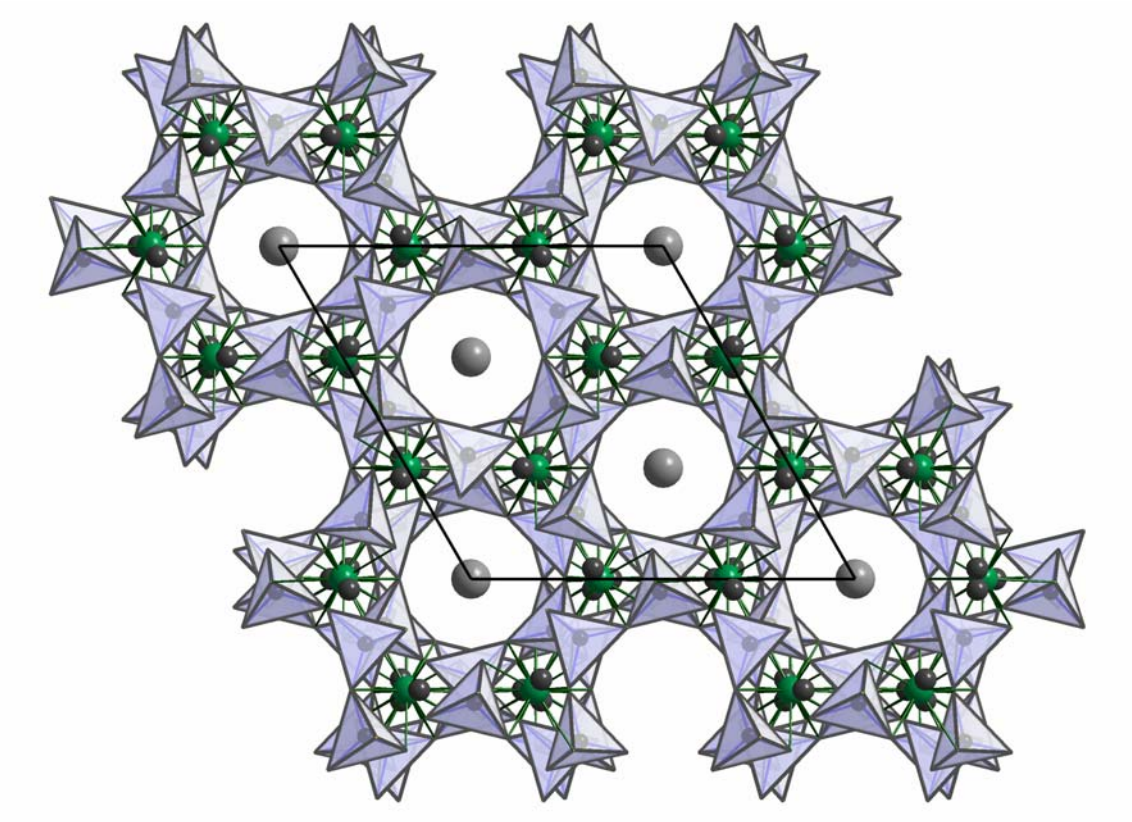

Figure 1. View of the structure of $CsLiU(PS_4)_2$ down the *c* axis illustrating the coordination of the uranium atoms and the linkage of the PS_4 tetrahedra.

The tunnels are filled with Cs^+ cations and have a diameter of approximately 6 Å, where the tunnel diameter is taken as the distance between "opposite" sulfur atoms, taking into account their atomic radii. The framework contains pseudotetrahedral U^{4+} centers bonded to four bidentate PS_4^{3-} ligands. The basic building block of this framework is the

$U(PS_4)_4$ unit shown in Figure 2. The $U(PS_4)_4$ unit exhibits crystallographically imposed *C2* symmetry; the central uranium atom is coordinated by four chelating PS_4^{3-} groups in a distorted square antiprismatic fashion, where the distortion of the coordination polyhedra may be caused by the strain within the four-membered US_2P ring or the S-P-S "bite angles" between 106.92(7)° and 113.93(8)°. Typical geometries for eight coordination are the bicapped trigonal prism or the square antiprism. A detailed analysis of the energetics of the U-S and P-S distances has shown only small energetic difference between these two arrangements,[21] and the preference for one alternative can be attributed to factors such as chelate ligand constraints, partially filled inner shells or hybridization effects. The U-S bond distances are unexceptional, selected values are compiled in Table 3. The average U-S distance is 2.838 Å in accordance with the sum of the ionic radii of the elements.[22] The average S-P-S "bite angle" of 110.43°, and the average U-S-P and S-U-S-angles of 91.68° and 69.36° are compatible with the presence of essentially planar US_2P rings. The P-U-P angles of 86.46(1)° (2x), 94.03(1)°, 119.00(1)° and 122.02(1)° (2x) indicate a compressional twist of the $U(S_2PS_2)_4$ "pseudotetrahedron". The thiophosphate groups are well defined by regular dimensions as indicated by P-S distances in the range 2.024(2)-2.047(2) Å. The mean value of 2.034 Å is in accordance with the P-S distances found in some metal orthothiophosphates.[23] According to the empirical rules of Pauling and Baur[24] it is established that the length of the S…S edges from a PS_4 tetrahedron shared with a cationic polyhedron is expected shorter than those of edges which are not shared. The corresponding S-P-S angles should also be found smaller. The observed S…S distances of the PS_4 tetrahedron in the structure clearly follow this rule with $d(S\ldots S)_{br}$ = 3.194(2) Å and 3.274(2) Å and $d(S\ldots S)_{free}$ ranging between 3.324(2) and 3.406 Å.

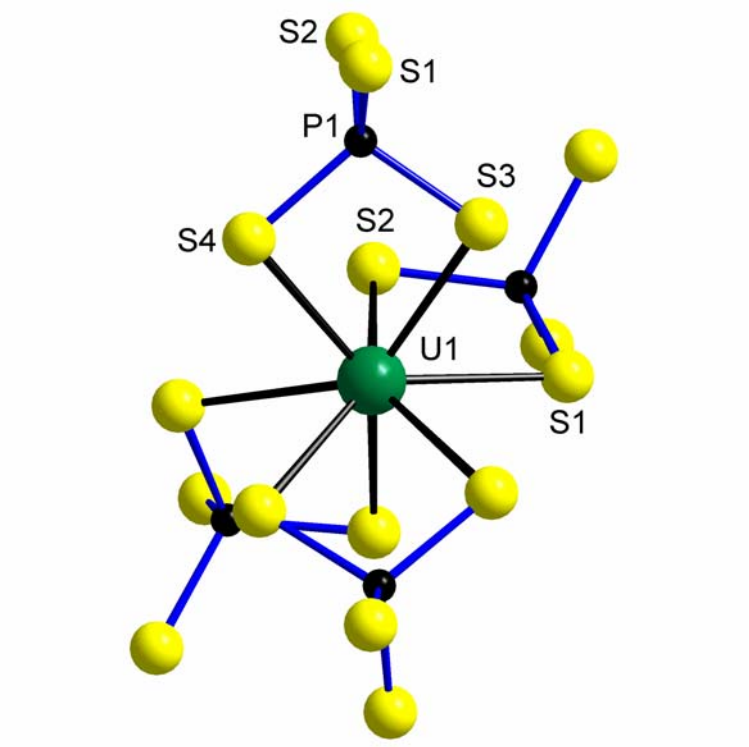

Figure 2. Coordination sphere of the U atoms in the structure of $CsLiU(PS_4)_2$.

An intriguing feature of $CsLiU(PS_4)_2$ is the tetrahedral coordination of the uranium centers by tetrahedral edge-bridging (μ-S_2PS_2) spacer units, which act as twofold bridging connectors. Therefore $CsLiU(PS_4)_2$ may be considered a chalcogenide analogue of zeolite frameworks whose structure is built up from tetrahedrally connected uranium centers and linearly connecting thiophosphate groups, with charge compensating cations in the channels of the zeotype framework. This is illustrated schematically in a wire frame plot in Figure 3, where the PS_4 groups are represented schematically by the central P atoms. The structure shown in Figure 3 is made up of 4- and 6-membered rings with the 4- and 6-rings forming channels along the twofold $(0\bar{1}0)$ and threefold (001) axes . The larger Cs^+ counter cations occupy the octahedral sites within these channels, whereas the smaller Li^+ cations are located at tetrahedral sites on cavities above/below the uranium atoms.

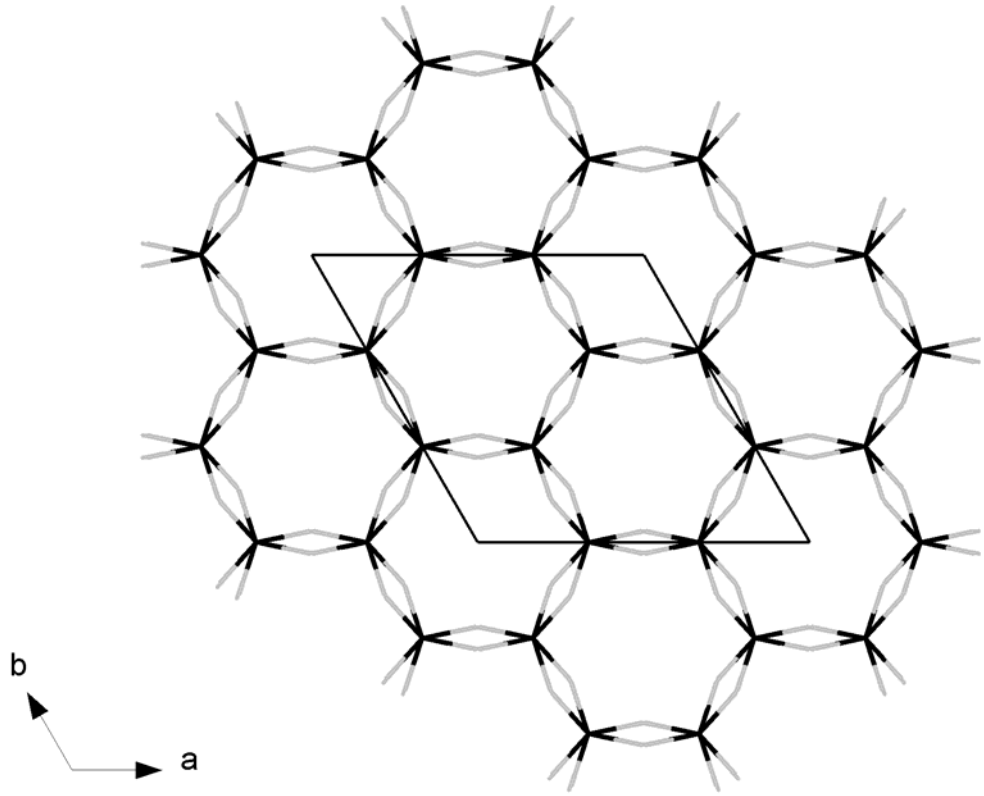

Figure 3. A schematic view of the three-dimensional framework structure of $CsLiU(PS_4)_2$ along the *c* direction. The PS_4 groups are represented only by the central P atoms of the PS_4 ligands for clarity.

It may be surprising, perhaps, that open-framework compounds can be synthesized at 700°C, i. e. under relatively harsh conditions, as it is commonly supposed that high-temperature procedures lead to dense, thermodynamically favored products rather than open, metastable phases. The success of the high-temperature technique may indicate that the structure is in fact not open, but that the cations rather fill the cavities and $CsLiU(PS_4)_2$ is effectively a dense phase. Still, once made and characterized, strategies for creating more open space in the structure may be employed, such as the exchange for smaller cations.[25]

Remarkably, except for a few examples such as $ATi_2(PS_4)_3$ (A = Li, Na, Ag),[23d,26,28] $TaPS_6$[23b] and $ANb_2P_2S_{12}$,[27] or $Ag_2NbTi_2P_6S_{25}$,[28] open frame-

work chalcogenide structures are obtained typically only with soft (according to Pearson) metals. However, high and variable coordination numbers of the early transition metals,[23,26-28] lanthanides,[29] or actinides[30] combined with the condensation equilibria of chalcophosphates[31] may lead to structural arrangements of astounding complexity, as the above examples indicate. The coordination preferences of the metal component are an important factor in the choice of the structure (and properties) of thiophosphates. The structures of the title compound and $U(P_2S_6)_2$ (**III**) indicate, that the coordination mode of the metal atom combined with the connectivity mode and size of the "linear" (rod-like) PS_4^{3-} or $P_2S_6^{2-}$ ligands may lead to the formation of complex network structures.

Based on a formal assignment of oxidation states the electronic structure of $CsLiU(PS_4)_2$ can be represented by $(Cs^+)(Li^+)(U^{4+})(PS_4^{3-})_2$. From this formula, an f^2 system with two unpaired electrons may be expected. The magnetic susceptibility of $CsLiU(PS_4)_2$ was measured as a function of temperature (4-300 K). The μ_{eff} of 2.83 μ_B at 300 K is consistent with an f^2 configuration.[32] The magnetic susceptibility of $CsLiU(PS_4)_2$ follows a Curie-Weiss type behavior with C = 1.14 cm^3 K/mol and θ = -49 K as apparent by the shape of the $1/\chi_{mol}$ vs. T and μ_{eff} vs. T curves. The negative value of θ indicates that antiferromagnetic interactions are present, although no antiferromagnetic ordering is observed down to 4 K. These observations are compatible with a large zero field splitting or uranium centers, which are magnetically coupled via the PS_4 ligands.

In conclusion, the formation of $CsLiU(PS_4)_2$ indicates that complex silicate or zeotype framework structures are not restricted to oxides or confined to the realm of coordination chemistry or soft-chemistry low-temperature approaches. Still, even oxidic open framework actinide compounds have been reported only recently.[33] Finally, it is apparent that similar to zeolites the inorganic template cations - in the present case Cs^+ and Li^+ - influence the anion framework profoundly, as the formally analogous $Na_2U(PS_4)_2$ (**VII**) crystallizes in a layer-type structure.

The formation of $CsLiU(PS_4)_2$ suggests, that chalcogenide open framework structures way beyond the well-known elements Al, Ge and P or the hexacoordinated transition metals to the eight-coordinated actinides such as uranium or thorium and early transition metals such as hafnium can be accessed. The combination of properties such as rigidity, coordination behavior, ligand dimensions, or thermal stability allows the use of the thiophosphate moieties for the synthesis of these "supramolecular" solid state aggregates.

6 $Cs_3UP_2S_8$, a coordination polymer based on an open tetrahedral network containing the unprecedented U=S thiouranyl unit

Introduction

Porous arrays on a nanometer scale are found in many crystalline compounds with tetrahedral oxide framework structures such as zeolites and AlPOs.[1] Recently, nanoporous framework structures based on non-oxide and/or non-tetrahedral units have attracted increasing attention because of their potential usage as new families of selective sorbents, ion exchangers or catalysts.[2] Except for organic coordination polymers,[3] most compounds with open framework structures are oxidic, but during the past few years significant progress towards the synthesis of open-framework chalcogenides has been made.[4-12] Most of them are based on group 3 or group 4 chalcogenide anions such as SnS_4^{4-},[13] $Sn_2S_6^{4-}$,[14] $Sn_2S_7^{6-}$,[15] $Sn_3S_7^{2-}$ [16] or $Sn_4S_{10}^{4-}$,[17] whose connectivity modes make them useful synthons for the construction of framework structures.

Tetrahedral network structures are, however, not restricted to main group elements or 3 *d* transition metals with low coordination numbers. For example, $CsLiU(PS_4)_2$ (**X**) and $U(P_2S_6)_2$ (**III**) contain three-dimensional silicate-type open framework structures. In uranium thiophosphates, the uranium atoms may be considered as coordination sites with tetrahedral connectivity, which are coordinated by P_xS_y groups. $Cs_3UP_2S_8$ may formally be considered a reduced variant of $CsLiU(PS_4)_2$ (**X**).

Experimental section

The following reagents were used as obtained: Cs (Chempur, 99.9 %), U (Kristallhandel Kelpin, 99.5 %), P_2S_5 (Aldrich, 99 %), S powder (Merck, 99.5 %), LiCl (Alfa Aesar, 99.996 %), CsCl (Acros, 99 %). All starting

compounds and products were examined by X-ray powder diffraction, using a Siemens D5000 diffractometer with a CuK_α source. Cs_2S was made following the procedure described in chapter 2. All substances were handled under argon atmosphere in a stainless steel glove box.

$Cs_3UP_2S_8$ (**XI**) was obtained originally by heating $CsU_2(PS_4)_3$ (**VI**) in an eutectic LiCl/CsCl mixture at 700°C. Dark red single crystals of $Cs_3UP_2S_8$ were obtained by annealing followed by slow cooling to room temperature over a duration of one week. Further experiments showed that $Cs_3UP_2S_8$ can also be prepared from a 500 mg mixture of uranium metal, sulfur, Cs_2S, and P_2S_5 with the molar ratio 4:8:1:3 in an evacuated quartz tube. The sample was heated in a furnace at a rate of 1°C/min up to 700°C and kept at this temperature for 3 days; subsequently, it was cooled to room temperature at a rate of 0.2°C/min. The resulting dark red powder was finely ground and 1.5 g of eutectic LiCl/CsCl mixture were added. After annealing the substance in an evacuated quartz tube for 7 days at 700°C it was cooled to room temperature in 3 days. Dark red hexagonal crystals were obtained by dissolving the halide melt with distilled water. Microprobe analysis of the crystals indicated the presence of cesium, uranium, phosphorus and sulfur in a 3:1:2:8 ratio.

Physical measurements

Crystal structure determination. The structure of $Cs_3UP_2S_8$ was determined from single crystal X-ray diffraction data. A single crystal of $Cs_3UP_2S_8$ was selected from the reaction mixture, embedded in a thin film of epoxy glue and fixed at the tip of a glass fiber on a Bruker SMART CCD diffractometer[18] equipped with a monochromated MoK_α source (λ= 0.71073 Å) and a graphite monochromator. The crystal to detector distance was 5 cm. Crystal decay was monitored by recollecting 50 initial frames at the end of the data collection. Data were collected by a scan of 0.3° in ω in groups of 600 frames at φ settings of 0°, 120° and 240°.

The exposure time was 30 s/frame. The collection of the intensity data was carried out with the program SMART.[18] Cell parameters were initially calculated from reflections taken from approximately 30 frames of reflections. The final lattice parameters were calculated from all reflections observed in the actual data collection. The data from the data collections were processed using the SAINT[19] program and corrected for absorption using SADABS.[20]

The structure was solved using direct methods which revealed the atomic positions and refined using the SHELXTL 5.1 program package.[21] The final refinement was carried out on F_O^2. Atomic scattering factors for spherical neutral free atoms were taken from standard sources and anomalous dispersion corrections were applied.[22] From the final refinement cycle the composition of the crystal used is $Cs_3UP_2S_8$. Calculations performed at an intermediate stage in which the relative positional occupancies were refined, revealed a disorder of the cation positions, but did not indicate any nonstoichiometry. The final coordinates and equivalent isotropic temperature factors of all atoms are given in Table 2.

FT-IR spectra. FT-IR spectra were recorded on solid samples in a CsI matrix. The samples were ground with dry CsI into a fine powder and pressed into transparent pellets. The spectra were recorded in the far-IR region (700-200 cm^{-1}, ≈ 5 cm^{-1} resolution) with a FT-IR spectrometer (2030 Galaxy-FT-IR, Mattson Instruments) equipped with a TGS/PE detector and a silicon beam splitter.

Results and discussion

$Cs_3UP_2S_8$ crystallizes in the rhombohedral space group $R\bar{3}$ with eighteen formula units per cell. Its structure is shown in Figure 1. It is based on a unique three-dimensional $U_2(S)_2(PS_4)_2(P_2S_6)^{6-}$ framework with large tunnels running parallel to the crystallographic *c* axis, where the disordered Cs^+ cations are located. The tunnels have a diameter of approximately 3.6 Å, where the tunnel diameter is taken as the distance between

"opposite" sulfur atoms, taking into account their *van der Waals* radii.[23] The framework contains U^{4+} centers with a pseudotetrahedral connectivity; Figure 2 illustrates that each U^{4+} is bonded to two bidentate PS_4^{3-} ligands and one tridentate $P_2S_6^{4-}$ ligand, which replaces one of the four bidentate thiophosphate ligands in the structures of $U(P_2S_6)_2$ (**III**) and $CsLiU(PS_4)_2$ (**X**), respectively. The fourth position of the coordination tetrahedron is occupied by a terminal sulfido ligand. The bond length order is $M{=}S_{terminal} < M{-}S_{bridging} < M{-}S_{triply\ bridging}$: the short U=S distance of 2.634(3) Å is compatible with the presence of a terminal sulfido ligand whereas the average $U{-}S_2PS_2$ and $U{-}S_3P{-}S$ separations of 2.808 Å and 2.954 Å are compatible with bis- and tris-chelating PS_4^{3-} or $P_2S_6^{4-}$ ligands.

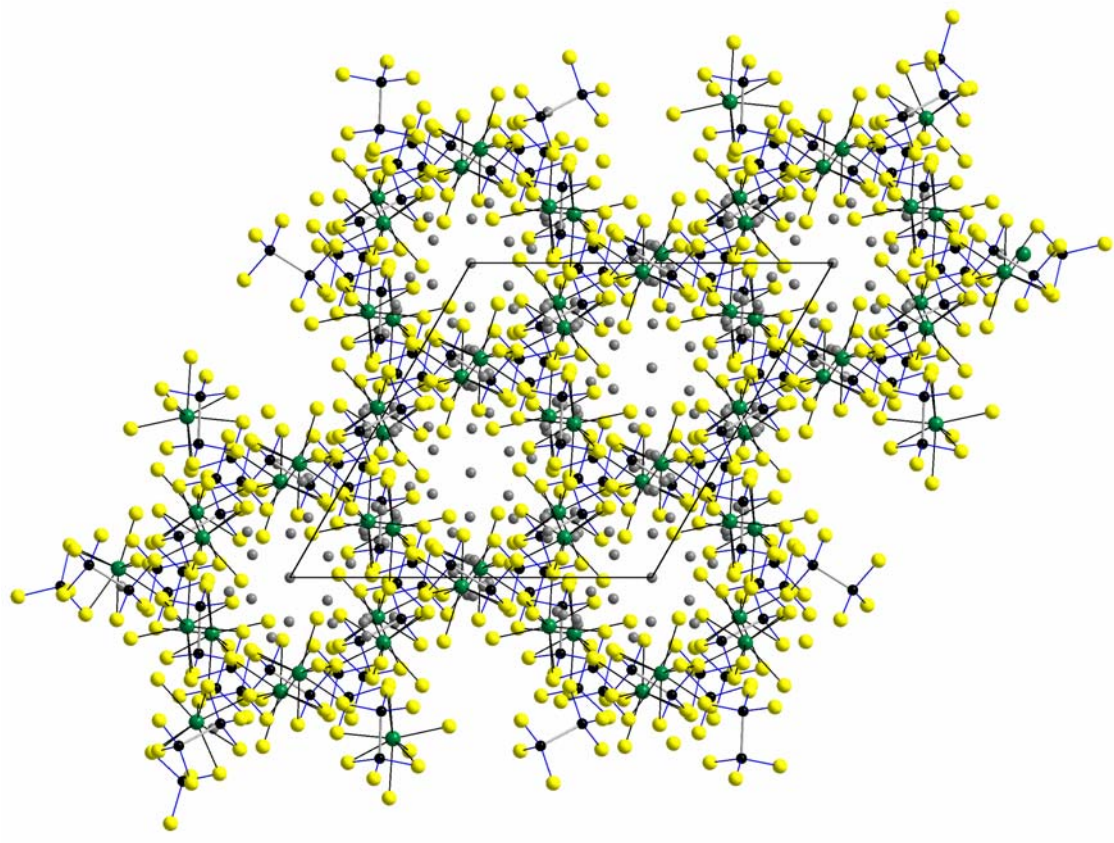

Figure 1. View of the unit cell down *c* illustrating the positions of the alkali metal cations in the structure channels.

The IR spectrum of $Cs_3UP_2S_8$ shows vibrations at 428 cm^{-1} and 457 cm^{-1} which may be assigned to the asymmetric and symmetric U=S vibrations, respectively. Corresponding values for the Nb=S vibrations in $[Nb_6S_{17}]^{4-}$ [24] or Cp*Nb(NAr)(S)(PMe_3)[25] are 483 cm^{-1} and 465 cm^{-1}, respectively, whereas 458 cm^{-1} and 435 cm^{-1} have been reported for the Nb=S stretching vibration in NbS_4^{3-} and TaS_4^{3-}, respectively.[26] The difference in the vibration frequencies may be accounted for by considering the reduced masses. Related results have been obtained for [Ta(Q)($Me_3SiNEt)_3N$] (Q = Se, Te)[27] and [Cp*Nb(NAr)PMe_3)Q] (Ar = 2,6-$iPrC_6H_3$; Q = S, Se, Te).[23] The U atoms in $Cs_3UP_2S_8$ display a slightly distorted square antiprismatic coordination, but it is well established that the two principal coordination geometries for eight-coordination, the bicapped trigonal prism or the square antiprism, are separated only by a small energetic difference.[28] The U-S single bond distances are unexceptional. The average U-S distance is 2.841 Å in accordance with the sum of the ionic radii.[29] The thiophosphate groups are well defined by regular dimensions as indicated by P-S distances in the range 2.007(4)-2.050(4) Å (mean: 2.026 Å), an average S-P-S "bite angle" of 110.9° and a P-P distance of 2.204(6) Å.

The most prominent feature of $Cs_3UP_2S_8$ is the terminal sulfido ligand. Terminal chalcogeno ligands are well established for M = Mo or W, but they are less common for the group 5 metals. Terminal chalcogeno ligands for the highly oxophilic group 4 metals have been a synthetic goal for a long time, and only recently terminal chalcogenido complexes have been stabilized with the aid of sterically demanding ligands.[30]

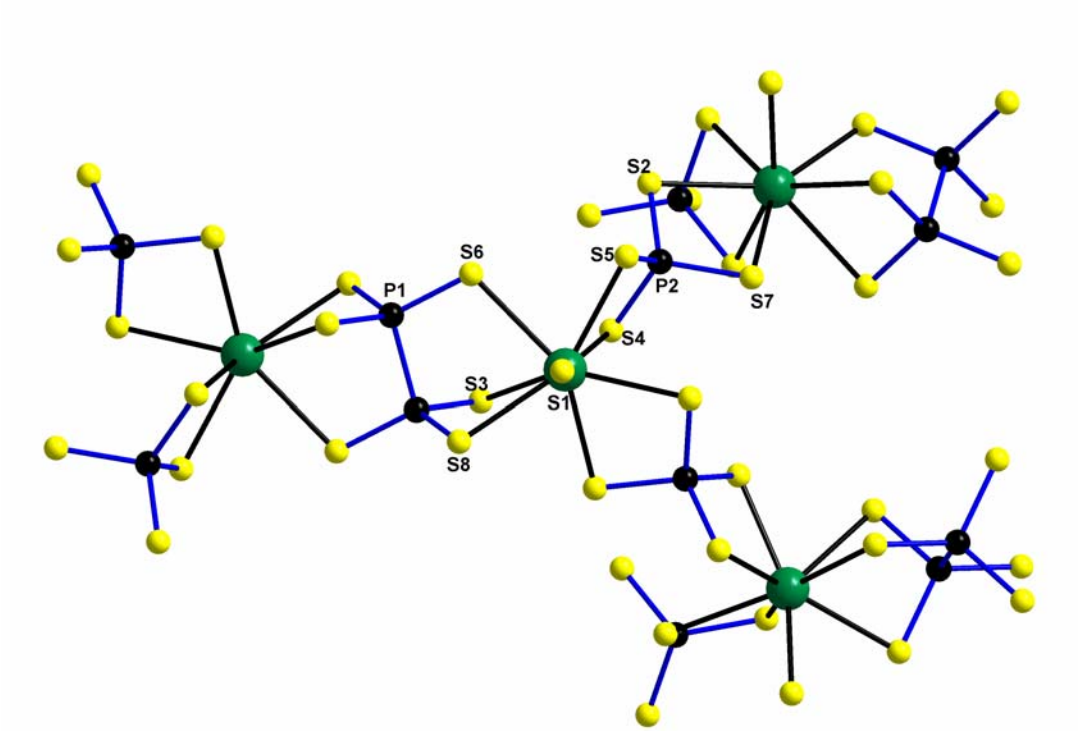

Figure 2. Fragment of the $[U(S)(PS_4)(P_2S_6)_{1/2}]^{3-}$ framework (with atomic labeling scheme) illustrating the pseudotetrahedral coordination geometry of the uranium atoms and the atom connectivity.

For the lanthanides or actinides the M=Q (Q = S, Se, Te) moiety is unknown. The U=S distance of 2.634(3) Å is approximately 0.2 Å shorter than the average U-S distances of 2.843 Å found in $CsLiU(PS_4)_2$ (**X**) and $U(P_2S_6)_2$ (**III**), slightly shorter than the Th=S distance of 2.743 Å in $Li_3Rb_6Th_3(S)S_2(PS_4)_5$ (**XIII**) but significantly longer than the M=S (M = Nb, Ta) distances of 2.196 and 2.204 Å in $[M_6S_{17}]^{4-}$ [24] or the Zr=Q distance of 2.650 Å in $[M(Te)\{TeSi(SiMe_3)_3\}_2dmpe_2]$,[30] if the differences of the ionic radii of Zr^{4+} (0.97 Å), Nb^{5+} (0.69 Å) and U^{4+} (0.87 Å), S^{2-} (1.84 Å) and Te^{2-} (1.87 Å) are taken into account. Still, the difference of approximately 0.2 Å between the U=S and U-$S_{bridging}$ distances is in good agreement with the Nb=S and Nb-$S_{bridging}$ distances typically observed for group 5 chalcogenides.

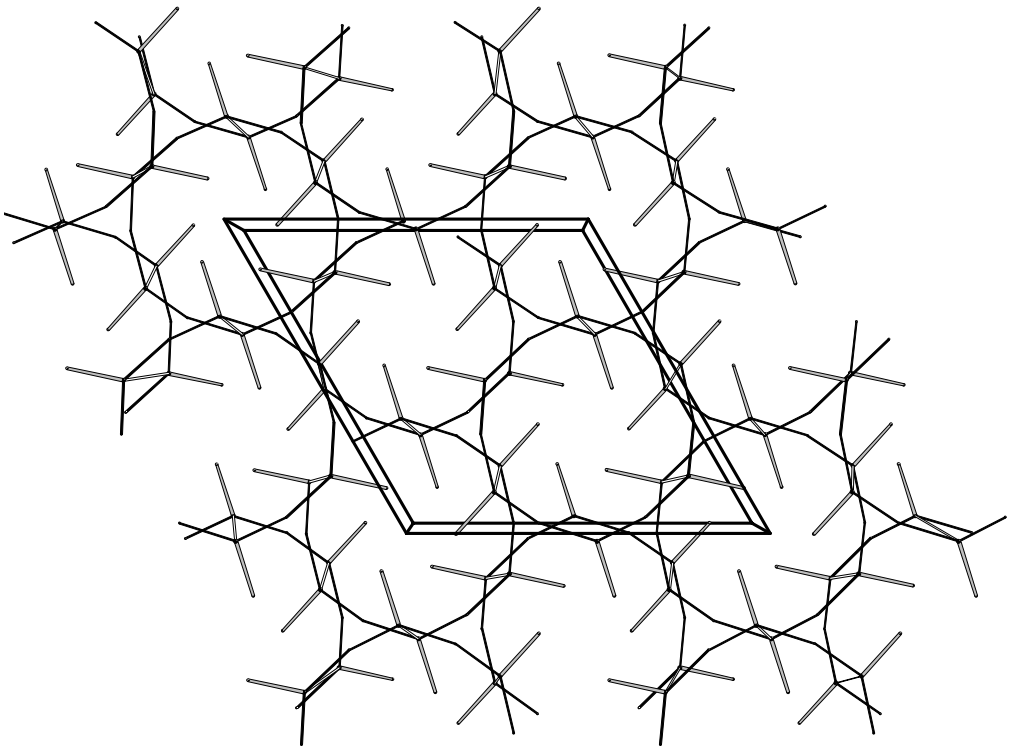

Figure 3. A schematic view of the three-dimensional framework structure of $Cs_3UP_2S_8$ along the *c* direction. The PS_4 groups are represented only by their central P atoms for clarity.

A second intriguing feature of $Cs_3UP_2S_8$ is the pseudotetrahedral coordination of the uranium centers by tetrahedral edge-briding (μ-S_2PS_2) spacer units, which act as twofold-bridging connectors. This leads to the formation of a framework structure as typically found for coordination polymers. Therefore $Cs_3UP_2S_8$ may be considered a topological chalcogenide analogue of open (alumo)silicate frameworks, whose structure is built up from pseudotetrahedrally connected uranium centers and linearly connecting thiophosphate groups, with charge compensating cations in the framework channels. The connectivity is illustrated schematically in a wire frame plot in Figure 3, where (for reasons of clarity) the PS_4 groups are represented by their central P atoms only. The structures of $Cs_3UP_2S_8$, $U(P_2S_6)_2$ (**III**) and $CsLiU(PS_4)_2$ (**X**) indicate, that many uranium thiophosphates might conceptually be assembled by a simple

LEGO-type approach according to the following recipe: (i) the U atoms act as pseudotetrahedral centers of connectivity, (ii) the bi- or tridentate thiophosphate ligands groups take the role of rod-like connectors, (iii) the general assemblage of corner sharing U(thiophosphate)$_4$ pseudotetrahedra follows the rules established for silicate networks. (iv) The structure of $Cs_3UP_2S_8$ presents an extension to these simple guidelines as the terminal =S moiety may substitute for a thiophosphate group but - as a terminal ligand – represents a dead end in the above connectivity pattern.

Finally, $Cs_3UP_2S_8$ may be regarded a reduced variant of the zeotype compound $CsLiU(PS_4)_2$ (**X**). In contrast to the well-known metal phosphorus trichalcogenides MPQ_3 (M = Mn, Fe, Co, Ni, Zn; Q = S, Se),[31] where low-lying metal *d* states have been shown to be acceptor levels (e. g. in alkali metal intercalation processes),[32] the highly electropositive U atoms in uranium thiophosphates such as $CsLiU(PS_4)_2$ (**X**) are unlikely to act as reduction sites, and the P atoms of the PS_4^{3-} anions are reduced to dithiophosphate (IV) $P_2S_6^{4-}$ groups. The isolated S^{2-} anion, which is expelled from the PS_4^{3-} anion in this reductive elimination step, remains bonded to the U atom and is captured in form of the sulfido group. The alkali cations engaged in the reduction process are taken up in the large pore channels of the framework. This view of the solid state synthesis of the title compound suggests that $Cs_3UP_2S_8$ may be accessible by a topotactic reaction from $CsLiU(PS_4)_2$ (**X**). The similarity of the connectivity patterns, the lattice constants as well as the resulting structure symmetries lend support to this hypothesis.

Conclusion

In conclusion, the synthesis and structure of $Cs_3UP_2S_8$ indicates that chalcogeno ligands may be stabilized even in the presence of the highly oxophilic metals from the actinide series. Furthermore, it supports the hypothesis that solid state compounds which are analogous to coor-

dination polymers are accessible through high-temperature solid state reactions, i. e. a solid state counterpart of supramolecular wet chemistry based on a simple LEGO-approach may be envisioned. Finally, it indicates that complex silicate or zeotype framework structures are not restricted to oxides or confined to the realm of coordination chemistry or soft-chemistry low-temperature approaches.

7 An unprecedented M=S unit in the structure of the novel thiophosphates $Li_3Rb_6M_3(S)S_2(PS_4)_5$ (M = Th, U)

Introduction

The chemistry of metal chalcogenides has attracted much interest in the past and an extensive set of binary, ternary and quaternary representatives has been obtained.[1,2] In many of these compounds the metal is bound to the chalcogen Q (Q = S, Se) in the form of the chalcogenido (Q^{2-}), perchalcogenido (Q_2^{2-}) or polychalcogenido (Q_n^{2-}) moieties. In addition, chalcogen containing ligands such as thiolates[3,4] (in coordination chemistry) or chalcophosphates[5] (in solid state chemistry) have added to the structural variety that is possible when chemically versatile metals M and chalcogens Q are present. This structural flexibility can be traced back to the large flexibility of Q as a coordinating ligand. For example, Q^{2-} may be bound in form of the M=S moiety, but it can act also as 2-, 3-, 4-, and 5-fold bridging ligand.[6] Similarly, the Q_2^{2-} group has been observed in an amazing number of coordination modes.[6,7] Whereas the M=Q moiety is quite common in the chemistry of Mo, W or Re, it is much less stable for the group 5 metals, and compounds containing this unit have never been described for the highly oxophilic group 4 metals or the lanthanides and actinides. Another possible reason for the apparent instability of the M=Q moiety seems to be its high reactivity, which at times may lead to coupling reactions; Bergman and co-workers showed[8] that like the $(Cp^*)_2Zr{=}NR$ and $(Cp^*)_2Zr{=}O$ complexes, the $(Cp^*)_2Zr{=}S$ complex could be generated *in situ*, and the existence of the Zr=S functional group was demonstrated in trapping experiments with alkynes, nitriles or dative ligands. The compounds $Li_3Rb_6U_3(S)S_2(PS_4)_5$ and $Li_3Rb_6Th_3(S)S_2(PS_4)_5$ contain the highly unusual M=S (M = Th, U) unit.

Experimental section

Starting materials were uranium metal powder (Kristallhandel Kelpin, 99.9 %), P_2S_5 (Aldrich, 99 %), Cs_2S, K_2S, S powder (Merck, 99.999 %), RbCl (Alfa Aesar, 99.8 %) and LiCl (Alfa Aesar, 99.996 %). All starting compounds and products were examined by X-ray powder diffraction, using a Siemens D5000 diffractometer with a CuK_α source. Alkali metal sulfides, A_2S (A = K, Cs) were made by reacting stoichiometric amounts of the elements in liquid ammonia as described in chapter 2.

$Li_3Rb_6U_3(S)S_2(PS_4)_5$ (XII). 300 mg (0.21 mmol) of a sample with the formal composition $CsU_2(PS_4)_5$ were sealed with 1.5 g of an eutectic LiCl/RbCl mixture under vacuum in a quartz ampoule with an outer diameter of 8 mm. The sample was placed in a programmable tube furnace and heated from room temperature up to 700°C at a rate of 10°C/h, kept at that temperature for 60 h and cooled down to room temperature at a rate of 0.5°C/min. The reaction product contained dark red needle-shaped crystals of $Rb_{11}U_7(PS_4)_{13}$ (**IX**) and small amounts of black plate-like crystals of $Li_3Rb_6U_3(S)S_2(PS_4)_5$ embedded in an amorphous LiCl/RbCl matrix. The LiCl/RbCl mixture could be removed by treating the product with dry methanol. Attempts to prepare $Li_3Rb_6U_3(S)S_2(PS_4)_5$ from high temperature reactions or from thiophosphate fluxes did not lead to the desired results.

$Li_3Rb_6Th_3(S)S_2(PS_4)_5$ (XIII). 300 mg (0.48 mmol) of a sample with the formal composition $K_2Th(PS_4)_2$ were sealed with 1.5 g of an eutectic LiCl/RbCl mixture under vacuum in a quartz ampoule with an outer diameter of 8 mm. The sample was placed in a programmable tube furnace and heated from room temperature up to 700°C at a rate of 10°C/h, kept at that temperature for 60 h and cooled down to room temperature at a rate of 0.5°C/min. The reaction product contained black plate-like crystals embedded in an amorphous LiCl/RbCl matrix. The LiCl/RbCl mixture could be removed by treating the product with dry methanol. The yield of the black crystalline material was approximately

90 % based on the initial metal content as judged by X-ray powder diffraction. Attempts to prepare $Li_3Rb_6Th_3(S)S_2(PS_4)_5$ from high temperature reactions or from thiophosphate fluxes did not lead to the desired results.

Crystal structure determination

The crystal structures of both compounds were determined from single crystal X-ray diffraction data. Single crystals of $Li_3Rb_6U_3(S)S_2(PS_4)_5$ and $Li_3Rb_6Th_3(S)S_2(PS_4)_5$ were selected from the reaction mixtures, embedded in a thin film of epoxy glue and fixed at the tip of a glass fiber on a Bruker SMART CCD diffractometer[9] equipped with a monochromated MoK_α source (λ= 0.71073 Å) and a graphite monochromator. The crystal to detector distance was 5 cm. Crystal decay was monitored by recollecting 50 initial frames at the end of the data collection. Data were collected by a scan of 0.3° in ω in groups of 600 frames at φ settings of 0°, 120° and 240°. The exposure time was 30 s/frame. The collection of the intensity data was carried out with the program SMART.[9] Cell parameters were initially calculated from reflections taken from approximately 30 frames of reflections. The final lattice parameters were calculated from all reflections observed in the actual data collection. The data from the data collections were processed using the SAINT[10] program and corrected for absorption using SADABS.[11] The structures were solved using direct methods which revealed the atomic positions and refined using the SHELXTL 5.1 program package.[12] The final refinements were carried out on F_O^2. Atomic scattering factors for spherical neutral free atoms were taken from standard sources and anomalous dispersion corrections were applied.[13]

From the final refinement cycle the compositions of the crystals used are $Li_3Rb_6U_3(S)S_2(PS_4)_5$ and $Li_3Rb_6Th_3(S)S_2(PS_4)_5$. The reasonableness of the anisotropic thermal parameters for the atoms in the structures suggests a

stoichiometric composition. Calculations performed at an intermediate stage in which the relative positional occupancies were refined, revealed a disorder of the cation positions, but did not indicate any non-stoichiometry. The positions of the disordered lithium atoms could not be determined. The final coordinates and equivalent isotropic temperature factors of all atoms are given in Tables 2 and 4.

Results and discussion

A perspective view of the crystal structure of $Li_3Rb_6M_3(S)S_2(PS_4)_5$ (M = Th, U) along the crystallographic ***b*** axis is provided in Figure 1. The structure is built up from two fragments which are illustrated in Figure 2.

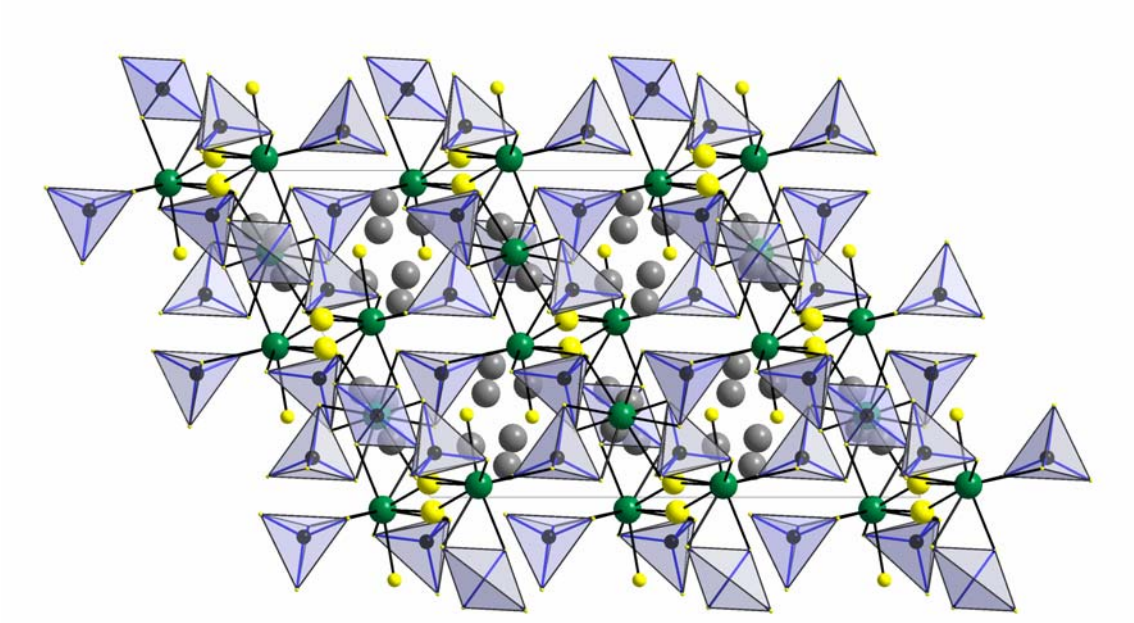

Figure 1. Crystal structure of $Li_3Rb_6M_3(S)S_2(PS_4)_5$ (M = Th, U), view along the crystallographic ***b*** axis.

Fragment 1, highlighted in Figure 2a, contains a dimeric unit consisting of M (Th, U) atoms interconnected by a sulfur bridge. In addition, three PS_4^{3-} anions are coordinated to the metals in a bidentate manner. The

square antiprismatic S coordination is completed by the highly unusual M=S unit. The Th1/U1-S2 bond in the M=S unit has a length of 2.744(2)/2.676(4) Å; it is significantly shorter than the other metal-sulfur bonds, which are in the range of 2.804(10)-2.922(3) Å for $Li_3Rb_6Th_3(S)S_2(PS_4)_5$ and 2.735(2)-2.923(1) Å for $Li_3Rb_6U_3(S)S_2(PS_4)_5$. The M1-S2 bond length is in accordance with the values expected for M=S double bonds. The rare thiouranyl unit is also present in the framework compound $Cs_3UP_2S_8$ (**XI**).

Another uncommon feature in the structure of $Li_3M_6Th_3(S)S_2(PS_4)_5$ is the existence of a singly μ-bridging S atom between two metal sites. The bridging S atom is displaced 0.56/0.66 Å (Th/U) from the ***4a*** site to a general position resulting in a disorder of S1 and M-S1-M angles of 153.7°/157.8°. While S_2 units coordinated to metal atoms are very popular among the group 5 chalcogenophosphates,[7] singly μ-bridging S atoms are very unusual in transition metal chalcogenides with coordination numbers higher than 4. The second fragment, which is shown in Figure 2b, contains a single metal atom coordinated by four bidentate PS_4^{3-} groups in a pseudotetrahedral fashion with average S-M-S angles of 67.9(1)/68.6(1)° for the S atoms of each PS_4^{3-} ligand.

Both fragments are interconnected in an alternating manner by the PS_4^{3-} groups to form chains running along the [201] direction. As fragment 2 is 4-connecting it acts also as a linking element to two other type-1 fragments along [001]. Since the M=S thio group of fragment 1 is in a terminal position, fragment 1 is 4-connecting as well by means of its μ-bridging sulfur atom and its three PS_4^{3-} groups.

Thus, the full 3D structure of the title compound is made up of two different 4- connected fragments, $M(S)S(PS_4)_3$ and $M(PS_4)_4$. It may be viewed as a silicate-analog open framework compound, where the Li^+ and Rb^+ counter cations are located in the voids of the network.

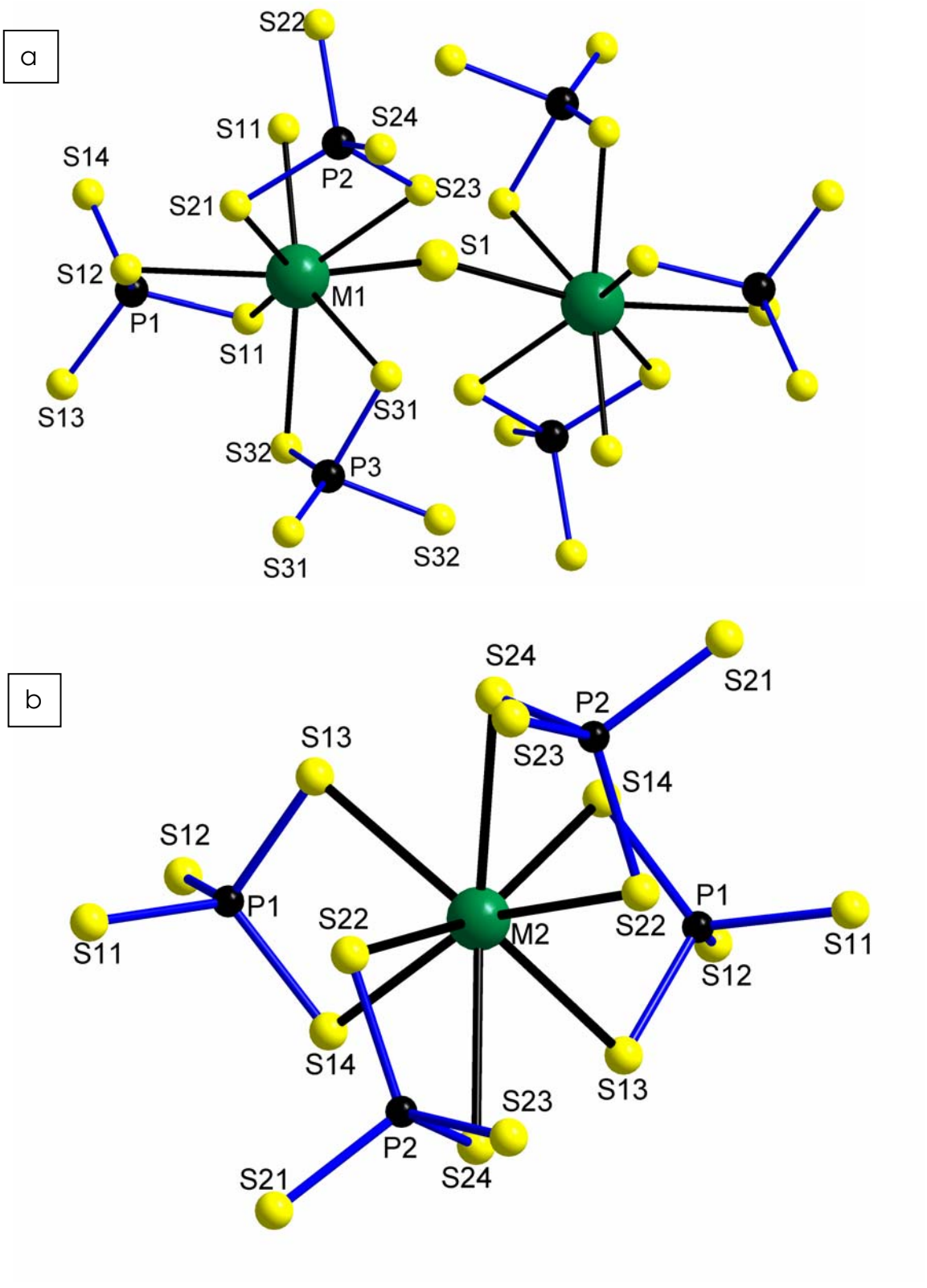

Figure 2. Fragments of the anionic framework (with atomic labeling scheme) highlighting the M=S unit, the μ-bridging S ligand, the pseudotetrahedral coordination geometry of the actinide atoms and the atom connectivity

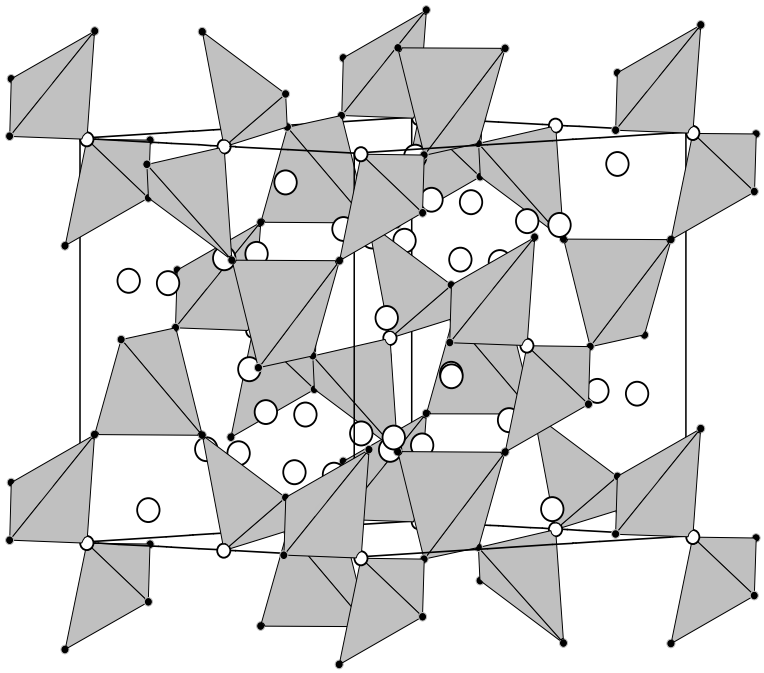

Figure 3. A schematic view of the three-dimensional framework structure of $Li_3Rb_6M_3(S)S_2(PS_4)_5$ (M = Th, U). The S atoms of the thiophosphate and M=S groups are omitted for clarity.

This is illustrated in Figure 3, where the polyhedra represent the pseudotetrahedral coordination of the M atoms. The structure is thus related to $U(P_2S_6)_2$ (**III**) and $CsLiU(PS_4)_2$ (**X**), two silicate-analog uranium thiophosphates, whose structures are based on tetrahedrally connected metal centers and twofold connecting $P_2S_6^{2-}$ or PS_4^{3-} thiophosphate groups. One may speculate about a potential template effect of the cations, in the present case Rb^+ and Li^+, as $Na_2U(PS_4)_2$ (**VII**) and $CsLiU(PS_4)_2$ (**X**) - formally analogous but with different cations - adopt very different structures.

$Li_3Rb_6Th_3(S)S_2(PS_4)_5$ and $Li_3Rb_6U_3(S)S_2(PS_4)_5$ belong to the large group of framework compounds based on 4-connected groups such GeS_4^{4-} [14] or the adamantane-type $[Ge_4Q_{10}]^{4-}$ (Q = S, Se) cage unit [15] whose tetrahedral topology makes them useful synthons to substitute for the ubiquitous TO_4 units from silicate or oxide chemistry.

8 Summary

The new thiophosphates **I**-**XIII** were prepared from reactive fluxes. **I**-**VIII** and **X** could be obtained from reactive thiophosphate melts; **IX**, **XI**, **XII** and **XIII** were synthesized by dissolving amorphous precursors in a eutectic alkali metal halide flux. The crystal structures of all compounds were determined by single-crystal X-ray diffraction methods.

UP_2S_6 (**I**) crystallizes in the ZrP_2S_6 structure type (tetragonal, $P4_2/m$). The uranium (IV) centers are arranged in a regular rectangular pattern and coordinated by the bidentate $P_2S_6^{4-}$ anions in a pseudo-tetrahedral fashion. These ligands act as square-planar connectors crosslinking four coplanar metal sites. Thus, the UP_2S_6 structure may be considered as a stuffed analogue of the PtS structure type with the S sites occupied by the uranium atoms and the Pt sites represented by the centers of gravity of the ligands.

The structure of UP_2S_7 (**II**) (orthorhombic, $Fddd$) is closely related to the monoclinic ZrP_2S_7 structure type. It consists of U^{4+} cations linked by $P_2S_7^{4-}$ ligands. A formal replacement of the anionic unit with a single pseudo ion located at the center of gravity results in the formation of a framework consisting of tetrahedrally connected atoms. This arrangement can be described as a distorted ZnS structure. The presence of the highly elongated anionic unit reduces the space filling of the unit cell significantly, the result is a 3D network containing large pores.

In the compound $U(P_2S_6)_2$ (**III**) (tetragonal, $I4_1/a$), the metal atoms are connected by bidentate $P_2S_6^{2-}$ anions. This arrangement can be considered as a pseudotetrahedral coordination of the uranium atoms by the quasilinear connectors. As a result, a three-dimensional framework system with large cavities is obtained. Three of these "super-diamond" type networks are inseparably interwoven in order to obtain optimum space filling.

$U_3(PS_4)_4$ (**IV**) (tetragonal, $I4_1/acd$) crystallizes in a defect variant of the $PrPS_4$ structure. The structure of $U_3(PS_4)_4$ consists of tetravalent uranium

atoms connected by PS_4^{3-} groups. The pseudotetrahedral coordination of the U atoms can be visualized by replacing the orthothiophosphate anions with single spherical pseudoanions. Each of these pseudoanions resides in a square planar coordination. The resulting framework structure can be described as a superstructure of the *anti*-PtS structure type, in which 25% of the sites occupied by the uranium centers remain empty.

Vibrational spectra, which were recorded for **I-III**, show good agreement between the obtained results and the expected values for the anionic units, while magnetic measurements confirm the presence of tetravalent uranium.

The introduction of alkali metal cations into the uranium thiophosphate systems led to the formation of polyanionic $U_xP_yS_z^{a-}$ frameworks or isolated Zintl-type anions.

The quaternary alkali metal uranium thiophosphate $Rb_5U(PS_4)_3$ (**V**) crystallizes in the $K_5U(PS_4)_3$ structure (monoclinic $P2_1/c$). This structure type represents the first actinide thiophosphate system containing Zintl-type anions. The centrosymmetric $[U_2(PS_4)_6]^{10-}$ unit consists of a $U_2(PS_4)_2$ core, which is terminated on each side by two PS_4^{3-} thiophosphate ligands in a bidentate fashion. The preparation of a solution containing the free anion $[U_2(PS_4)_6]^{10-}$ was attempted, however, the Zintl anion disintegrates upon contact with the solvent and the S_3^- radical anion is formed instead.

The anionic framework of $CsU_2(PS_4)_3$ (**VI**) (monoclinic, $P2_1/c$) can be described as a system of $[U_2(PS_4)_6]^{10-}$ building blocks linked by additional uranium atoms. The compound contains two different one-dimensional tunnel systems running parallel to the *b* axis. The larger tunnels are filled with the Cs^+ cations (fractionally distributed over three distinct crystallographic sites) whereas the smaller ones remain empty. The arrangement of the cations in the cavities can be visualized as a system of distorted planar hexagonal layers parallel to the $(\bar{1}02)$ plane.

$Na_2U(PS_4)_2$ (**VII**) crystallizes in the monoclinic space group Cc. The structure contains linear $[U_2(PS_4)_5]_x$ chains running along $[110]$ and $[\bar{1}10]$

linked by additional uranium atoms. The resulting framework consists of two 2D $[U(PS_4)_2]_x$ layers per unit cell with disordered sodium cations residing in the cavities and in the *van der Waals* gap between the layers. The arrangement of the PS_4 tetrahedra linking the uranium atoms in the structure of $Na_2U(PS_4)_2$ shows an important difference to the $U_2(PS_4)_6$ building blocks found in **V**, **VI** and **VIII**. While these units are centrosymmetric, the bridging tetrahedra in **VII** are related by a twofold rotation axis, resulting in a distorted D_{2h} symmetry for the $U_2(PS_4)_6$ entity. $Na_2U(PS_4)_2$ crystals exhibit a systematic non-merohedral twinning which simulates a larger, orthorhombic cell with $c' = 2\ c^*\sin\beta$. However, the monoclinic habit of the crystals and the large value of c' were taken as evidences of a lower symmetry.

The crystal structure of $K_{11}U_7(PS_4)_{13}$ (**VIII**) (tetragonal, $I\bar{4}2d$) contains a tunnel system composed of eight interlocking $U_7(PS_4)_{13}$ screw helices with the alkali metal cations residing inside the framework channels. These helices are built up from uranium atoms interconnected by PS_4 tetrahedral units. In order to achieve chain commensurability, distortions of the US_8 coordination polyhedra are necessary; this leads to a ninefold S-coordination for one of the uranium atoms. Single crystals of the isostructural compound $Rb_{11}U_7(PS_4)_{13}$ (**IX**) could only be obtained by dissolving the amorphous precursor UPS_5 in an eutectic LiCl/RbCl melt.

The anionic framework of $CsLiU(PS_4)_2$ (**X**) (rhombohedral, $R\bar{3}c$) is a unique three-dimensional $[U(PS_4)_2]^{2-}$ system consisting of pseudotetrahedral U^{4+} centers bonded to four bidentate PS_4^{3-} ligands, which act as quasilinear connectors. The structure contains large tunnels running parallel to the crystallographic c axis. The larger cesium counter cations occupy the octahedral sites within these channels, whereas the smaller lithium cations are located at tetrahedral sites on cavities above/below the uranium atoms. It is apparent that, similar to the results found for zeolites, the diameter of the templating alkali metal cations influences the formation of the anionic framework profoundly, as the formally analogous $Na_2U(PS_4)_2$ (**VII**) crystallizes in a layer-type structure.

Magnetic susceptibility measurements performed for **VIII** and **X** revealed that the uranium atoms are in both cases magnetically coupled via the PS_4 groups. Below the Néel temperature, antiferromagnetic ordering can be observed. In the paramagnetic region, **X** shows Curie-Weiss type behavior, in **VIII**, a modified Curie-Weiss law is observed.

The crystal structure of $Cs_3UP_2S_8$ (**XI**) (rhombohedral, $R\bar{3}$) may be regarded as a reduced variant of the $CsLiU(PS_4)_2$ (**X**) structure type. A reduction of 50% of the PS_4 units in the parent compound leads to the formation of one $P_2S_6^{4-}$ group and two S^{2-} anions from two PS_4^{3-} anions. The dithiophosphate(IV) unit acts as a triply bridging quasilinear connector between two adjacent uranium centers. The S^{2-} units, which are expelled from the orthothiophosphate anions in the reductive elimination step, remain bonded to the U atoms as terminal sulfido ligands. The resulting three-dimensional $U_2(S)_2(PS_4)_2(P_2S_6)^{6-}$ framework contains large tunnels running parallel to the crystallographic *c* axis, where the charge compensating Cs^+ cations are located. This interpretation of **XI** as a reduced variant of **X** suggests that the compound may be accessible by a topotactic reaction. The similar lattice constants of the unit cells, the related connectivity patterns for both crystal structures, as well as the resulting structure symmetry lend support to this hypothesis.

The isotype compounds $Li_3Rb_6U_3(S)S_2(PS_4)_5$ (**XII**) and $Li_3Rb_6Th_3(S)S_2(PS_4)_5$ (**XIII**) crystallize in the monoclinic space group *C2/c*. Their structure contains different connectivity patterns for the two actinide atom sites. While one is coordinated by four bidentate PS_4^{3-} groups in a pseudotetrahedral fashion, the second atom is linked to only three PS_4^{3-} anions. The coordination polyhedron is completed by a single S atom, which acts as a sulfur bridge between two metal cations and the terminal M=S group. The actinide centers are interconnected by the PS_4^{3-} groups, the result is a wide-meshed network structure, with the counter cations residing in the cavities.

The investigated compounds contain tetravalent actinide cations, which are coordinated in a square antiprismatic fashion by eight sulfur

atoms. With the thiophosphate anions $P_xS_y^{z-}$ acting in most cases as bidentate ligands, the result is a pseudotetrahedral connectivity for the metal centers. The general assemblage of these corner-sharing U(thiophosphate)$_4$ pseudotetrahedra follows the rules established for silicate networks. The structures of **XI**-**XIII** present an extension to these simple guidelines, as the =S unit may act as a substitute for a thiophosphate group but - as a terminal ligand - represents a dead end in the connectivity pattern.

A comparison of the crystal structures of **VI**-**XIII** shows that the pore size of these "zeotype" compounds is not only determined by the stoichiometry of the educts, but also by the radii of the templating alkali metal cations residing in the cavities. Another method to obtain optimum space filling in a crystal structure is the formation of several interpenetrating frameworks, which fill each other's empty cages and tunnels. In systems containing metal centers with a (pseudo)tetrahedral environment and rigid quasilinear connectors, diamondoid frameworks are observed. The number of interwoven identical units is determined by the length of the connecting rod-like ligand. While this behaviour is often present in the crystal structures of coordination compounds obtained from solutions, **III** is one of the few examples for the formation of interpenetrating networks during a high-temperature reaction.

The requirements of both large cavities and linear connectors in the same structure explains the absence of interpenetrating networks in the other ternary uranium thiophosphate compounds UP_2S_6 (**I**), UP_2S_7 (**II**) and $U_3(PS_4)_4$ (**IV**).

The multitude of connectivity patterns observed in the crystal structures of **I**-**XIII** leads to the belief that transition metal thiophosphates might conceptually be assembled by a simple LEGO-type approach with the different $P_xS_y^{z-}$ anions acting as connectors between pseudotetrahedrally coordinated metal centers.

Appendix

Chapter 2

Table 1. Crystallographic data for compounds **I-IV**.

	I	**II**	**III**	**IV**
empirical formula	UP_2S_6	UP_2S_7	$U(P_2S_6)_2$	$U_3(PS_4)_4$
formula weight	492.33	524.39	746.63	1350.93
crystal system	tetragonal	orthorhombic	tetragonal	tetragonal
space group	*P4₂/m*	*Fddd*	*I4₁/a*	*I4₁/acd*
a [Å]	6.8058(7)	8.9966(15)	12.8776(9)	10.7440(9)
b [Å]	6.8058(7)	15.287(2)	12.8776(9)	10.7440(9)
c [Å]	9.7597(14)	30.319(5)	9.8367(10)	19.097(2)
V [Å³]	452.06(9)	4169.8(12)	1631.2(2)	2204.4(4)
Z	2	16	6	2
ρ_{calcd} [g cm^{-3}]	3.617	3.341	3.040	2.035
Temperature [K]	203(2)	203(2)	203(2)	183(2)
μ (MoK_α) [mm^{-1}]	19.605	17.207	11.850	11.890
θ range [°]	2.99 - 28.22	2.71 - 28.35	2.61 - 28.22	3.43 - 28.29
index ranges	$-9 \le h \le 8$	$-11 \le h \le 10$	$-5 \le h \le 17$	$-14 \le h \le 13$
	$-9 \le k \le 9$	$-20 \le k \le 6$	$-11 \le k \le 16$	$-14 \le k \le 7$
	$-13 \le l \le 12$	$-26 \le l \le 40$	$-12 \le l \le 10$	$-25 \le l \le 24$
measured reflections	4181	2561	2708	6040
independent reflections	591	1256	1003	690
observed reflections [$I > 2\sigma(I)$]	511	888	913	543
R_{int}	0.0437	0.0588	0.0327	0.0490
parameters	25	48	39	30
goodness-of-fit on F²	1.363	0.954	1.024	1.126
R values	*R1* = 0.0322	*R1* = 0.0449	*R1* = 0.0270	*R1* = 0.0330
[$I > 2\sigma(I)$]	*wR2* = 0.0627	*wR2* = 0.0877	*wR2* = 0.0595	*wR2* = 0.0901
R values	*R1* = 0.0384	*R1* = 0.0775	*R1* = 0.0320	*R1* = 0.0413
(for all data)	*wR2* = 0.0637	*wR2* = 0.0955	*wR2* = 0.0610	*wR2* = 0.0923
residual electron density [e*Å^{-3}]	1.192 / -3.425	1.780 / -2.150	2.211 / -1.291	1.838 / -3.302

Table 2. Atom coordinates [x 10^4] and isotropic thermal parameters [$Å^2$ x 10^3] of UP_2S_6 (**I**). U(eq) is defined as one third of the trace of the orthogonalized matrix U_{ij}.

	x	y	z	U(eq)
U(1)	0	0	2500	9(1)
P(1)	-606(4)	3485(4)	0	8(1)
S(1)	-2191(3)	3207(3)	1732(2)	13(1)
S(2)	1812(4)	1717(4)	0	9(1)

Table 3. Selected bond distances [Å] for UP_2S_6 (**I**).

U(1)-S(1) (4x)	2.748(2)	P(1)-S(1) (2x)	2.014(2)
U(1)-S(2) (4x)	2.973(2)	P(1)-S(2)	2.038(4)
		P(1)-P(1)	2.221(5)

Table 4. Atom coordinates [x 10^4] and isotropic thermal parameters [$Å^2$ x 10^3] of UP_2S_7 (**II**). U(eq) is defined as one third of the trace of the orthogonalized matrix U_{ij}.

	x	y	z	U(eq)
U(1)	1250	1250	152(1)	11(1)
P(1)	1187(4)	3195(2)	689(1)	12(1)
S(1)	1826(3)	66(2)	3069(1)	13(1)
S(2)	890(3)	4069(2)	197(1)	16(1)
S(3)	2851(3)	247(2)	762(1)	15(1)
S(4)	1250	4026(2)	1250	16(1)

Table 5. Selected bond distances [Å] for UP_2S_7 (**II**).

U(1)-S(3) (2x)	2.801(3)	P(1)-S(3)	2.009(4)
U(1)-S(2) (2x)	2.825(3)	P(1)-S(2)	2.021(4)
U(1)-S(1) (2x)	2.885(3)	P(1)-S(1)	2.063(4)
U(1)-S(1) (2x)	2.939(3)	P(1)-S(4)	2.123(3)

Table 6. Atom coordinates [x 10^4] and isotropic thermal parameters [$Å^2$ x 10^3] of $U(P_2S_6)_2$ (**III**). U(eq) is defined as one third of the trace of the orthogonalized matrix U_{ij}.

	x	y	z	U(eq)
U(1)	0	1/4	1/8	11(1)
P(1)	62(1)	662(1)	3808(1)	13(1)
S(1)	1681(1)	1840(1)	6774(1)	17(1)
S(2)	1195(1)	1681(1)	3480(1)	19(1)
S(3)	-1812(1)	-1557(1)	-238(1)	16(1)

Table 7. Selected bond distances [Å] for $U(P_2S_6)_2$ (**III**).

U(1)-S(3) (4x)	2.812(1)	P(1)-S(2)	1.989(2)
U(1)-S(2) (4x)	2.879(1)	P(1)-S(3)	1.997(2)
		P(1)-S(1)	2.107(2)
		P(1)-S(1)	2.113(2)

Table 8. Atom coordinates [x 10^4] and isotropic thermal parameters [$Å^2$ x 10^3] of $U_3(PS_4)_4$ (**IV**). U(eq) is defined as one third of the trace of the orthogonalized matrix U_{ij}.

	x	y	z	U(eq)	sof
U(1)	0	2500	1250	13(1)	
U(2)	0	2500	3750	22(1)	0.5
P(1)	363(2)	0	2500	10(1)	
S(1)	919(2)	1097(2)	85(1)	22(1)	
S(2)	2513(2)	3213(2)	878(1)	16(1)	

Table 9. Selected bond distances [Å] for $U_3(PS_4)_4$ (**IV**).

U(1)-S(1) (4x)	2.8628(17)	P(1)-S(2) (2x)	2.037(2)
U(1)-S(2) (4x)	2.8949(17)	P(1)-S(1) (2x)	2.039(2)
U(2)-S(2) (4x)	2.8691(16)		
U(2)-S(1) (4x)	3.1222(19)		

Table 10. Vibrational spectra [cm^{-1}] of UP_2S_6 (**I**).

UP_2S_6			$MnPS_3$		Assignments for $P_2S_6^{4-}$ (*D_{3d}*)
162.3	m	R	154	m	R'_{xy} PS_3?
241.1	m	R	244	vs	T'_{xy} PS_3
262.8	m	R	273	vs	δ_d PS_3
385.5	vs	R	378	vs	ν_s PS_3
457	m	IR	450	m	ν P-P
555.8	m	R	566	w	ν_d PS_3
594	s	IR	572	vs	ν_d PS_3
595.8	w	R	579	m	ν_d PS_3

Table 11. Vibrational spectra [cm^{-1}] of UP_2S_7 (**II**).

UP_2S_7			$Ag_4P_2S_7$		Assignments for $P_2S_7^{4-}$ (C_2)
195.7	vw	R	210	s	δ PS_3 + δ PSP
245.7	w	R	255	m	δ PS_3 + δ PSP
272.3	vw	R	285	m	δ PS_3 + δ PSP
			411;	vs;	ν_S PS_3
410.2	vs	R	389	vs	ν_S PSP
413	w	IR	405	m	ν_S PS_3
457	s	IR	454	s	ν_{as} PSP
512	w	IR	512	s	ν_a PS_3
560.8	vw	R	550	w	ν_a PS_3
575	w	IR	570	m	ν_a PS_3
592	w	IR	596	m	ν_a PS_3
608.4	vw	R	601	w	ν_a PS_3

Table 12. Vibrational spectra [cm^{-1}] of $U(P_2S_6)_2$ (**III**).

$U(P_2S_6)_2$			$Ag_2P_2S_6$		Assignments for $P_2S_6^{2-}$ (D_{2h})
152.3	w	R	143	m	*rock* PS_2
238.2	w	R	233	W	*wag* PS_2
257.3	w	R	259	m	*wag* PS_2
319.6	vw	R	299	m	δ PS_2 (t)
403	s	IR	395	ms	ν_s PS_2 (b)
403.8	m	R	398	s	ν_s PS_2 (b)
429.5	vs	R	418	vs	ν_a PS_2 (b)
608.1	vw	R	612	w	ν_a PS_2 (t)

Table 13. Parameters F_2, F_4, F_6, ζ, $e_\sigma(d)$; $e_\pi(d)$ [cm^{-1}] and basis set for UP_2S_6 (**I**), UP_2S_7 (**II**) and $U(P_2S_6)_2$ (**III**).

F_2	189.4
F_4	33.47
F_6	3.927
ζ	1800.104
e_σ(2.81 Å)	1124.0
e_π(2.81 Å)	136.5
basis set:	^3P, ^3F, ^3H, ^1S, ^1D, ^1G, ^1I

Table 1. Crystallographic data for compounds **V**-**VII**.

	V	**VI**	**VII**
empirical formula	$Rb_5U(PS_4)_3$	$CsU_2(PS_4)_3$	$Na_2U(PS_4)_2$
formula weight	1143.01	1448.80	602.43
crystal system	monoclinic	monoclinic	monoclinic
space group	$P2_1/c$	$P2_1/c$	Cc
a [Å]	14.780(7)	12.0989(12)	10.4130
b [Å]	17.820(8)	8.8165(8)	19.5475
c [Å]	9.759(4)	20.367(2)	35.9241
β [°]	108.804(7)	122.314(2)	98.322
V [Å³]	2433.4(19)	1836.1(3)	7235.29
Z	4	4	20
ρ_{calcd} [g cm^{-3}]	3.120	3.931	2.765
Temperature [K]	203(2)	182(2)	203(2)
μ (MoK_α) [mm^{-1}]	17.821	21.174	12.607
θ range [°]	2.29 - 28.24	2.13 - 28.27	2.16 - 28.31
index ranges	$-18 \le h \le 15$,	$-11 \le h \le 16$	$-13 \le h \le 13$
	$-23 \le k \le 15$,	$-11 \le k \le 11$	$-25 \le k \le 26$
	$-11 \le l \le 12$	$-27 \le l \le 27$	$-47 \le l \le 47$
measured reflections	12031	8222	33693
independent reflections	5677	4328	17227
observed reflections	2834	3180	10569
[$I > 2\sigma(I)$]			
R_{int}	0.0800	0.0362	0.0770
parameters	191	185	619
goodness-of-fit on F^2	0.804	0.988	1.034
R values	*R1* = 0.0483	*R1* = 0.0362	*R1* = 0.0751
[$I > 2\sigma(I)$]	*wR2* = 0.0715	*wR2* = 0.0763	*wR2* = 0.1794
R values	*R1* = 0.1345	*R1* = 0.0624	*R1* = 0.1311
(for all data)	*wR2* = 0.0846	*wR2* = 0.0988	*wR2* = 0.2087
residual electron	2.352 / -2.113	3.929 / -1.722	6.126 / -2.614
density [e*Å^{-3}]			

Table 2. Atom coordinates [x 10^4] and isotropic thermal parameters [$Å^2$ x 10^3] of $Rb_5U(PS_4)_3$ (**V**). U(eq) is defined as one third of the trace of the orthogonalized matrix U_{ij}.

	x	y	z	U(eq)
U(1)	3350(1)	5017(1)	8893(1)	15(1)
Rb(1)	2020(1)	8056(1)	5861(2)	40(1)
Rb(2)	246(1)	4752(1)	2279(1)	26(1)
Rb(3)	-879(1)	6981(1)	3583(1)	33(1)
Rb(4)	3231(1)	4978(1)	4391(1)	35(1)
Rb(5)	5446(1)	7048(1)	7386(2)	44(1)
S(1)	3111(2)	6277(2)	7074(4)	30(1)
S(2)	872(2)	6678(2)	6978(4)	27(1)
S(3)	1367(2)	6272(2)	3941(3)	25(1)
S(4)	4126(2)	6406(2)	313(4)	24(1)
S(5)	4751(2)	4784(2)	1741(3)	25(1)
S(6)	3737(3)	3850(2)	7221(5)	63(1)
S(7)	2804(2)	3565(2)	9460(3)	21(1)
S(8)	2102(2)	5092(2)	595(3)	21(1)
S(9)	1632(2)	4911(2)	6511(3)	19(1)
S(10)	4456(4)	6328(2)	3836(5)	73(2)
S(11)	2313(2)	3504(2)	2623(4)	29(1)
S(12)	535(2)	3659(2)	9528(3)	24(1)
P(1)	1675(2)	6059(2)	6064(4)	17(1)
P(2)	4876(2)	5924(2)	2230(4)	28(1)
P(3)	1906(2)	3922(2)	595(3)	18(1)

Table 3. Selected bond distances [Å] for $Rb_5U(PS_4)_3$ (**V**).

U(1)-S(6)	2.812(5)	P(1)-S(3)	2.009(5)
U(1)-S(1)	2.813(3)	P(1)-S(2)	2.026(4)
U(1)-S(7)	2.817(3)	P(1)-S(1)	2.068(5)
U(1)-S(9)	2.843(3)	P(1)-S(9)	2.096(4)
U(1)-S(8)	2.856(3)	P(2)-S(6)	1.986(5)
U(1)-S(4)	2.888(3)	P(2)-S(10)	1.997(5)
U(1)-S(5)	2.911(3)	P(2)-S(4)	2.031(5)
U(1)-S(5)	3.083(3)	P(2)-S(5)	2.081(4)
		P(3)-S(12)	2.012(4)
		P(3)-S(11)	2.016(4)
		P(3)-S(7)	2.082(5)
		P(3)-S(8)	2.107(4)

Table 4. Atom coordinates [x 10^4] and isotropic thermal parameters [$Å^2$ x 10^3] of $CsU_2(PS_4)_3$ (**VI**). U(eq) is defined as one third of the trace of the orthogonalized matrix U_{ij}.

	x	y	z	U(eq)	sof
U(1)	1567(1)	6374(1)	4848(1)	9(1)	
U(2)	5219(1)	2254(1)	2033(1)	9(1)	
Cs(1)	1356(5)	857(9)	3314(4)	33(1)	0.534
Cs(2)	1940(50)	977(13)	3540(20)	57(9)	0.292
Cs(3)	2620(90)	1200(60)	3780(30)	65(12)	0.174
S(1)	620(3)	5902(3)	5879(2)	10(1)	
S(2)	700(3)	2641(4)	1355(2)	14(1)	
S(3)	1428(3)	5551(4)	159(2)	12(1)	
S(4)	1579(3)	4785(4)	3656(2)	16(1)	
S(5)	2237(3)	7407(4)	2692(2)	15(1)	
S(6)	2554(3)	1440(4)	660(2)	12(1)	
S(7)	3453(3)	631(4)	2419(2)	12(1)	
S(8)	3525(3)	4515(3)	2051(2)	10(1)	
S(9)	4520(3)	4353(4)	829(2)	12(1)	
S(10)	5394(3)	266(4)	1044(2)	18(1)	
S(11)	6207(3)	2725(3)	3640(2)	11(1)	
S(12)	6727(3)	2734(4)	443(2)	19(1)	
P(1)	1823(3)	947(4)	1347(2)	10(1)	
P(2)	3297(3)	5479(3)	1064(2)	9(1)	
P(3)	7089(3)	1262(4)	1299(2)	11(1)	

Table 5. Selected bond distances [Å] for $CsU_2(PS_4)_3$ (**VI**).

U(1)-S(12)	2.713(3)	P(1)-S(2)	2.025(4)
U(1)-S(2)	2.755(3)	P(1)-S(7)	2.032(4)
U(1)-S(3)	2.809(3)	P(1)-S(1)	2.049(4)
U(1)-S(4)	2.810(3)	P(1)-S(6)	2.062(4)
U(1)-S(6)	2.864(3)	P(2)-S(3)	2.015(4)
U(1)-S(1)	2.908(3)	P(2)-S(9)	2.039(4)
U(1)-S(11)	2.916(3)	P(2)-S(8)	2.060(4)
U(1)-S(1)	3.005(3)	P(2)-S(11)	2.063(4)
U(2)-S(10)	2.764(3)	P(3)-S(12)	2.025(4)
U(2)-S(9)	2.818(3)	P(3)-S(10)	2.027(4)
U(2)-S(5)	2.822(3)	P(3)-S(5)	2.029(4)
U(2)-S(11)	2.850(3)	P(3)-S(4)	2.036(4)
U(2)-S(8)	2.872(3)		
U(2)-S(8)	2.931(3)		
U(2)-S(7)	3.003(3)		
U(2)-S(6)	3.015(3)		
U(2)-S(7)	3.283(3)		

Table 6. Atom coordinates [x 10^4] and isotropic thermal parameters [$Å^2$ x 10^3] of $Na_2U(PS_4)_2$ (**VII**). U(eq) is defined as one third of the trace of the orthogonalized matrix U_{ij}.

	x	y	z	U(eq)	sof
U(1)	539(1)	5359(1)	2766(1)	16(1)	
U(2)	2070(1)	2853(1)	835(1)	16(1)	
U(3)	2560(3)	1250(1)	4300(1)	23(1)	
U(4)	3083(1)	7149(1)	2765(1)	18(1)	
U(5)	4621(1)	4655(1)	836(1)	19(1)	
Na(1)	470(20)	3806(10)	4736(6)	19(7)	0.593
Na(2)	810(20)	105(15)	3217(7)	91(9)	
Na(3)	1301(16)	1318(10)	2030(7)	42(5)	
Na(4)	1620(20)	4090(10)	4459(8)	25(9)	0.407
Na(5)	1900(17)	2428(12)	5364(6)	65(6)	
Na(6)	2872(19)	2726(10)	3198(7)	67(6)	
Na(7)	3577(16)	1177(10)	6548(7)	46(5)	
Na(8)	3832(18)	3727(9)	2017(6)	28(4)	
Na(9)	3970(40)	3980(20)	3365(10)	26(19)	0.218
Na(10)	4017(18)	201(11)	392(6)	63(6)	
Na(11)	5060(40)	3681(14)	3842(10)	36(11)	0.493
Na(12)	5210(40)	3540(18)	3355(8)	31(12)	0.289
Na(13)	6112(19)	1232(10)	1642(6)	38(5)	
S(1)	221(11)	43(6)	7401(4)	19(2)	
S(2)	498(19)	815(9)	3795(6)	66(5)	
S(3)	606(12)	1974(7)	3065(3)	24(3)	
S(4)	680(14)	2041(6)	1297(4)	33(3)	
S(5)	897(16)	4010(7)	2976(5)	60(5)	
S(6)	918(12)	1170(6)	6448(4)	28(3)	
S(7)	1027(16)	1676(7)	4808(4)	45(3)	
S(8)	1152(12)	5370(7)	3583(3)	27(3)	
S(9)	1358(13)	2460(7)	3937(4)	40(4)	
S(10)	1450(13)	403(6)	1280(4)	27(3)	
S(11)	1573(12)	3610(6)	1447(4)	24(3)	
S(12)	1708(15)	50(6)	4651(4)	34(4)	
S(13)	1870(13)	530(7)	5527(3)	26(3)	
S(14)	1902(11)	2857(7)	26(3)	32(3)	

S(15)	1955(9)	4311(5)	651(3)	9(2)
S(16)	1959(11)	4878(5)	2217(3)	17(2)
S(17)	2037(13)	2595(7)	6176(4)	44(4)
S(18)	2228(17)	1524(7)	612(4)	40(4)
S(19)	2927(16)	1446(7)	7968(5)	53(5)
S(20)	3007(11)	2587(6)	2403(4)	28(3)
S(21)	3216(12)	5050(7)	1413(4)	37(3)
S(22)	3229(13)	5694(7)	2953(4)	37(3)
S(23)	3232(15)	7063(6)	3573(4)	36(3)
S(24)	3328(15)	580(9)	3089(5)	49(4)
S(25)	3486(17)	40(9)	3961(5)	51(4)
S(26)	3684(12)	464(6)	7283(3)	23(3)
S(27)	3781(12)	6333(6)	2159(3)	19(2)
S(28)	3838(16)	2443(7)	4628(4)	44(4)
S(29)	3936(15)	4565(7)	37(4)	39(4)
S(30)	4058(11)	2388(6)	1393(3)	22(3)
S(31)	4249(12)	6024(6)	612(4)	39(4)
S(32)	4320(19)	1595(8)	3805(6)	67(5)
S(33)	4415(12)	1111(6)	2155(3)	19(2)
S(34)	4448(12)	2094(6)	7300(4)	22(3)
S(35)	4493(16)	1914(9)	5504(5)	49(4)
S(36)	4555(12)	3174(6)	640(3)	23(3)
S(37)	4795(14)	899(7)	4797(4)	45(4)
S(38)	4942(15)	154(7)	1165(5)	47(4)
S(39)	5581(10)	1794(6)	2939(3)	18(2)
S(40)	6129(12)	2567(7)	2203(4)	35(3)
P(1)	0(14)	3148(7)	0(3)	34(4)
P(2)	145(12)	1837(6)	3600(4)	36(4)
P(3)	818(11)	1247(6)	982(4)	19(2)
P(4)	857(14)	659(7)	5007(5)	49(4)
P(5)	1605(10)	4545(5)	1170(3)	10(2)
P(6)	3628(13)	5402(6)	2396(4)	25(3)
P(7)	4140(12)	1255(7)	7642(4)	26(3)
P(8)	4323(12)	656(6)	3604(3)	23(3)
P(9)	4720(11)	2032(5)	2402(3)	9(2)
P(10)	5494(12)	2885(6)	1169(4)	22(3)

Table 7. Selected bond distances [Å] for $Na_2U(PS_4)_2$ (**VII**).

U(1)-S(5)	2.752(14)	P(1)-S(35)	1.96(2)
U(1)-S(33)	2.756(11)	P(1)-S(37)	2.000(18)
U(1)-S(24)	2.758(16)	P(1)-S(28)	2.028(18)
U(1)-S(16)	2.792(10)	P(1)-S(14)	2.050(19)
U(1)-S(22)	2.860(14)	P(2)-S(9)	2.025(18)
U(1)-S(39)	2.874(11)	P(2)-S(23)	2.03(2)
U(1)-S(26)	2.890(12)	P(2)-S(3)	2.067(19)
U(1)-S(8)	2.912(12)	P(2)-S(2)	2.13(2)
U(2)-S(18)	2.731(14)	P(3)-S(4)	1.936(19)
U(2)-S(11)	2.760(13)	P(3)-S(31)	1.999(18)
U(2)-S(35)	2.810(16)	P(3)-S(10)	2.024(17)
U(2)-S(30)	2.816(10)	P(3)-S(18)	2.188(19)
U(2)-S(4)	2.840(14)	P(4)-S(13)	2.02(2)
U(2)-S(36)	2.847(12)	P(4)-S(12)	2.042(19)
U(2)-S(14)	2.885(12)	P(4)-S(29)	2.07(2)
U(2)-S(15)	2.923(9)	P(4)-S(7)	2.129(18)
U(3)-S(7)	2.722(14)	P(5)-S(15)	2.004(14)
U(3)-S(2)	2.739(18)	P(5)-S(21)	2.031(16)
U(3)-S(37)	2.804(12)	P(5)-S(11)	2.084(17)
U(3)-S(32)	2.815(14)	P(5)-S(38)	2.099(17)
U(3)-S(28)	2.854(15)	P(6)-S(1)	1.871(17)
U(3)-S(12)	2.864(13)	P(6)-S(27)	2.026(17)
U(3)-S(25)	2.889(17)	P(6)-S(16)	2.040(17)
U(3)-S(9)	2.897(14)	P(6)-S(22)	2.176(19)
U(4)-S(3)	2.713(12)	P(7)-S(19)	1.878(19)
U(4)-S(40)	2.774(15)	P(7)-S(26)	2.026(19)
U(4)-S(34)	2.772(12)	P(7)-S(5)	2.10(2)
U(4)-S(39)	2.852(11)	P(7)-S(34)	2.101(18)
U(4)-S(19)	2.853(14)	P(8)-S(32)	1.97(2)
U(4)-S(27)	2.877(11)	P(8)-S(24)	1.991(19)

U(4)-S(23)	2.890(15)	P(8)-S(8)	1.997(17)
U(4)-S(22)	2.921(15)	P(8)-S(25)	2.047(19)
U(5)-S(10)	2.726(12)	P(9)-S(33)	2.012(15)
U(5)-S(13)	2.757(12)	P(9)-S(40)	2.015(16)
U(5)-S(31)	2.803(10)	P(9)-S(39)	2.061(17)
U(5)-S(21)	2.812(14)	P(9)-S(20)	2.087(16)
U(5)-S(15)	2.840(10)	P(10)-S(17)	1.858(17)
U(5)-S(29)	2.859(14)	P(10)-S(30)	2.043(17)
U(5)-S(6)	2.899(13)	P(10)-S(36)	2.086(19)
U(5)-S(36)	2.978(12)	P(10)-S(6)	2.119(17)

Table 8. Correlation between cation diameter and pore diameter.

Compound		cation Ø [Å][12]		pore Ø [Å]
$CsLiU(PS_4)_2$	(**X**)	3.64	(Cs)	6
$CsU_2(PS_4)_3$	(**VI**)			6
$A_{11}U_7(PS_4)_{13}$	(**IX**)	3.20	(Rb)	4.9
	(**VIII**)	3.02	(K)	4.8
$Na_2U(PS_4)_2$	(**VII**)	2.32		---

Table 1. Crystallographic data for compounds **VIII** and **IX**.

	VIII	**IX**
empirical formula	$K_{11}U_7(PS_4)_{13}$	$Rb_{11}U_7(PS_4)_{13}$
formula weight	4166.04	4676.11
crystal system	tetragonal	tetragonal
space group	$I\bar{4}2d$	$I\bar{4}2d$
a [Å]	32.048(2)	32.164(1)
c [Å]	17.321(1)	17.724(1)
V [Å³]	17789.9(18)	18336.4(13)
Z	8	8
ρ_{calcd} [g cm^{-3}]	3.111	3.388
Temperature [K]	203(2)	183(2)
μ (MoK_α) [mm^{-1}]	14.689	19.554
θ range [°]	2.01 - 28.29	2.00 - 28.31
index ranges	$-42 \le h \le 42$, $-42 \le k \le 42$, $-22 \le l \le 23$	$-42 \le h \le 37$, $-38 \le k \le 42$, $-17 \le l \le 23$
measured reflections	81364	79281
independent reflections	11046	11401
observed reflections [$I > 2\sigma(I)$]	6272	7018
R_{int}	0.1890	0.2001
parameters	379	378
goodness-of-fit on F^2	0.845	0.963
R values	*R1* = 0.0535	*R1* = 0.0545
[$I > 2\sigma(I)$]	*wR2* = 0.0799	*wR2* = 0.1105
R values	*R1* = 0.1189	*R1* = 0.1288
(for all data)	*wR2* = 0.0911	*wR2* = 0.1348
residual electron density [e*Å^{-3}]	3.060 / -1.245	3.348 / -3.547

Table 2. Atom coordinates [x 10^4] and isotropic thermal parameters [$Å^2$ x 10^3] of $K_{11}U_7(PS_4)_{13}$ (**VIII**). U(eq) is defined as one third of the trace of the orthogonalized matrix U_{ij}.

	x	y	z	U(eq)	sof
U(1)	119(1)	1519(1)	2118(1)	26(1)	
U(2)	1222(1)	844(1)	2387(1)	20(1)	
U(3)	3065(1)	1808(1)	1252(1)	21(1)	
U(4)	4238(1)	1/4	1/8	21(1)	
S(1)	17(2)	976(2)	849(3)	39(1)	
S(2)	58(2)	945(2)	4525(3)	61(2)	
S(3)	267(1)	2633(1)	4940(3)	30(1)	
S(4)	305(2)	682(2)	2637(3)	36(1)	
S(5)	501(1)	2664(1)	331(3)	29(1)	
S(6)	717(1)	6232(2)	347(3)	32(1)	
S(7)	728(2)	1520(2)	3295(3)	34(1)	
S(8)	756(2)	3890(2)	2999(3)	51(2)	
S(9)	877(1)	1457(1)	1318(3)	30(1)	
S(10)	922(2)	468(2)	1018(3)	32(1)	
S(11)	1025(1)	612(1)	3936(2)	30(1)	
S(12)	1344(1)	5034(1)	247(3)	24(1)	
S(13)	1573(2)	2597(2)	3621(3)	58(2)	
S(14)	1676(1)	1585(1)	2649(3)	27(1)	
S(15)	1855(1)	926(1)	1251(3)	25(1)	
S(16)	1959(1)	592(1)	3200(3)	25(1)	
S(17)	2010(2)	4771(2)	3483(3)	49(2)	
S(18)	2197(1)	1906(1)	1049(3)	30(1)	
S(19)	2668(1)	1317(1)	2304(3)	28(1)	
S(20)	2871(1)	2494(1)	229(2)	24(1)	
S(21)	2900(2)	1289(2)	23(3)	35(1)	
S(22)	3010(2)	335(1)	667(3)	36(1)	
S(23)	3598(1)	1121(1)	1378(3)	25(1)	

S(24)	3741(1)	3002(1)	164(3)	26(1)	
S(25)	3743(2)	1985(2)	273(3)	36(1)	
S(26)	4630(1)	1735(1)	1412(3)	28(1)	
P(1)	479(2)	916(2)	3730(3)	58(2)	
P(2)	645(2)	999(2)	609(3)	28(1)	
P(3)	2092(1)	1426(1)	1803(3)	24(1)	
P(4)	3326(1)	859(1)	430(3)	23(1)	
P(5)	3454(1)	2533(2)	2769(3)	28(1)	
P(6)	4984(1)	1851(1)	457(3)	21(1)	
P(7)	145(2)	1/4	1/8	22(1)	
K(1)	124(2)	3113(2)	3210(3)	68(2)	
K(2)	1765(2)	3727(2)	3108(3)	75(2)	
K(3)	3125(1)	423(1)	2475(2)	42(1)	
K(4)	4565(1)	719(1)	1172(3)	54(1)	
K(5)	1365(2)	1/4	1/8	85(3)	
K(6)	6965(2)	1/4	1/8	42(2)	
K(7a)	102(4)	-570(4)	1273(4)	95(5)	0.5
K(7b)	-102(4)	570(4)	1273(4)	98(5)	0.5

Table 3. Selected bond distances [Å] for $K_{11}U_7(PS_4)_{13}$ (**VIII**).

U(1)-S(17)	2.753(5)	P(1)-S(2)	1.930(8)
U(1)-S(22)	2.775(5)	P(1)-S(11)	2.032(7)
U(1)-S(9)	2.803(4)	P(1)-S(4)	2.110(7)
U(1)-S(1)	2.822(5)	P(1)-S(7)	2.226(9)
U(1)-S(7)	2.822(5)	P(2)-S(8)	1.984(7)
U(1)-S(6)	2.834(4)	P(2)-S(10)	2.047(7)
U(1)-S(4)	2.889(5)	P(2)-S (9)	2.052(7)
U(1)-S(5)	2.892(4)	P(2)-S(1)	2.057(7)
U(2)-S(14)	2.821(4)	P(3)-S(15)	2.015(6)
U(2)-S(10)	2.828(5)	P(3)-S(14)	2.044(6)
U(2)-S(15)	2.839(4)	P(3)-S(18)	2.046(6)
U(2)-S(12)	2.851(4)	P(3)-S(19)	2.069(6)
U(2)-S(11)	2.855(4)	P(4)-S(22)	2.005(6)
U(2)-S(16)	2.867(4)	P(4)-S(6)	2.007(6)
U(2)-S(9)	2.916(5)	P(4)-S(23)	2.040(6)
U(2)-S(4)	3.015(5)	P(4)-S(21)	2.066(6)
U(2)-S(7)	3.110(5)	P(5)-S(13)	1.936(7)
U(2)-P(1)	3.337(5)	P(5)-S(25)	2.032(7)
U(3)-S(19)	2.722(4)	P(5)-S(20)	2.061(6)
U(3)-S(21)	2.751(5)	P(5)-S(24)	2.084(6)
U(3)-S(23)	2.798(4)	P(6)-S(16)	2.024(6)
U(3)-S(25)	2.813(5)	P(6)-S(12)	2.031(6)
U(3)-S(20)	2.891(4)	P(6)-S(26)	2.040(6)
U(3)-S(20) (2x)	2.916(4)	P(6)-S(3)	2.045(6)
U(3)-S(24) (2x)	2.933(5)	P(7)-S(5) (2x)	2.028(6)
U(4)-S(26) (2x)	2.769(4)	P(7)-S(17) (2x)	2.029(6)
U(4)-S(3) (2x)	2.803(5)		
U(4)-S(25) (2x)	2.847(5)		
U(4)-S(24) (2x)	2.942(4)		

Table 4. Atom coordinates [x 10^4] and isotropic thermal parameters [$Å^2$ x 10^3] of $Rb_{11}U_7(PS_4)_{13}$ (**IX**). U(eq) is defined as one third of the trace of the orthogonalized matrix U_{ij}.

	x	y	z	U(eq)
U(1)	109(1)	1514(1)	2077(1)	16(1)
U(2)	1226(1)	852(1)	2375(1)	12(1)
U(3)	3067(1)	1807(1)	1230(1)	11(1)
U(4)	4246(1)	1/4	1/8	12(1)
S(1)	20(2)	979(2)	842(3)	27(1)
S(2)	84(2)	956(2)	4495(3)	29(1)
S(3)	268(2)	2633(2)	4960(3)	20(1)
S(4)	301(2)	701(2)	2655(3)	18(1)
S(5)	480(2)	2672(2)	357(3)	21(1)
S(6)	716(2)	1515(2)	3262(3)	23(1)
S(7)	725(2)	6221(2)	379(3)	20(1)
S(8)	766(2)	3919(2)	2961(3)	31(2)
S(9)	875(2)	1454(2)	1321(3)	17(1)
S(10)	922(2)	464(2)	1053(3)	19(1)
S(11)	1032(2)	631(2)	3900(3)	20(1)
S(12)	1345(2)	5024(2)	227(3)	16(1)
S(13)	1555(2)	2554(2)	3672(3)	32(1)
S(14)	1684(2)	1596(2)	2595(3)	18(1)
S(15)	1856(2)	926(2)	1253(3)	17(1)
S(16)	1958(2)	594(2)	3162(3)	16(1)
S(17)	2012(2)	4751(2)	3479(3)	29(2)
S(18)	2204(2)	1899(2)	1032(3)	18(1)
S(19)	2669(2)	1323(2)	2265(3)	19(1)
S(20)	2873(1)	2504(2)	263(3)	12(1)
S(21)	2904(2)	1286(2)	26(3)	25(1)
S(22)	3034(2)	334(2)	651(3)	22(1)
S(23)	3605(2)	1132(2)	1331(3)	15(1)

S(24)	3745(2)	3008(2)	211(3)	17(1)
S(25)	3748(2)	1991(2)	279(3)	20(1)
S(26)	4633(2)	1740(2)	1388(3)	17(1)
P(1)	500(2)	948(2)	3689(3)	21(1)
P(2)	645(2)	991(2)	615(3)	15(1)
P(3)	2093(2)	1428(2)	1780(3)	14(1)
P(4)	3332(2)	865(2)	401(3)	16(1)
P(5)	3459(2)	2514(2)	2732(3)	15(1)
P(6)	4991(2)	1852(2)	449(3)	14(1)
P(7)	124(2)	1/4	1/8	15(2)
Rb(1)	128(1)	3113(1)	3209(1)	42(1)
Rb(2)	1784(1)	3694(1)	3109(1)	35(1)
Rb(3)	3138(1)	428(1)	2467(1)	27(1)
Rb(4)	4580(1)	694(1)	1166(2)	30(1)
Rb(5)	1368(1)	1/4	1/8	52(1)
Rb(6)	6955(1)	1/4	1/8	26(1)
Rb(7)	0	0	1291(3)	98(2)

Table 5. Selected bond distances [Å] for $Rb_{11}U_7(PS_4)_{13}$ (**IX**).

U(1)-S(17)	2.771(6)	P(1)-S(2)	1.956(8)
U(1)-S(22)	2.787(5)	P(1)-S(11)	2.028(8)
U(1)-S(1)	2.801(6)	P(1)-S(6)	2.092(8)
U(1)-S(9)	2.809(5)	P(1)-S(4)	2.100(8)
U(1)-S(7)	2.846(5)	P(2)-S(8)	1.968(8)
U(1)-S(6)	2.866(6)	P(2)-S(1)	2.051(8)
U(1)-S(5)	2.878(6)	P(2)-S(10)	2.065(7)
U(1)-S(4)	2.878(5)	P(2)-S(9)	2.081(8)
U(2)-S(10)	2.828(5)	P(3)-S(15)	2.015(7)
U(2)-S(14)	2.840(5)	P(3)-S(14)	2.026(8)
U(2)-S(12)	2.848(5)	P(3)-S(18)	2.045(8)
U(2)-S(15)	2.850(5)	P(3)-S(19)	2.071(8)
U(2)-S(16)	2.861(5)	P(4)-S(22)	2.007(8)
U(2)-S(11)	2.863(5)	P(4)-S(21)	2.040(8)
U(2)-S(9)	2.919(5)	P(4)-S(7)	2.046(8)
U(2)-S(4)	3.054(5)	P(4)-S(23)	2.056(8)
U(2)-S(6)	3.117(6)	P(5)-S(13)	1.948(8)
U(2)-P(1)	3.312(6)	P(5)-S(25)	2.055(8)
U(3)-S(19)	2.727(5)	P(5)-S(24)	2.068(8)
U(3)-S(21)	2.763(6)	P(5)-S(20)	2.079(7)
U(3)-S(23)	2.780(5)	P(6)-S(16)	2.005(7)
U(3)-S(25)	2.825(6)	P(6)-S(12)	2.025(8)
U(3)-S(20)	2.891(5)	P(6)-S(26)	2.040(7)
U(3)-S(20) (2x)	2.914(5)	P(6)-S(3)	2.047(7)
U(3)-S(24) (2x)	2.939(5)	P(7)-S(5) (2x)	2.031(7)
U(4)-S(26) (2x)	2.755(5)	P(7)-S(17) (2x)	2.034(8)
U(4)-S(3) (2x)	2.803(5)		
U(4)-S(25) (2x)	2.866(6)		
U(4)-S(24) (2x)	2.942(5)		

Table 1. Crystallographic data for $CsLiU(PS_4)_2$ (**X**).

	X
empirical formula	$CsLiU(PS_4)_2$
formula weight	696.30
crystal system	rhombohedral
space group	$R\bar{3}c$
a [Å]	15.2797(7)
c [Å]	28.7782(19)
V [Å³]	5818.7(5)
Z	18
ρ_{calcd} [g cm^{-3}]	3.577
Temperature [K]	182(2)
μ (MoK_α) [mm^{-1}]	16.816
θ range [°]	2.67 - 28.29
index ranges	$-18 \le h \le 20$
	$-20 \le k \le 15$
	$-38 \le l \le 36$
measured reflections	11667
independent reflections	1619
observed reflections	1291
[I > 2 σ (I)]	
R_{int}	0.0333
parameters	62
goodness-of-fit on F^2	1.055
R values	*R1* = 0.0239
[I > 2 σ (I)]	*wR2* = 0.0582
R values	*R1* = 0.0346
(for all data)	*wR2* = 0.0617
residual electron density [e*Å^{-3}]	2.371 / -2.853

Table 2. Atom coordinates [x 10^4] and isotropic thermal parameters [$Å^2$ x 10^3] of $CsLiU(PS_4)_2$ (**X**). U(eq) is defined as one third of the trace of the orthogonalized matrix U_{ij}.

	x	y	z	U(eq)
U(1)	6678(1)	6667	4167	11(1)
S(1)	6667(1)	5216(1)	4811(1)	14(1)
S(2)	8485(1)	7546(1)	4652(1)	25(1)
S(3)	5813(1)	6737(1)	5032(1)	18(1)
S(4)	6577(1)	8479(1)	4267(1)	21(1)
P(1)	6274(1)	8223(1)	4958(1)	12(1)
Li(1)	6667	6978(10)	5833	24(3)
Cs(2)	3333	6667	4167	81(1)
Cs(3)	3333	6667	5904(1)	26(1)

Table 3. Selected bond distances [Å] for $CsLiU(PS_4)_2$ (**X**).

U(1)-S(2) (2x)	2.768(1)	P(1)-S(3)	2.024(2)
U(1)-S(3) (2x)	2.845(1)	P(1)-S(1) (2x)	2.028(2)
U(1)-S(4) (2x)	2.864(1)	P(1)-S(4)	2.036(1)
U(1)-S(1) (2x)	2.884(1)	P(1)-S(2) (2x)	2.047(2)

Table 1. Crystallographic data for $Cs_3UP_2S_8$ (**XI**).

	XI
empirical formula	$Cs_3UP_2S_8$
formula weight	955.18
crystal system	rhombohedral
space group	$R\bar{3}$
a [Å]	16.5217(8)
c [Å]	35.132(2) Å
V [Å³]	8305.0(8)
Z	18
ρ_{calcd} [g cm^{-3}]	3.438
Temperature [K]	182(2)
μ (MoK_α) [mm^{-1}]	15.673
θ range [°]	2.72 - 28.29
index ranges	$-21 \le h \le 22$
	$-21 \le k \le 22$
	$-46 \le l \le 46$
measured reflections	25488
independent reflections	4591
observed reflections	3587
[I > 2 σ (I)]	
R_{int}	0.0592
parameters	167
goodness-of-fit on F^2	1.104
R values	*R1* = 0.0518
[I > 2 σ (I)]	*wR2* = 0.1436
R values	*R1* = 0.0687
(for all data)	*wR2* = 0.1491
residual electron density [e*Å^{-3}]	3.948 / -4.520

Table 2. Atom coordinates [x 10^4] and isotropic thermal parameters [$Å^2$ x 10^3] of $Cs_3UP_2S_8$ (**XI**). U(eq) is defined as one third of the trace of the orthogonalized matrix U_{ij}.

	x	y	z	U(eq)	sof
U(1)	3617(1)	2071(1)	662(1)	13(1)	
S(1)	100(2)	1396(2)	2665(1)	20(1)	
S(2)	1151(2)	3877(2)	110(1)	21(1)	
S(3)	1992(2)	1208(2)	1207(1)	20(1)	
S(4)	2164(2)	433(2)	380(1)	23(1)	
S(5)	2306(2)	2229(2)	3080(1)	19(1)	
S(6)	2452(2)	2178(2)	2109(1)	21(1)	
S(7)	2568(3)	2911(3)	509(1)	28(1)	
S(8)	2790(2)	131(2)	1998(1)	23(1)	
P(1)	2934(2)	2020(2)	1600(1)	15(1)	
P(2)	3055(2)	189(2)	58(1)	17(1)	
Cs(1)	50(3)	218(6)	4748(1)	43(5)	0.167
Cs(2)	1108(1)	3129(1)	1146(4)	42(3)	0.349
Cs(3)	1184(7)	3061(6)	1172(2)	36(2)	0.616
Cs(4)	1401(5)	723(5)	4167(3)	65(3)	0.169
Cs(5)	1470(4)	2740(4)	3940(2)	63(2)	0.076
Cs(6)	1874(3)	3886(3)	2622(3)	48(2)	0.790
Cs(7)	0	0	1910(1)	25(1)	
Cs(8)	0	0	3398(1)	53(1)	
Cs(9)	0	0	0	39(1)	

Table 3. Selected bond distances [Å] for $Cs_3UP_2S_8$ (**XI**).

U(1)-S(1)	2.634(3)	P(1)-P(1)	2.204(6)
U(1)-S(4)	2.753(3)	P(1)-S(3)	2.011(4)
U(1)-S(7)	2.762(3)	P(1)-S(8)	2.017(4)
U(1)-S(5)	2.842(3)	P(1)-S(6)	2.026(4)
U(1)-S(2)	2.872(3)	P(2)-S(2)	2.007(4)
U(1)-S(8)	2.909(3)	P(2)-S(7)	2.034(4)
U(1)-S(6)	2.943(3)	P(2)-S(5)	2.038(4)
U(1)-S(3)	3.013(3)	P(2)-S(4)	2.050(4)

Table 1. Crystallographic data for compounds **XII** and **XIII**.

	XII	**XIII**
empirical formula	$Li_3Rb_6U_3(S)S_2(PS_4)_5$	$Li_3Rb_6Th_3(S)S_2(PS_4)_5$
formula weight	2139.96	2121.99
crystal system	monoclinic	monoclinic
space group	C2/c	C2/c
a [Å]	18.467(2)	18.6028(14)
b [Å]	18.222(2)	18.4125(12)
c [Å]	14.6568(16)	14.8304(10)
β [°]	123.417(2)	123.2900(10)
V [Å³]	4116.8(8)	4246.2(5)
Z	4	4
ρ_{calcd} [g cm^{-3}]	3.453	3.319
Temperature [K]	183(2)	183(2)
μ (MoK_α) [mm^{-1}]	20.190	18.642
θ range [°]	2.24 - 28.30	2.21 - 28.31
index ranges	$-24 \le h \le 24$	$-24 \le h \le 24$
	$-24 \le k \le 24$	$-24 \le k \le 24$
	$-19 \le l \le 19$	$-19 \le l \le 19$
measured reflections	16995	18655
independent reflections	5108	5244
observed reflections [$I > 2\sigma(I)$]	3262	3863
R_{int}	0.1089	0.0500
parameters	242	242
goodness-of-fit on F^2	0.948	1.002
R values	*R1* = 0.0680	*R1* = 0.0435
[$I > 2\sigma(I)$]	*wR2* = 0.1574	*wR2* = 0.0981
R values	*R1* = 0.1157	*R1* = 0.0668
(for all data)	*wR2* = 0.1780	*wR2* = 0.1038
residual electron density [e*Å^{-3}]	3.684 / -2.141	2.227 / -2.753

Table 2. Atom coordinates [x 10^4] and isotropic thermal parameters [$Å^2$ x 10^3] of $Li_3Rb_6U_3(S)S_2(PS_4)_5$ (**XII**). U(eq) is defined as one third of the trace of the orthogonalized matrix U_{ij}.

	x	y	z	U(eq)	sof
U(1)	1150(1)	1147(1)	5385(1)	18(1)	
U(2)	0	5882(1)	2500	20(1)	
S(1)	157(6)	83(5)	436(8)	38(2)	0.5
S(2)	3156(3)	4084(2)	2485(4)	34(1)	
S(11)	1940(3)	231(2)	635(4)	37(1)	
S(12)	2145(3)	3660(2)	4118(5)	43(1)	
S(13)	3699(3)	210(3)	518(4)	41(1)	
S(14)	1027(3)	4920(4)	2171(5)	66(2)	
S(21)	3334(3)	2398(2)	3846(4)	30(1)	
S(22)	3852(4)	2070(3)	2016(4)	53(2)	
S(23)	4922(3)	3161(2)	695(6)	53(2)	
S(24)	4959(3)	1348(2)	598(4)	37(1)	
S(31)	435(8)	1763(8)	1494(11)	29(3)	0.315
S(32)	834(12)	569(10)	3432(14)	50(5)	0.315
S(33)	333(19)	2182(10)	3677(14)	81(9)	0.318
S(34)	1168(12)	1198(13)	3533(16)	61(6)	0.318
S(35)	1056(13)	1927(9)	3617(11)	70(7)	0.367
S(36)	295(8)	700(7)	1592(10)	34(3)	0.367
P(1)	1885(3)	4743(2)	3791(4)	27(1)	
P(2)	4318(3)	2257(2)	3624(4)	27(1)	
P(3)	0	1380(4)	2500	42(2)	
Rb(1)	53(2)	3472(2)	3273(3)	36(1)	0.5
Rb(2)	1514(4)	2901(4)	1558(5)	85(3)	0.440
Rb(3)	1991(3)	2809(3)	948(4)	80(2)	0.560
Rb(4)	2422(11)	765(4)	3136(5)	50(2)	0.725
Rb(5)	2820(20)	654(7)	3365(19)	31(5)	0.275
Rb(6)	4679(3)	4169(2)	2104(4)	65(2)	0.5

Table 3. Selected bond distances [Å] for $Li_3Rb_6U_3(S)S_2(PS_4)_5$ (**XII**).

U(1)-S(2)	2.676(4)	P(1)-S(14)	2.026(7)
U(1)-S(34)	2.735(18)	P(1)-S(12)	2.026(6)
U(1)-S(36)	2.769(12)	P(1)-S(13)	2.028(6)
U(1)-S(1)	2.793(18)	P(1)-S(11)	2.049(6)
U(1)-S(32)	2.799(8)	P(2)-S(21)	2.031(6)
U(1)-S(33)	2.817(17)	P(2)-S(24)	2.034(6)
U(1)-S(12)	2.826(4)	P(2)-S(23)	2.036(6)
U(1)-S(11)	2.833(4)	P(2)-S(22)	2.044(7)
U(1)-S(21)	2.836(4)	P(3)-S(34) (2x)	1.86(2)
U(1)-S(23)	2.841(4)	P(3)-S(35) (2x)	1.990(15)
U(1)-S(35)	2.876(13)	P(3)-S(32) (2x)	2.026(16)
U(1)-S(1)	2.920(13)	P(3)-S(33) (2x)	2.078(18)
U(1)-S(31)	2.923(9)	P(3)-S(36) (2x)	2.099(14)
U(2)-S(14) (2x)	2.813(5)	P(3)-S(31) (2x)	2.147(13)
U(2)-S(13) (2x)	2.832(5)		
U(2)-S(22) (2x)	2.833(5)		
U(2)-S(24) (2x)	2.875(5)		

Table 4. Atom coordinates [x 10^4] and isotropic thermal parameters [$Å^2$ x 10^3] of $Li_3Rb_6Th_3(S)S_2(PS_4)_5$ (**XIII**). U(eq) is defined as one third of the trace of the orthogonalized matrix U_{ij}.

	x	y	z	U(eq)	sof
Th(1)	1145(1)	1147(1)	5378(1)	17(1)	
Th(2)	0	5883(1)	2500	20(1)	
S(1)	157(4)	69(3)	442(5)	38(1)	0.5
S(2)	3154(2)	4084(1)	2466(2)	35(1)	
S(11)	1964(2)	239(1)	646(2)	35(1)	
S(12)	2133(2)	3664(2)	4120(3)	43(1)	
S(13)	3700(2)	199(2)	517(2)	44(1)	
S(14)	1035(2)	4894(2)	2176(2)	65(1)	
S(21)	3339(2)	2385(1)	3847(2)	30(1)	
S(22)	3854(2)	2093(2)	2043(3)	59(1)	
S(23)	4907(2)	3144(2)	689(3)	52(1)	
S(24)	4964(2)	1358(2)	596(2)	41(1)	
S(31)	435(5)	1779(5)	1511(6)	32(2)	0.321
S(32)	806(7)	566(6)	3380(7)	51(3)	0.321
S(33)	305(9)	2176(6)	3630(7)	62(4)	0.308
S(34)	1170(7)	1184(10)	3505(8)	73(5)	0.308
S(35)	1033(8)	1925(5)	3598(6)	65(4)	0.371
S(36)	310(4)	692(4)	1625(5)	33(2)	0.371
P(1)	1883(2)	4743(2)	3789(2)	31(1)	
P(2)	4322(2)	2253(1)	3642(2)	27(1)	
P(3)	0	1383(2)	2500	39(1)	
Rb(1)	43(1)	3466(1)	3273(2)	36(1)	0.5
Rb(2)	1502(2)	2924(2)	1558(3)	84(2)	0.438
Rb(3)	1989(2)	2817(2)	967(3)	99(2)	0.562
Rb(4)	2432(9)	756(3)	3143(4)	49(2)	0.715
Rb(5)	2809(17)	643(5)	3339(13)	35(3)	0.285
Rb(6)	4675(2)	4152(2)	2103(2)	64(1)	0.5

Table 5. Selected bond distances [Å] for $Li_3Rb_6Th_3(S)S_2(PS_4)_5$ (**XIII**).

Th(1)-S(2)	2.744(2)	P(1)-S(14)	2.036(4)
Th(1)-S(34)	2.804(10)	P(1)-S(12)	2.038(4)
Th(1)-S(36)	2.833(6)	P(1)-S(13)	2.038(4)
Th(1)-S(1)	2.838(5)	P(1)-S(11)	2.041(4)
Th(1)-S(32)	2.876(10)	P(2)-S(21)	2.027(3)
Th(1)-S(33)	2.880(10)	P(2)-S(24)	2.027(4)
Th(1)-S(12)	2.884(3)	P(2)-S(23)	2.042(4)
Th(1)-S(11)	2.885(3)	P(2)-S(22)	2.049(4)
Th(1)-S(21)	2.888(2)	P(3)-S(34) (2x)	1.879(11)
Th(1)-S(23)	2.896(3)	P(3)-S(35) (2x)	1.976(9)
Th(1)-S(35)	2.908(8)	P(3)-S(32) (2x)	2.016(10)
Th(1)-S(1)	2.932(5)	P(3)-S(33) (2x)	2.054(10)
Th(1)-S(31)	2.967(7)	P(3)-S(36) (2x)	2.111(8)
Th(2)-S(14) (2x)	2.875(3)	P(3)-S(31) (2x)	2.154(9)
Th(2)-S(13) (2x)	2.877(3)		
Th(2)-S(22) (2x)	2.896(3)		
Th(2)-S(24) (2x)	2.922(3)		

References

Chapter 1

1 Kresge, C. T.; Leonowicz, M. E.; Roth, W. J.; Vartuli, J. C. U.S. Pat. Patent 5,098,684, **1992**.

2 Kutz, N. A. in *Perspectives in Molecular Sieve Science* (Eds.: Flank, W. H.; Whyte, T. E.), *ACS Symp. Ser.* **1988** ,*368*, 532.

3 Ratnasamy, P.; Kumar, R. *Catal. Today* **1991**, *9*, 329-416.

4 Bellussi, G.; Rigutto, M. S. in *Advanced Zeolite Science and Applications* (Eds.: Jansen, J. C.; Stöcker, M.; Karge, H. G.; Weitkamp, J.) *Stud. Surf. Sci. Catal.* **1994**, *85*, 177.

5 Flanigen, E. M.; Patton, R. L.; Wilson, S. T. in *Innovation in Zeolite Materials Science* (Eds.: Grobet, P. J.; Mortier, W. J.; Vansant, E. F.; Schulz-Ekloff, G.) *Stud. Surf. Sci. Catal.* **1988**, *37*, 13.

6 Wilson, S. T. in *Introduction to Zeolite Science and Practice* (Eds.: van Bekkum, H.; Flanigen, E. M.; Jansen, J. C.) *Stud. Surf. Sci. Catal.* **1991**, *58*, 137.

7 Martens, J. A.; Jacobs, P. A. *Advanced Zeolite Science and Applications* (Eds.: Jansen, J. C.; Stöcker, M.; Karge, H. G.; Weitkamp, J.) *Stud. Surf. Sci. Catal.* **1994**, *85*, 653.

8 Pauling, L. *Die Natur der chemischen Bindung*, Verlag Chemie, Weinheim, **1988**.

9 Bedard, R. L.; Vail, L. D.; Wilson, S. T.; Flanigen, E. M. (UOP) U.S. Pat. Patent 4,880,761, **1989**; Bedard, R. L.; Vail, L. D.; Wilson, S. T.; Flanigen, E. M. (UOP), U.S. Pat. Patent 4,933,068, **1990**; Bedard, R. L.; Wilson, S. T.; Vail, L. D.; Bennett, J. M.; Flanigen, E. M. in *Zeolites: Facts, Figures and Future* (Eds.: Jacobs, P. A.; van Santen, R. A.), Elsevier, Amsterdam, **1989**.

10 (a) Yaghi, O.; Sun, Z.; Richardson, D. A.; Groy, T. L. *J. Am. Chem. Soc*. **1994**, *116*, 807-808.

(b) Achak, O.; Pivan, J. Y.; Maunaye, M.; Louër, M.; Louër, D. *J. Alloys Compd*. **1995**, *219*, 111-115.

(c) Achak, O.; Pivan, J. Y.; Maunaye, M.; Louër, M.; Louër, D. *J. Solid State Chem*. **1996**, *121*, 473-478.

11 Tan, K.; Darovsky, A.; Parise, J. B. *J. Am. Chem. Soc*. **1995**, *117*, 7039-7040.

12 Bowes, C. L.; Lough, A. J.; Malek, A.; Ozin, G. A.; Petrov, S.; Young, D. *Chem. Ber*. **1996**, *129*, 283-287.

13 MacLachlan, M. J.; Coombs, N.; Ozin, G. A. *Nature* **1999**, *397*, 681-684.

14 Wachhold, M.; Rangan, K. K.; Billinge, S. J. L.; Petkov, V.; Heising, J.; Kanatzidis, M. G. *Adv. Mater*. **2000**, *12*, 85-91.

15 MacLachlan, M. J.; Petrov, S.; Bedard, R. L.; Manners, I.; Ozin, G. A., *Angew. Chem*. **1998**, *110*, 2186-2189. *Angew. Chem. Int. Ed. Engl*. **1998**, *37*, 2076-2079.

16 (a) Angenault, J.; Cieren, X.; Wallez, G.; Quarton, M. *J. Solid State Chem*. **2000**, *153*, 55-65.

(b) Cieren, X.; Angenault, J.; Couturier, J.C.; Jaulmes, S.; Quarton, M.; Robert, F. *J. Solid State Chem*. **1996**, *121*, 230-236.

(c) Derstroff, V.; Tremel, W.; Regelsky, G.; Schmedt auf der Günne, J.; Eckert, H. *Solid State Sciences* **2002**, *4*, 731-745.

(d) McCarthy, T.; Kanatzidis, M. G. *J. Alloys Comp.* **1996,** *236*, 70-85.

17 (a) Gauthier, G.; Evain, M.; Jobic, S.; Brec, R. *Solid State Sciences* **2002**, *4*, 1361-1366.

(b) Hess, R. F.; Abney, K. D.; Burris, J. L.; Hochheimer, H. D.; Dorhout, P. K. *Inorg. Chem*. **2001**, *40***,** 2851-2059.

(c) Wibbelmann, C.; Brockner, W.; Eisenmann, B.; Schäfer, H. *Z. Naturforsch.* **1984**, *39A*, 190-194.

18 (a) Klingen, W.; Eulenberger, G.; Hahn, H. *Z. Anorg. Allg. Chem.* **1973**, *401*, 97-112.

(b) Prouzet, E.; Ouvrard, G.; Brec, R. *Mater. Res. Bull.* **1986**, *21*, 195-200.

(c) Ouvrard, G.; Fréour, R.; Brec, R.; Rouxel, J. *Mater. Res. Bull.* **1985**, *20*, 1053-1062.

(d) Ouvrard, G.; Brec, R.; Rouxel, J. *Mater. Res. Bull.* **1985**, *20*, 1181-1189.

19 (a) Klingen, W.; Ott, R.; Hahn, H. *Z. Anorg. Allg. Chem*. **1973**, *396*, 271-278.

(b) Wiedenmann, A.; Rossat-Mignod, J.; Louisy, A.; Brec, R.; Rouxel, J. *Solid State Commun*. **1981**, *40*, 1067-1072.

20 Brec, R. *Solid State Ionics*, **1986**, *22*, 3-30.

21 (a) Brec, R.; Schleich, D. M.; Ouvrard, G.; Louisy, A.; Rouxel, J. *Inorg. Chem*. **1979**, *18*, 1814-1818.

(b) Clément, R.; Doeuff, M.; Gledel, C. *J. Chim. Phys.* **1988**, *85*, 1053-1057.

22 Foot, P. J. S.; Katz, T.; Patel, S. N.; Nevett, B. A.; Piercy, A. R.; Balchin, A. A. *Phys. Stat. Sol. A* **1987**, *100***,** 10-29.

23 (a) Manríquez, V.; Galdámez, A.; Ponce, J.; Brito, I.; Kasaneva, J. *Mater. Res. Bull*. **1999**, *34*, 123-130.

(b) Zhang, D.; Qin, J.; Yakushi, K.; Nakazawa, Y.; Ichimura, K. *Mat. Sci. Eng. A* **2000**, *286*, 183-187.

(c) Sukpirom, N.; Oriakhi, C. O.; Lerner, M. M. *Mater. Res. Bull*. **2000**, *35*, 325-331.

24 Yang, D.; Westreich, P.; Frindt, R. F. *J. Solid State Chem*. **2002**, *166*, 421-425.

25 Lagadic, I.; Lacroix, P. G.; Clément, R. *Chem. Mater*. **1997**, *9*, 2004-2012.

26 (a) Colombet, P.; Leblanc, A.; Danot, M.; Rouxel, J. *Nouv. J. Chim*. **1983**, *7*, 333-338.

(b) Lee, S.; Ouvrard, G.; Colombet, P.; Brec, R. *Mater. Res. Bull*. **1986**, *21*, 917-928.

(c) Ouili, Z.; Leblanc, A.; Colombet, P. *J. Solid State Chem*. **1987**, *66*, 86-94.

(d) Colombet, P.; Leblanc, A.; Danot, M.; Rouxel, J. *J. Solid State Chem*. **1982**, *41*, 174-184.

27 (a) Pfeiff, R.; Kniep, R. *Z. Naturforsch*. **1993**, *48 b*, 1270-1274.
(b) Pfeiff, R.; Kniep, R. *J. Alloys Comp*. **1992**, *186*, 111-133.
(c) Bourdon, X.; Maisonneuve, V.; Cajipe, V. B.; Payen, C.; Fischer, J. E. *J. Alloys Comp*. **1999**, *283*, 122-127.
(d) Ouvrard, G.; Brec, R. *Mater. Res. Bull*. **1988**, *23*, 1199-1209.

28 Jandali, M. Z.; Eulenberger, G.; Hahn, H. *Z. Anorg. Allg. Chem*. **1978**, *447*, 105-118.

29 Wang, Z.; Willett, R. D.; Laitinen, R. A.; Cleary, D. A. *Chem. Mater.* **1995**, *7*, 856-858.

30 Ouvrard, G.; Fréour, R.; Brec, R.; Rouxel, J. *Mater. Res. Bull*. **1985**, *20*, 1053-1062.

31 Diehl, R.; Carpentier, C.-D. *Acta Cryst*. **1978**, *B 34*, 1097-1105.

32 Jandali, M. Z.; Eulenberger, G.; Hahn, H. *Z. Anorg. Allg. Chem*. **1980**, *470*, 39-44.

33 Simon, A.; Peters, K.; Peters, E.; Hahn, H. *Z. Anorg. Allg. Chem.* **1982**, *491*, 295-300.

34 Do, J.; Kim, J.; Lah, S.; Yun, H. *Bull. Korean Chem. Soc*. **1993**, *14*, 678-681.

35 Simon, A.; Hahn, H.; Peters, K. *Z. Naturforsch*. **1985**, *40 b*, 730-732.

36 Brec, R.; Ouvrard, G.; Evain, M.; Grenouilleau, P.; Rouxel, J. *J. Solid State Chem*. **1983**, *47*, 174-184.

37 Grenouilleau, P.; Brec, R.; Evain, M.; Rouxel, J. *Rev. Chim. Miner*. **1983**, *20*, 628-635.

38 Brec, R.; Grenouilleau, P.; Evain, M., Rouxel, J. *Rev. Chim. Miner*. **1983**, *20*, 295-304.

39 Brec, R.; Evain, M.; Grenouilleau, P.; Rouxel, J. *Rev. Chim. Miner*. **1983**, *20*, 283-294.

40 Brec, R.; Fréour, R.; Ouvrard, G.; Soubeyroux, J. L.; Rouxel, J. *Mater. Res. Bull*. **1983**, *18*, 689-696.

41 Evain, M.; Brec, R.; Ouvrard, G.; Rouxel, J. *J. Solid State Chem.* **1985**, *56*, 12-20.

42 Evain, M.; Brec, R., Ouvrard, G.; Rouxel, J. *Mater. Res. Bull.* **1984**, *19*, 41-48.

43 Evain, M.; Lee, S.; Queignec, M.; Brec, R. *J. Solid State Chem.* **1987**, *71*, 139-153.

44 Fiechter, S.; Kuhs, W. F.; Nitsche, R. *Acta Crystallogr.* **1980**, *B36*, 2217-2220.

45 Evain, M.; Queignec, M.; Brec, R.; Rouxel, J. *J. Solid State Chem.* **1985**, *56*, 148-157.

46 Evain, M.; Queignec, M.; Brec, R.; Sourisseau, C. *J. Solid State Chem.* **1988**, *75*, 413-431.

47 Chondroudis, K.; Kanatzidis, M. G.; Sayettat, J.; Jobic, S.; Brec, R. *Inorg. Chem.* **1997**, *36*, 5859-5868.

48 Bither, T. A.; Donohue, P. C.; Young, H. S. *J. Solid State Chem.* **1971**, *3*, 300-307.

49 Derstroff, V.; Ksenofontov, V.; Gütlich, P.; Tremel, W. *Chem. Commun.* **1998**, 187-188.

50 Derstroff, V.; Ensling, J.; Ksenofontov, V.; Gütlich, P.; Tremel, W. *Z. Anorg. Allg. Chem.* **2002**, *628*, 1346-1354.

Chapter 2

1 Zachariasen, W. H. *Acta Cryst.* **1949**, *2*, 291-296.

2 Ferro, R. *Z. Anorg. Allg. Chem.* **1954**, *275*, 320-326.

3 Potel, M.; Brochu, R.; Padiou, J.; Grandjean, D. *C. R. Séances Acad. Sci. Ser. C* **1972**, *275*, 1419-1421.

4 Tougait, O.; Potel, M.; Noel, H. *Inorg. Chem.* **1998**, *37*, 5088-5091.

5 Stoewe, K. *J. Solid State Chem.* **1996**, *127*, 202-210.

6 Tougait, O.; Potel, M.; Levet, J. C.; Noel, H. *Eur. J. Solid State Inorg. Chem.* **1998**, *35*, 67-76.

7 (a) Ben Salem, A.; Meerschaut, A.; Rouxel, J. *C. R. Séances Acad. Sci. Ser. C* **1984**, *299*, 617-619.

(b) Stoewe, K. *Z. Anorg. Allg. Chem.* **1996**, *622*, 1419-1422.

8 Noel, H. *Inorg. Chim. Acta* **1985**, *109*, 205-207.

9 Chondroudis, K.; Kanatzidis, M. G. *J. Am. Chem. Soc.* **1997**, *119*, 2574-2575.

10 Briggs Piccoli, P. M.; Abney, K. D.; Schoonover, J. D.; Dorhout, P. K. *Inorg. Chem*. **2001**, *40***,** 4871-4875.

11 (a) Hess, R. F.; Abney, K. D.; Burris, J. L.; Hochheimer, H. D.; Dorhout, P. K. *Inorg. Chem*. **2001**, *40***,** 2851-2059.

(b) Chondroudis, K.; Kanatzidis, M. G. *C. R. Séances Acad. Sci.* **1996**, *322*, 887-894.

12 (a) Pearson, W. B. *Z. Krist.* **1985**, *171*, 23-39.

(b) Do, J.; Kim, J.; Lah, S.; Yun, H. *Bull. Korean Chem. Soc.* **1993**, *14*, 678-681.

(c) Baskin, Y.; Shalek, P. D. *J. Am. Ceram. Soc.* **1969**, *52*, 341-342.

13 Gieck, C.; Rocker, F.; Ksenofontov, V.; Gütlich, P.; Tremel, W. *Angew. Chem*. **2001**, *113*, 946-948; *Angew. Chem. Int. Ed.* **2001**, *40*, 908-911.

14 Neitzel, S. Ph. D. Thesis, Mainz, **1999**.

15 *POWDERCELL*, Version 2.3; Kraus, G.; Nolze, W.: Berlin, Germany, **1999**.

16 (a) Weiss, A.; Witte, H. *Magnetochemie: Grundlagen, Anwendungen*, Verlag Chemie: Weinheim, **1973**.

(b) Lueken, H. *Einführung in die Magnetochemie*, RWTH Aachen: Aachen, **1988**.

(c) Selwood, P. W. *Magnetochemistry*, Interscience Publishers: New York, **1956**.

(d) Mabbs, F. E.; Machin, J. D. *Magnetism and Transition Metal Complexes*, Chapman and Hall: London, **1973**.

17 *SMART*, 5th ed.; Siemens Analytical X-ray Systems, Inc.: Madison, WI, **1998**.

18 *SAINT*, 4th ed.; Siemens Analytical X-ray Systems, Inc.: Madison, WI, **1998**.

19 Sheldrick, G. M. *SADABS*; University of Göttingen: Göttingen, **1997**.

20 Sheldrick, G. M. *SHELXTL 5.1*; Siemens Analytical X-ray Systems, Inc.: Madison, WI, **1998**.

21 Wilson, A. J. C. (editor) *International Tables for Crystallography*, *Volume C*, Kluwer Academic Publishers: Dordrecht **1992**.

22 Simon, A.; Peters, K.; Peters, E.; Hahn, H. *Z. Anorg. Allg. Chem.* **1982**, *491*, 295-300.

23 Lott, D. R.; Fincher, T.; LeBret, G. C.; Cleary, D. A. *J. Solid State Chem.* **1999**, *143*, 239-245.

24 Spek, A. L. *PLATON*; University of Utrecht: Utrecht, **2003**.

25 Hamilton, W. C. *Acta Cryst*. **1965**, *18*, 502-510.

26 Wibbelmann, C.; Brockner, W.; Eisenmann, B.; Schäfer, H. *Z. Naturforsch.* **1984**, *39A*, 190-194.

27 (a) Volodina, A. N.; Kuvshinova, T. B.; Maksimova, S. I.; Muravev, E. N.; Niyazov, S. A.; Orlovskii, V. P.; Palkina, K. K.; Chibiskova, N. T. *Zh. Neorg. Khim.* **1987**, *32*, 2899-2901.

(b) Palkina, K. K.; Maksimova, S. I.; Chibiskova, N. T.; Kuvshinova, T. B.; Volodina, A. N. *Izv. Akad. Nauk SSSR*, *Neorg. Mater.* **1984**, *20*, 1557-1560.

(c) Palkina, K. K.; Kuvshinova, T. B.; Maksimova, S. I.; Chibiskova, N. T.; Tripolskaya, T. A. *Izv. Akad. Nauk SSSR*, *Neorg. Mater.* **1989**, *25*, 1555-1556.

28 (a) Le Rolland, B.; McMillan, P.; Molinie, P.; Colombet, P. *Eur. J.Solid State Inorg. Chem.* **1990**, *27*, 715-724.

(b) Le Rolland, B.; Molinie, P.; Colombet, P.; *C. R. Séances Acad. Sci. Ser.II*, **1998**, *310*, 1201-1206.

29 (a) LeBret, G. C.; McCoy, H. C.; Kittelstved, K. R.; Cleary, D. A., Twamley, B. *Inorg. Chim. Acta* **2003**, *343*, 141-146.

(b) Gauthier, G.; Jobic, S.; Boucher, F.; Macaudière, P.; Huguenin, D.; Rouxel, J.; Brec, R.; *Chem. Mater.* **1998**, *10*, 2341-2347.

30 Groenvold, F.; Haraldsen, H.; Kjekshus, A. *Acta Chem. Scand*. **1966**, *20*, 577-579.

31 Ermer, O.; Eling, A. *Angew. Chem*. **1988**, *100*, 856-859; *Angew. Chem. Int. Ed. Engl.* **1988**, *27*, 829-833.

32 Riedel, R.; Greiner, A.; Miehe, G.; Dressler, W.; Fuess, H.; Bill, J.; Aldinger, F. *Angew. Chem.* **1997**, *109*, 657-660; *Angew. Chem. Int. Ed. Engl.* **1997**, *36*, 603-606.

33 (a) Hirsch, K. A.; Venkataraman, D.; Wilson, S. R.; Moore, J. S.; Lee, S. *J. Chem. Soc., Chem. Commun.* **1995**, 2199-2200.

(b) Hirsch, K. A.; Wilson, S. C.; Moore, J. S. *Chem. Eur. J.* **1997**, *3*, 765-771.

34 Toffoli, P.; Rouland, J. C.; Khodadad, P.; Rodier, N. *Acta Cryst.* **1985**, *C41*, 645-647.

35 Angenault, J.; Cieren, X.; Wallez, G.; Quarton, M. *J. Solid State Chem*. **2000**, *153*, 55-65.

36 Cieren, X.; Angenault, J.; Couturier, J.C.; Jaulmes, S.; Quarton, M.; Robert, F. *J. Solid State Chem*. **1996**, *121*, 230-236.

37 Derstroff, V.; Tremel, W.; Regelsky, G.; Schmedt auf der Günne, J.; Eckert, H. *Solid State Sciences* **2002**, *4*, 731-745.

38 McCarthy, T.; Kanatzidis, M. G. *J. Alloys Comp.* **1996,** *236*, 70-85.

39 Evenson, C. R.; Dorhout, P. K. *Inorg. Chem*. **2001**, *40*, 2884-2891.

40 (a) Tremel, W; Kleinke, H.; Derstroff, V.; Reisner, C. *J. Alloys Comp.* **1995,** *219*, 73-82.

(b) Derstroff, V.; Tremel, W. *Z. Naturforsch*. **2003**, *to be submitted for publication.*

41 Derstroff, V.; Ensling, J.; Ksenofontov, V.; Gütlich, P.; Tremel, W. *Z. Anorg. Allg. Chem.* **2002**, *628*, 1346-1354.

42 Derstroff, V. Ph. D. Thesis, Mainz **1998**.

43 Müller, A.; Jostes, R.; Flemming, V.; Potthast, R. *Inorg. Chim. Acta* **1980**, *44*, L33-L35.

44 (a) Coucouvanis , D.; Simhon, E. D.; Baenzinger, N. C. *J. Amer. Chem. Soc.* **1980**, *102*, 6644-6646.
(b) Callahan, K. P.; Piliero, P. A. *J. Chem. Soc., Chem. Commun.* **1979**, 13-14.

45 Kopnin, E.; Coste, S.; Jobic, S.; Evain, M.; Brec, R. *Mater. Res. Bull.* **2000**, *35*, 1401-1410.

46 Gieck, C.; Derstroff, V.; Block, T.; Felser, C.; Regelsky, G.; Ksenofontov, V.; Gütlich, P.; Eckert, H.; Tremel, W. *Chem. Eur. J.* **2003**, *submitted for publication.*

47 Cieren, X.; Angenault, J.; Couturier, J.-C.; Jaulmes, S.; Quarton, M.; Robert, F. *J. Solid State Chem.* **1996**, *121*, 230-235.

48 Derstroff, V.; Regelsky, G.; Eckert, H.; Tremel, W. *J. Chem. Soc., Dalton Trans.* **2003**, *to be submitted for publication*.

49 Derstroff V.; Tremel W. *Chem. Commun.* **1998**, 913-914.

50 Nakamoto, K. *Infrared and Raman Spectra of Inorganic and Coordination Compounds, Part A, 5th edition*, John Wiley & Sons: New York, **1997**.

51 Poizat, O.; Sourisseau, C.; Mathey, Y. *J. Solid State Chem.* **1988**, *72*, 272-282.

52 (a) Toffoli, P.; Khodadad, P.; Rodier, N. *Acta Cryst.* **1977**, *B33*, 1492-1494.
(b) Sourisseau, C., *unpublished results*.

53 Sourisseau, C.; Fragnaud, P.; Prouzet, E.; Brec, R. *J. Solid State Chem.* **1994**, *112*, 299-304.

54 Urland, W. *Chem. Phys.* **1976,** *14*, 393-401.

55 Urland, W. *Chem. Phys.* Lett. **1977**, *46*, 457-460.

56 Lueken, H. *Magnetochemie*, Teubner-Verlag, Stuttgart, **1999**.

57 Johnston, D. R.; Satten, R. A.; Schreiber, C. L.; Wong, E. Y. *J. Chem. Phys.* **1966**, *44*, 3141-3143.

58 Urland, W. *Chem. Phys.* **1979**, *38*, 407-412.

59 Urland, W. *Chem. Phys. Lett.* **1979**, *62*, 525-528.

60 Becker, A.; Urland, W. *Z. Anorg. Allg. Chem.* **1999**, *625*, 1033-1036.

61 Bleaney, B. *Proc. Roy. Soc. London, Sect. A* **1963**, *276*, 19-27.

62 Urland, W. *Z. Naturforsch.* **1980**, *35a*, 247-251.

63 Amoretti, G.; Blaise, A.; Fournier, J. M.; Caciuffo, R. Larroque, J.; Osborn, R.; Tylor, A. D.; Bowden, Z. A. *J. Magn. Magn. Mater.* **1995**, *139*, 339-346.

64 Troc, R. *Inorg. Chim. Acta* **1987**, *140*, 67-77.

65 Kaczorowski, D.; Pöttgen, R.; Gajek, Z.; Zygmunt A.; Jeitschko, W. *J. Phys. Chem. Solids* **1993**, *54*, 723-732.

66 Warren, K. D. *Inorg. Chem*. **1977** ,*16*, 2008-2011.

67 Gajek, Z.; Mulak, J. *J. Phys. Cond. Matter* **1992**, *4*, 427-444.

68 Hatscher, S. T.; Urland, W. *Mater. Res. Bull.* **2003**, *38*, 99-112.

69 Hatscher, S. T.; Urland, W. *Z. Anorg. Allg. Chem*. **2002**, *628*, 1673-1677.

Chapter 3

1 (a) Kanatzidis, M. G. *Curr. Opin. Solid State Mater. Sci.* **1997**, *2*, 139-149.

(b) Kanatzidis, M. G.; Sutorik, A. C.*Progr. Inorg. Chem.* **1995**, *43*, 151-265.

2 (a) Tremel, W.; Kleinke, H.; Derstroff, V.; Reisner, C. *J. Alloys Comp.* **1995**, *219*, 73-82.

(b) Hess, R. F.; Gordon, P. L.; Tait, C. D.; Abney, K. D.; Dorhout, P. K. *J. Amer. Chem. Soc.* **2002**, *124*, 1327-1333.

(c) Evenson, C. R.; Dorhout, P. K. *Inorg. Chem.* **2001**, *40*, 2884-2891.

3 (a) Briggs Piccoli, P. M.; Abney, K. D.; Schoonover, J. D.; Dorhout, P. K. *Inorg. Chem.* **2000**, *39*, 2970-2976.

(b) Briggs Piccoli, P. M.; Abney, K. D.; Schoonover, J. D.; Dorhout, P. K. *Inorg. Chem.* **2001**, *40*, 4871-4875.

(c) Evenson, C. R.; Dorhout, P. K. *Inorg. Chem.* **2001**, *40*, 2875-2883.

4 Derstroff, V.; Ksenofontov, V.; Gütlich, P.; Tremel, W. *Chem. Commun.* **1998**, 187-188.

5 Hess, R. F.; Abney, K. D.; Burris, J. L.; Hochheimer, H. D.; Dorhout, P. K. *Inorg. Chem.* **2001**, *40*, 2851-2859.

6 Derstroff, V., Ph. D. Thesis, Mainz **1998**.

7 Derstroff, V.; Ensling, J.; Ksenofontov, V.; Gütlich, P.; Tremel, W. *Z. Anorg. Allg. Chem.* **2002**, *628*, 1346-1354.

8 Zones, S. I.; Hwang, S.-J. *Chem. Mater.* **2002,** *14*, 313-320.

9 *SMART*, 5th ed.; Siemens Analytical X-ray Systems, Inc., Madison, WI, **1998**.

10 *SAINT*, 4th ed.; Siemens Analytical X-ray Systems, Inc., Madison, WI, **1998**.

11 Sheldrick, G. M.: *SADABS*; University of Göttingen: Göttingen, **1997**.

12 Sheldrick, G. M.: *SHELXTL 5.1*, Siemens Analytical X-ray Systems, Inc., Madison, WI, **1998**.

13 Wilson, A. J. C. (editor) *International Tables for Crystallography*, *Volume C*, Kluwer Academic Publishers: Dordrecht **1992**.

14 (a) Kortüm, G. *Reflectance Spectroscopy*, Springer, New York, **1969**.

(b) Clarke, R. J. H. *J. Chem. Educ.* **1964**, *41*, 488-492.

(c) Wendlandt, W. W.; Hecht, H. G. *Reflectance Spectroscopy (Chemical Analysis, Vol. 21)*, Interscience, New York, **1966**.

15 The solution was prepared by suspending 10 mg of finely ground $Rb_5U(PS_4)_3$ in 5 ml of toluene saturated with 2,2,2 crypt under argon atmosphere. To this mixture, 1 ml of previously dried acetonitrile was added and stirred. The resulting blue-green solution can be stored for several weeks in a sealed vial, but quickly forms a light yellow oxidation product upon contact with air.

16 Mathey, Y.; Clement, R.; Sourisseau, C.; Lucazeau, G. *Inorg. Chem.* **1980**, *19*, 2773-2779.

17 Sourisseau, C.; Fragnaud, P.; Prouzet, E.; Brec, R. *J. Solid State Chem.* **1994**, *112*, 299-306.

18 Pätzmann, U.; Brockner, H. *Z. Naturforsch.* **1983**, *38A*, 27-36.

19 Chondroudis, K.; Kanatzidis, M. G.; Sayettat, J.; Jobic, S.; Brec, R. *Inorg. Chem.* **1997**, *36*, 5859-5868.

20 Seel, F.; Güttler, H. J. *Angew. Chem.* **1973**, *85*, 416-417; *Angew. Chem. Int. Ed. Engl.* **1973**, *12*, 420-421.

21 (a) Daoudi, A.; Lamire, M.; Levet, J. C.; Noel, H. *J. Solid State Chem*. 1996, *123*, 331-337.

(b) Noel, H. *J. Solid State Chem*. **1984**, *52*, 203-210.

22 (a) Corbett, J. D. *Chem. Rev*. **1985**, *85*, 383-403.

(b) Bolle, U.; Tremel, W. *J. Chem. Soc., Chem. Commun.*, **1992**, 93-94.

(c) Bolle, U.; Tremel, W. *J. Chem. Soc., Chem. Commun.*, **1994**, 217-218.

23 Tarling, S. E.; Barnes, P.; Klinowski, J. *Acta Crystallogr.*, **1988**, *B44*, 128-135.

24 (a) Shannon, R. D.; Prewitt, C. T. *Acta Crystallogr.*, **1969**, *B25*, 925-946.

(b) Shannon, R. D.; Prewitt, C. T. *Acta Crystallogr.*, **1970**, *B26*, 1046-1048.

25 (a) Gauthier, G.; Guillen, F.; Jobic, S.; Deniard, P.; Macaudiere, P.; Fouassier, C.; Brec, R. *C. R. Séances Acad. Sci. Ser.II*, **1999**, *2*, 611-616.

(b) Evenson, C. R.; Dorhout, P. K. *Inorg. Chem.* **2001**, *40*, 2409-2414.

(c) Marking, G. A.; Kanatzidis, M. G. *J. Alloys Comp.* **1997**, *259*, 122-128.

26 (a) Wu, P.; Lu, Y.-J.; Ibers, J. A. *J. Solid State Chem*. **1992**, *97*, 383-390.

(b) Wu, P.; Ibers, J. A. *J. Solid State Chem*. **1993**, *107*, 347-355.

(c) Aitken, J. A.; Marking, G. A.; Evain, M.; Iordanidis, L. Kanatzidis, M. G. *J. Solid State Chem*. **2000**, *153*, 158-169.

(d) Bucher, C. K.; Hwu, S.-J. *Inorg. Chem.* **1994**, *33*, 5831-5835.

27 (a) Löken, S.; Tremel, W. *Z. Anorg. Allg. Chem.* **1998**, *624*, 1588-1594.

(b) Wu, P.; Ibers, J. A., *Acta Crystallogr.* **1993**, *C49*, 126-129.

(c) Guo, H.-Y.; Li, Z.-H.; Yang, L.; Wang, P.; Huang, X.-Y.; Li, J. *Acta Crystallogr.* **2001**, *C57*, 1237-1238.

(d) Liao, J.-H.; Kanatzidis, M. G. *Chem. Mater.* **1993**, *5*, 1561-1569.

(e) Wu, P.; Ibers, J. A. *J. Solid State Chem*. **1994**, *110*, 156-161.

(f) Marking, G. A.; Hanko, J. A.; Kanatzidis, M. G. *Chem. Mater.* **1998**, *10*, 1191-1199.

(g) Klepp, K. O.; Fabian, F. *Eur. J. Solid State Inorg. Chem.* **1997**, *34*, 1155-1163.

(h) Chondroudis, K.; Kanatzidis, M. G. *J. Solid State Chem*. **1998**, *136*, 79-86.

(i) Chondroudis, K.; Kanatzidis, M. G. *J. Chem. Soc., Chem. Commun.*, **1996**, 1371-1372.

(j) Chen, X.; Huang, X.-Y.; Fu, A.-H.; Li, J.; Zhang, L.-D.; Guo, H.-Y. *Chem. Mater.* **2000**, *12*, 2385-2391.

28 (a) Schimek, G. L.; Kolis, J. W. *Acta Crystallogr.* **1997**, *C53*, 991-992.

(b) Jerome, J. E.; Wood, P. T.; Pennington, W. T.; Kolis, J. W. *Inorg. Chem.* **1994**, *33*, 1733-1734.

(c) Kanatzidis, M. G.; Chou, J.-H. *J. Solid State Chem*. **1996**, *127*, 186-201.

(d) Löken, S.; Tremel, W. *Eur. J. Inorg. Chem.* **1998**, 283-289.

(e) Wachhold, M.; Kanatzidis, M. G. *Inorg. Chem.* **1999**, *38*, 3863-3870.

(f) Wachhold, M.; Kanatzidis, M. G. *Inorg. Chem.* **1999**, *38*, 4178-4180.

(g) Kanatzidis, M. G; Wachhold, M. *Z. Anorg. Allg. Chem.* **2000**, *626*, 1901-1904.

(h) Wachhold, M.; Kanatzidis, M. G. *Inorg. Chem.* **2000**, *39*, 2337-2343.

29 Chou, J.-H.; Hanko, J. A.; Kanatzidis, M. G. *Inorg. Chem.* **1997,** *36*, 4-9.

30 Chou, J.-H.; Kanatzidis, M. G. *Inorg. Chem.* **1994,** *33***,** 1001-1002.

31 Ahari, H.; Garcia, A.; Kirkby, S.; Ozin, G. A.; Young, D.; Lough, A. J. *J. Chem. Soc., Dalton Trans.*, **1998**, 2023-2027.

32 (a) Hirsch, K. A.; Venkataraman, D.; Wilson, S. R.; Moore, J. S.; Lee, S. *Chem. Commun.* **1995**, 2199-2200.
(b) Hirsch, K. A.; Wilson, S. C.; Moore, J. S. *Chem. Eur. J.* **1997**, *3*, 765-771.

33 Cieren, X.; Angenault, J.; Couturier, J-C.; Jaulmes, S.; Quarton, M.; Robert, F. *J. Solid State Chem*. **1996**, *121*, 230-235.

Chapter 4

1 Glatzel, E. *Ber. Dtsch. Chem. Ges.* **1891**, *24*, 3886-3899.

2 Rouxel, J. in *The Synthesis and Reactivity of Solids*, Vol. 2, (Ed.: Mallouk, T. T.); JAI London, **1994**; pp. 27-91.

3 Brec, R. *Solid State Ionics*, **1986**, *22*, 3-30.

4 Kanatzidis, M. G. *Curr. Opin. Solid State Mater. Sci*. **1997**, *2*, 139-149.

5 Kanatzidis, M. G.; Sutorik, A. C. *Progr. Inorg. Chem.* **1995**, *43*, 151-265.

6 Brec, R.; Fréour, R.; Ouvrard, G.; Soubeyroux, J. L.; Rouxel, J. *Mater. Res. Bull*. **1983**, *18*, 689-696.

7 Fiechter, S.; Kuhs, W. F.; Nitsche, R. *Acta Crystallogr*. **1980**, *B36*, 2217-2220.

8 Grenouilleau, P.; Brec, R.; Evain, M.; Rouxel, J. *Rev. Chim. Miner*. **1983**, *20*, 628-635.

9 Ouvrard, G.; Fréour, R.; Brec, R.; Rouxel, J. *Mater. Res. Bull*. **1985**, *20*, 1053-1062.

10 (a) Grenouilleau, P.; Brec, R.; Evain, M.; Rouxel, J. *Rev. Chim. Miner*. **1983**, *20*, 295-305;
(b) Jandali, M. Z.; Eulenberger, G.; Hahn, H. *Z. Anorg. Allg. Chem*. **1985**, *530*, 144-154.

11 Durand, E.; Evain, M.; Brec, R .*J. Solid State Chem*. **1993**, *102*, 146-155.

12 Brec, R.; Ouvrard, G. *Solid State Ionics* **1983**, *9-10*, 481-484.

13 Brec, R.; Evain, M.; Grenouilleau, P.; Rouxel, J. *Rev. Chim. Miner*. **1983**, *20*, 283-294.

14 Evain, M.; Brec, R., Ouvrard, G.; Rouxel, J. *Mater. Res. Bull*. **1984**, *19*, 41-48.

15 Evain, M.; Brec, R.; Ouvrard, G.; Rouxel, J. *J. Solid State Chem*. **1985**, *56*, 12-20.

16 Wibbelmann, C.; Brockner, W.; Eisenmann, B.; Schäfer, H. *Z. Naturforsch.* **1984**, *39A*, 190-194.

17 Chondroudis, K.; Kanatzidis, M. G. *Inorg. Chem.* **1998**, *37*, 3792-3797.

18 Evenson, C. R.; Dorhout, P. K. *Inorg. Chem.* **2001**, *40*, 2884-2891.

19 Evenson, C. R.; Dorhout, P. K. *Inorg. Chem.* **2001**, *40*, 2875-2883.

20 Gauthier, G.; Jobic, S.; Brec, R.; Rouxel, J. *Inorg. Chem.* **1998**, *37*, 2332-2333.

21 Gauthier, G.; Jobic, S.; Danaire, V.; Brec, R.; Evain, M. *Acta Crystallogr.* **2000**, *C56*, 117.

22 Chondroudis, K.; Kanatzidis, M. G. *Inorg. Chem*. **2000**, *39*, 1525-1533.

23 Chen, J. H.; Dorhout, P. K. *Inorg. Chem*. **1995**, *34*, 5705-5706.

24 Chen, J. H.; Dorhout, P. K.; Ostenson, J. E. *Inorg. Chem*. **1996**, *36*, 5627-5633.

25 Chondroudis, K.; McCarthy, T.; Kanatzidis, M. G. *Inorg. Chem*. **1996**, *35*, 840-844.

26 Do, J.; Kim, J.; Lah, S.; Yun, H., *Bull. Korean. Chem. Soc*. **1993**, *14*, 678-681.

27 Chondroudis, K.; Kanatzidis, M. G. *C. R. Séances Acad. Sci. Ser. B* **1996**, *322*, 887-894.

28 (a) Briggs Piccoli, P. M.; Abney, K. D.; Schoonover, J. R.; Dorhout, P. K. *Inorg. Chem*. **2000**, *39*, 2970-2976

(b) Hess, R. F.; Abney, K. D.; Burris, J. L.; Hochheimer, H. D.; Dorhout, P. K. *Inorg. Chem.* **2001**, *40*, 2851-2859.

29 Chondroudis, K.; Kanatzidis, M. G. *J. Am. Chem. Soc*. **1997**, *119*, 2574-2575.

30 Gieck, C.; Ksenofontov, V.; Gütlich, P.; Tremel, W. *Angew. Chem*. **2001**, *113*, 946-948; *Angew. Chem. Int. Ed. Engl*. **2001**, 40, 908-911.

31 Evain, M.; Queignec, M.; Brec, R.; Rouxel, J. *J. Solid State Chem*. **1985**, *56*, 148-1587.

32 Derstroff, V., Ph. D. Dissertation, University of Mainz: Mainz, **1997**.

33 Cieren, X.; Angenault, J.; Couturier, J.-C.; Jaulmes, S.; Quarton, M.; Robert, F. *J. Solid State Chem.* **1996**, *121*, 230-235.

34 Regelsky, G., Ph. D. Dissertation, University of Münster: Münster, **2000**.

35 SMART, 5th ed.; Siemens Analytical X-ray Systems, Inc.: Madison, WI, **1998**.

36 SAINT, 4th ed.; Siemens Analytical X-ray Systems, Inc.: Madison, WI, **1998**.

37 Sheldrick, G. M.: SADABS; University of Göttingen: Göttingen, **1997**.

38 Sheldrick, G. M. *SHELXTL* 5.1, Siemens Analytical X-ray Systems, Inc.: Madison, WI, **1998**.

39 Wilson, A. J. C. (editor) *International Tables for Crystallography*, *Volume C*, Kluwer Academic Publishers: Dordrecht **1992**.

40 Kortüm, G. *Reflectance Spectroscopy*; Springer, New York, **1969**.

41 Clarke, R. J. H. *J. Chem. Educ*. **1964**, *41*, 488.

42 Wendlandt, W. W.; Hecht, H. G. *Reflectance Spectroscopy* (Chemical Analysis, Vol. 21). Interscience, New York, **1966**.

43 Haberditzl, W. *Magnetochemie*, Akademie Verlag, Berlin, **1968**.

44 Daoudi, A.; Lamire, M.; Levet, J. C.; Noel, H. *J. Solid State Chem*. **1996**, *123*, 331-336.

45 Suski, W. *Bull. Acad. Pol. Sci.* **1976**, *24*, 75-81.

46 Daoudi, A.; Noel, H. *Inorg. Chim. Acta* **1987**, *140*, 93-95.

47 Noel, H.; Le Marouille, J. Y. *J. Solid State Chem*. **1984**, *52*, 197-202.

48 Noel, H. *J. Solid State Chem*. **1984**, *52*, 203-210.

49 Shannon, R. D. *Acta Crystallogr.* **1976**, *A32*, 751-767.

50 Bürger, H.; Falius, H. *Z. Anorg. Allg. Chem*. **1968**, *363*, 24-32.

51 Sourisseau, C.; Cavagnat, R.; Jobic, S.; Brec, R. *J. Raman Spectrosc*. **1999**, *30*, 721-731.

52 Pätzmann, U.; Brockner, H. *Z. Naturforsch.* **1983**, *38A*, 27-36.

53 Chondroudis, K.; Kanatzidis, M. G. *J. Solid State Chem*. **1998**, *136*, 328-332.

54 Freeman, A. J.; Keller, C. *Handbook on the Physics and Chemistry of the Actinides*; *Vol. 6*, Elsevier, New York, **1991**, pp. 337-366.

55 Lueken, H. *Magnetochemie*, Teubner, Stuttgart, **1999**.

56 Wertheim, G. K.; Guggenheim, H. J.; Levinstein, H. J.; Buchanan, D. N. E.; Sherwood, R. C. *Phys. Rev.* **1968**, *173*, 614-616.

Chapter 5

1 Meier, W. H.; Olson, D. H.; Baerlocher, C. *Atlas of Zeolite Structures*, 4th edn., Elsevier, Amsterdam **1996**, Zeolites, 17, A1-A6.

2 Hyde, B. G.; Andersson, S. Inorganic Crystal Structures. Wiley, New York, **1989**, chap. 15.

3 Wells, A. F. *Structural Inorganic Chemistry*, 5th ed., Clarendon Press, Oxford, **1984**.

4 Breck, D. W. *Zeolite Molecular Sieves*, Wiley & Sons, New York, **1974**.

5 Batten, S. R.; Robson, R. *Angew. Chem*. **1998**, *110*, 1559-1595. *Angew. Chem., Int. Ed. Engl*. **1998**, *37*, 1460-1494.

6 (a) Parise, J. B. *Science* **1991**, *251*, 293-294.
(b) Wang, X.; Liebau, F. *J. Solid State Chem*. **1994**, *111*, 385-389.

7 Simon, U.; Schüth, F.; Schunk, S. Wang, X.; Liebau, F. **1997**, *Angew. Chem*. **1997**, *109*, 1138-1140; *Angew. Chem. Int. Ed. Engl*. **1997**, *109*, 1121-1124.

8 MacCarthy, T. J.; Tanzer, T. A.; Kanatzidis, M. G. *J. Am. Chem. Soc*. **1995**, *117*, 1294-1301.

9 Bedard, R. L.; Vail, L. D.; Wilson, S. T.; Flanigen, E. M. (UOP) U.S. Pat. Patent 4,880,761, **1989**; Bedard, R. L.; Vail, L. D.; Wilson, S. T.; Flanigen, E. M. (UOP), U.S. Pat. Patent 4,933,068, **1990**; Bedard, R. L.; Wilson, S. T.; Vail, L. D.; Bennett, J. M.; Flanigen, E. M. in *Zeolites: Facts, Figures and Future* (Eds.: Jacobs, P. A.; van Santen, R. A.), Elsevier, Amsterdam, **1989**.

10 (a) Yaghi, O.; Sun, Z.; Richardson, D. A.; Groy, T. L. *J. Am. Chem. Soc*. **1994**, *116*, 807-808.

(b) Achak, O.; Pivan, J. Y.; Maunaye, M.; Louër, M.; Louër, D. *J. Alloys Compd*. **1995**, *219*, 111-115.

(c) Achak, O.; Pivan, J. Y.; Maunaye, M.; Louër, M.; Louër, D. *J. Solid State Chem*. **1996**, *121*, 473-478.

11 Tan, K.; Darovsky, A.; Parise, J. B. *J. Am. Chem. Soc*. **1995**, *117*, 7039-7040.

12 Bowes, C. L.; Lough, A. J.; Malek, A.; Ozin, G. A.; Petrov, S.; Young, D. *Chem. Ber*. **1996**, *129*, 283-287.

13 (a) MacLachlan, M. J.; Coombs, N.; Ozin, G. A. *Nature* **1999**, *397*, 681-684.

(b) Wachhold, M.; Rangan, K. K.; Billinge, S. J. L.; Petkov, V.; Heising, J.; Kanatzidis, M. G. *Adv. Mater*. **2000**, *12*, 85-91.

14 MacLachlan, M. J.; Petrov, S.; Bedard, R. L.; Manners, I.; Ozin, G. A., *Angew. Chem*. **1998**, *110*, 2186-2189. *Angew. Chem. Int. Ed. Engl*. **1998**, *37*, 2076-2079.

15 (a) Krebs, B.; Pohl, S., *Z. Naturforsch.* **1971**, *26B*, 853-854.

(b) Pohl, S.; Krebs, B. *Z. Anorg. Allg. Chem*. **1976**, *424*, 265-272.

16 *SMART*, 5th ed.; Siemens Analytical X-ray Systems, Inc.: Madison, WI, **1998**.

17 *SAINT*, 4th ed.; Siemens Analytical X-ray Systems, Inc.: Madison, WI, **1998**.

18 Sheldrick, G. M. *SADABS*; University of Göttingen: Göttingen, **1997**.

19 Sheldrick, G. M. *SHELXTL 5.1*; Siemens Analytical X-ray Systems, Inc.: Madison, WI, **1998**.

20 Wilson, A. J. C. (editor) *International Tables for Crystallography*, *Volume C*, Kluwer Academic Publishers: Dordrecht **1992**.

21 Cotton, F. A.; Wilkinson, G. *Advanced Inorganic Chemistry*, 4th Ed., pp- 53-55, John Wiley & Sons, New York, **1980**.

22 Shannon, R. D. *Acta Crystallogr*. **1976**, *A32*, 751-767.

23 (a) Zimmermann, H.; Carpentier, C. D.; Nitsche, R. *Acta Crystallogr.* **1975**, *B31*, 2003-2006.

(b) Fiechter, S.; Kuhs, W. F.; Nitsche, R. *Acta Crystallogr*. **1980**, *B36*, 2217-2220.

(c) McCarthy, T.; Kanatzidis, M. G. *Chem. Mater.* **1993**, *5*, 1061-1063.

(d) Cieren, X.; Angenault, J.; Couturier, J.-C.; Jaulmes, S.; Quarton, M.; Robert, F. *J. Solid State Chem.* **1996**, *121*, 230-235.

(e) Löken, S.; Tremel, W. *Eur. J. Inorg. Chem.* **1998**, 283-289.

(f) Derstroff, V.; Ksenofontov, V.; Gütlich, P.; Tremel, W. *J. Chem. Soc., Chem. Commun*. **1998,** 187-188.

(g) Derstroff, V.; Tremel, W. *J. Chem. Soc., Chem. Commun*. **1998**, 913-14.

(h) Derstroff, V.; Regelsky, G.; Tremel, W. *J. Chem. Soc., Chem. Commun*. **2003**, submitted for publication.

24 (a) Pauling, L. *Die Natur der chemischen Bindung*, *Verlag Chemie*, Weinheim, **1962**.

(b) Baur, W. H. in Structure and Bonding in Crystals, Vol. II, (Eds.: O´Keefe, M. and Navrotsky, A.), Vol, II, Academic Press, New York, **1981**, pp. 31.

25 Chondroudis, K.; Kanatzidis, M. G. *J. Solid State Chem.* **1998**, *136*, 328-332.

26 Derstroff, V.; Regelsky, G.; Gieck, C.; Suard, E.; Eckert, H.; Tremel, W., *to be submitted for publication.*

27 Gieck, C.; Derstroff, V.; Regelsky, G.; Felser, C.; Block, T.; Ksenofontov, V.; Gütlich, P.; Eckert, H.; Tremel, W. *Chem. Eur. J.*, **2003**, submitted for publication.

28 Angenault, J.; Cieren, X.; Wallez, G.; Quarton, M. *J. Solid State Chem*. **2000**, *153*, 55-65.

29 (a) Wibbelmann, C.; Brockner, W.; Eisenmann, B.; Schäfer, H. *Z. Naturforsch*. **1984**, *39A*, 190-194.

(b) Chen, J. H.; Dorhout, P. K. *Inorg. Chem*. **1995**, *34*, 5705-5706.

(c) Chen, J. H.; Dorhout, P. K., Ostenson, J. E. *Inorg. Chem*. **1996**, *36*, 5627-5633.

(d) Chondroudis, K.; McCarthy, T.; Kanatzidis, M. G. *Inorg. Chem*. **1996**, *35*, 840-844.

30 (a) Do, J.; Kim, J.; Lah, S.; Yun, H. *Bull. Korean Chem. Soc*. **1993**, *14*, 678-681.

(b) Chondroudis, K.; Kanatzidis, M. G. *CR Acad. Sci. Paris* **1996**, *322*, 887-894.

(c) Briggs Piccoli, P. M.; Abney, K. D.; Schoonover, J. R.; Dorhout, P. K. *Inorg. Chem*. **2000**, *39*, 2970-2976.

(d) Chondroudis, K.; Kanatzidis, M. G. *J. Am. Chem. Soc*. **1997**, *119*, 2574-2575.

31 Interestingly, the channels of the $TaPS_6$ framework may be filled with chalcogen chains or alkali metal cations. See for example:

(a) Evain, M.; Queignec, M.; Brec, R.; Rouxel, J. *J. Solid State Chem.* **1988**, *75*, 148-158.

(b) Evain, M.; Queignec, M.; Brec, R.; Sourisseau, C. *J. Solid State Chem.* **1988**, *75*, 413-431.

32 Lueken, H. *Magnetochemie*, Teubner, Stuttgart, **1999**.

33 Halasyamani, P. S.; Walker, S. M.; O´Hare, D. *J. Am. Chem. Soc*. **1999**, *121*, 7415-7416.

Chapter 6

1 Meier, W. H.; Olson, D. H.; Baerlocher, C. *Atlas of Zeolite Structures*, 4th edn., Elsevier, Amsterdam **1996**, *Zeolites*, *17*, A1-A6.

2 (a) Breck, D. W. *Zeolite Molecular Sieves*, Wiley & Sons, New York, **1974**.

(b) Thomas, J. M.; Raja, R.; Sankar, G.; Bell, R. G. *Nature* **1999**, *398*, 227-230.

3 (a) Batten, S. R.; Robson, R. *Angew. Chem*. **1998**, *110*, 1559-1595; *Angew. Chem., Int. Ed. Engl*. **1998**, *37*, 1460-1494.

(b) Eddaoudi, M.; Moler, D.; Li, H.; Reineke, T. M.; O´Keeffe, M.; Yaghi, O. M. *Acc. Chem. Res*. **2001**, *34*, 319-330.

4 (a) Parise, J. B. *Science* **1991**, *251*, 293-294.

(b) Wang, X.; Liebau, F. *J. Solid State Chem*. **1994**, *111*, 385-389.

5 (a) zum Hebel, P.; Krebs, B.; Grüne, M.; Müller-Warmuth, W. *Solid State Ionics* **1990**, *43*, 133-142.

(b) Hiltmann, F.; zum Hebel, P.; Hammerschmidt, A.; Krebs, B. *Z. Anorg. Allg. Chem.* **1993**, *619*, 293-302.

(c) Hammerschmidt, A.; zum Hebel, P.; Hiltmann, F.; Krebs, B. *Z. Anorg. Allg. Chem.* **1996**, *622*, 76-84.

(d) Conrad, O.; Jansen, C.; Krebs, B. *Angew. Chem.* **1998**, *110*, 3396-3407; *Angew. Chem., Int. Ed. Engl.* **1998**, *37*, 3208-3218.

6 (a) Li, H.; Laine, A.; O´Keeffe, M.; Yaghi, O. M. *Science* **1999**, *283*, 1145-1147.

(b) Li, H.; Eddaoudi, M.; Laine, A.; O´Keeffe, M.; Yaghi, O. M. *J. Am. Chem. Soc.* **1999**, *121*, 6096-6097.

(c) Li, H.; Kim, J.; Groy, T. L.; O´Keeffe, M.; Yaghi, O. M. *J. Am. Chem. Soc.* **2001**, *123*, 4867-4868.

7 Simon, U.; Schüth, F.; Schunk, S.; Wang, X.; Liebau, F. *Angew. Chem.* **1997**, *109*, 1138-1140; *Angew. Chem. Int. Ed. Engl.* **1997**, *109*, 1121-1124.

8 MacCarthy, T. J.; Tanzer, T. A.; Kanatzidis, M. G. *J. Am. Chem. Soc.* **1995**, *117*, 1294-1301.

9 Bedard, R. L.; Vail, L. D.; Wilson, S. T.; Flanigen, E. M. (UOP), U.S. Pat. Patent 4,880,761, **1989**; Bedard, R. L.; Vail, L. D.; Wilson, S. T.; Flanigen, E. M. (UOP), U.S. Pat. Patent 4,933,068, **1990**; Bedard, R. L.; Wilson, S. T.; Vail, L. D.; Bennett, J. M.; Flanigen, E. M. in *Zeolites: Facts, Figures and Future* (Eds.: Jacobs, P. A.; van Santen, R. A.), Elsevier, Amsterdam, **1989**.

10 (a) MacLachlan, M. J.; Coombs, N.; Ozin, G. A. *Nature* **1999**, *397*, 681-684.

(b) Wachhold, M.; Rangan, K. K.; Billinge, S. J. L.; Petkov, V.; Heising, J.; Kanatzidis, M. G. *Adv. Mater.* **2000**, *12*, 85-91.

11 MacLachlan, M. J.; Petrov, S.; Bedard, R. L.; Manners, I.; Ozin, G. A. *Angew. Chem.* **1998**, *110*, 2186-2189. *Angew. Chem. Int. Ed. Engl.* **1998**, *38*, 2076-2079.

12 Trikalitis, P. N.; Rangan, K. K.; Bakas, T.; Kanatzidis, M. G. *Nature* **2001**, *410*, 671-675.

13 Schiwy, W.; Pohl, S.; Krebs, B. *Z. Anorg. Allg. Chem.* **1973**, *402*, 77-86.

14 Krebs, B.; Pohl, S.; Schiwy, W. *Z. Anorg. Allg. Chem.* **1972**, *393*, 241-252.

15 Schiwy, W.; Blutau, C.; Gäthke, D.; Krebs, B. *Z. Anorg. Allg. Chem.* **1975**, *412*, 1-10.

16 Sheldrick, W. S.; Braunbeck, H.-G. *Z. Naturforsch.* **1990**, **45b**, 1643-1646.

17 Krebs, B. *Angew. Chem.* **1983**, *95*, 113-134; *Angew. Chem., Int. Ed. Engl.* **1983**, *22*, 113-134.

18 *SMART*, 5th ed.; Siemens Analytical X-ray Systems, Inc.: Madison, WI, **1998**.

19 *SAINT*, 4th ed.; Siemens Analytical X-ray Systems, Inc.: Madison, WI, **1998**.

20 Sheldrick, G. M. *SADABS*; University of Göttingen: Göttingen, **1997**.

21 Sheldrick, G. M. *SHELXTL 5.1*; Siemens Analytical X-ray Systems, Inc.: Madison, WI, **1998**.

22 Wilson, A. J. C. (editor) *International Tables for Crystallography*, *Volume C*, Kluwer Academic Publishers: Dordrecht **1992**.

23 (a) Pauling, L. *Die Natur der chemischen Bindung*, Verlag Chemie, Weinheim, **1962**.

(b) Baur, W. H. in *Structure and Bonding in Crystals*, Vol. II, (Eds.: O´Keefe M. and Navrotsky, A.), Academic Press, New York, **1981**, pp. 31.

24 Sola, J.; Do, Y.; Berg, J. M.; Holm, R. H. *Inorg. Chem.* **1985**, *24*, 1706-1713.

25 Siemeling, U.; Gibson, V. *Chem. Commun.* **1992**, 1670-1671.

26 Lee, S. C.; Holm, R. H. *J. Am. Chem. Soc.* **1990**, *112*, 9654-9655.

27 Christou, V.; Arnold, J. *Angew. Chem.* **1993**, *105*, 1551-1553; *Angew. Chem. Int. Ed. Engl.* **1993**, *32*, 1450-1452.

28 Cotton, F. A.; Wilkinson, G. *Advanced Inorganic Chemistry*, 4th Ed., 53-55, John Wiley & Sons, New York, **1980**.

29 Shannon, R. D. *Acta Crystallogr.* **1976**, *A32*, 751-767.

30 Christou, V.; Arnold, J. *J. Am. Chem. Soc.* **1992**, *114*, 6240-6242.

31 Brec, R. *Solid State Ionics*, **1986**, *22*, 3-30.

32 Whangbo, M.-H.; Brec, R.; Ouvrard, G.; Rouxel, J. *Inorg. Chem.* **1985**, *24*, 2459-2461.

Chapter 7

1 Hulliger, F. *Structure and Bonding* **1968**, *4*, 83-229.

2 Kanatzidis, M. G. *Phosphorus Sulfur* **1994**, *93*, 159-172.

3 Stephan, D. W.; Nadasdi, T. T. *Coord. Chem. Rev.* **1996**, *147*, 147-208.

4 Krebs, B.; Henkel, G. *Angew. Chem.* **1991**, *103*, 785-804; *Angew. Chem. Int. Ed. Engl.* **1991**, *30*, 769-788.

5 (a) Derstroff, V.; Tremel, W. *Chem. Commun.* **1998**, 913-914.
(b) Evenson, C. R.; Dorhout, P. K. *Inorg. Chem.* **2001**, *40*, 2884-2891.
(c) Briggs Piccoli, P. M.; Abney, K. D.; Schoonover, J. D.; Dorhout, P. K. *Inorg. Chem.* **2001**, *40*, 4871-4875.
(d) Gieck, C.; Tremel, W. *Chem. Eur. J.* **2002**, *8*, 2980-2987.
(e) Hess, R. F.; Gordon, P. L.; Tait, C. D.; Abney, K. D.; Dorhout, P. K. *J. Amer. Chem. Soc.* **2002**, *124*, 1327-1333.
6 Roof, L. C.; Kolis, J. C. *Chem. Rev.* **1993**, *93*, 1037-1080.
7 Rouxel,. J. *J. Solid State Chem.* **1986**, *61*, 305-321.
8 Carney, M. J.; Walsh, P. J.; Hollander, F. J.; Bergman, R. G. *Organometallics* **1992**, *11*, 761-777.
9 *SMART*, 5th ed.; Siemens Analytical X-ray Systems, Inc., Madison, WI, **1998**.
10 *SAINT*, 4th ed.; Siemens Analytical X-ray Systems, Inc., Madison, WI, **1998**.
11 Sheldrick, G. M.: *SADABS*; University of Göttingen: Göttingen, **1997**.
12 Sheldrick, G. M.: *SHELXTL 5.1*, Siemens Analytical X-ray Systems, Inc., Madison, WI, **1998**.
13 Wilson, A. J. C. (editor) *International Tables for Crystallography*, *Volume C*, Kluwer Academic Publishers: Dordrecht **1992**.
14 Chen, L.; Klar, P. J.; Heimbrodt, W.; Oberender, N.; Kempe, D.; Fröba, M. *Appl. Phys. Lett.* **2000**, *77*, 3965-3967.
15 (a) MacLachlan, M. J.; Coombs, N.; Ozin, G. A. *Nature* **1999**, *397*, 681-684.
(b) Wachhold, M.; Rangan, K. K.; Billinge, S. J. L.; Petkov, V.; Heising, J.; Kanatzidis, M. G. *Adv. Mater.* **2000**, *12*, 85-91.

Danksagung

Ich möchte mich ganz herzlich bei allen bedanken, die zum Gelingen meiner Dissertation beigetragen haben.

- Herrn Professor Dr. W. Tremel für seine Diskussionsbereitschaft und sein Interesse an meiner Arbeit
- Frau S. Hennig für zahlreiche Messungen am Einkristall-Diffraktometer
- Frau Dr. S. Neitzel und Herrn Dr. V. Derstroff für die Einführung in die verwendeten Arbeitstechniken sowie viele gute Ideen
- Herrn F. Rocker und Herrn Dr. J. Neuhausen für ihre Unterstützung und ihre Hilfsbereitschaft
- Herrn Dr. M. Bartz und Herrn Dr. J. Küther für Untersuchungen am Rasterelektronenmikroskop
- Herrn Dr. V. Ksenofontov für die Durchführung magnetischer Messungen sowie Herrn Professor Dr. W. Urland und Herrn Dr. S. T. Hatscher für die Auswertung der Daten
- Herrn PD Dr. L. Nasdala für die Aufnahme von Raman-Spektren
- Frau U. Zmij und Herrn Dr. A. Höfer für die Aufnahme von IR-Spektren
- Herrn Dr. M. Kocher für erste Untersuchungen an $K_{11}U_7(PS_4)_{13}$
- allen Mitgliedern des Arbeitskreises für die gute Zusammenarbeit und die angenehme Atmosphäre
- Herrn Dr. S. D. Hoffmann für die Korrektur des Manuskriptes
- meiner Mutter, Frau L. Kolb, die mir mein Chemiestudium ermöglichte

Eidesstattliche Erklärung

Hiermit versichere ich, dass ich die vorliegende Dissertation selbstständig verfasst und keine anderen als die angegebenen Hilfsmittel verwendet habe. Alle der Literatur entnommenen Stellen sind als solche gekennzeichnet.

Mainz, September 2003